WILEY-BLACKWELL

Cladistics 30 (2014) 67–106

Cladistics

10.1111/cla.12025

Phantoms of Gondwana?—phylogeny of the spider subfamily Mynogleninae (Araneae: Linyphiidae)

Holger Frick[a,b,*] and Nikolaj Scharff[b,c]

[a]*Department of Invertebrates, Natural History Museum of Bern, Bernastrasse 15, 3005 Bern, Switzerland;* [b]*Department of Entomology, Natural History Museum of Denmark, Zoological Museum, University of Copenhagen, Universitetsparken 15, 2100 Copenhagen, Denmark;* [c]*Center of Macroecology, Evolution and Climate, Biological Institute, Universitetsparken 15, 2100 Copenhagen, Denmark*

Accepted 25 February 2013

Abstract

This is the first genus-level phylogeny of the subfamily Mynogleninae. It is based on 190 morphological characters scored for 44 taxa: 37 mynoglenine taxa (ingroup) representing 15 of the 17 known genera and seven outgroup taxa representing the subfamilies Stemonyphantinae, Linyphiinae (Linyphiini and Micronetini), and Erigoninae, and a representative of the family Pimoidae, the sister-group to Linyphiidae. No fewer than 147 of the morphological characters used in this study are new and defined for this study, and come mainly from male and female genitalia. Parsimony analysis with equal weights resulted in three most parsimonious trees of length 871. The monophyly of the subfamily Mynogleninae and the genera *Novafroneta*, *Parafroneta*, *Laminafroneta*, *Afroneta*, *Promynoglenes*, *Metamynoglenes*, and *Haplinis* are supported, whereas *Pseudafroneta* is paraphyletic. The remaining seven mynoglenine genera are either monotypic or represented by only one taxon. Diagnoses are given for all genera included in the analysis. The evolution of morphological traits is discussed and we summarize the diversity and distribution patterns of the 124 known species of mynoglenines. The preferred topology suggests a single origin of mynoglenines in New Zealand with two dispersal events to Africa, and does not support Gondwana origin.

Introduction

Linyphiidae are the most species-rich spider family within the superfamily Araneoidea, a large clade that includes one-third of all described spider species (Blackledge et al., 2009). Linyphiidae have a worldwide distribution but are most diverse in colder regions. At higher latitudes, this family dominates the spider faunas. For instance, 41% of the Danish spider fauna (216 of the 523 species) are linyphiids (Scharff and Gudik-Sørensen, 2006) and most species are widely distributed in northern Europe. At lower latitudes, the family is well represented but constitutes a much smaller fraction of the total spider fauna (Scharff, 1992, 1993; Sørensen et al., 2002).

The family represents the second most diverse family of spiders, with 4429 described species (Platnick, 2013) in 590 genera, surpassed only by the family Salticidae, with 5570 species in 591 genera.

The spider family Linyphiidae has been divided into a number of different subfamilies, most of which are not monophyletic according to modern phylogenetic studies. Currently used subfamilies of Linyphiidae are Stemonyphantinae, Mynogleninae, Erigoninae, and Linyphiinae (Micronetini plus Linyphiini; Arnedo et al., 2009), of which Mynogleninae with 17 genera and 124 species are one of the smallest and most recently established. Most species have been described within the past 35 years. The subfamily Mynogleninae was established by Lehtinen (1967: 250) for *Mynoglenes insolens* Simon, 1905 (now *Haplinis rufocephala* (Urquhart, 1888)) and is "mainly characterized by the presence of numerous metatarsal trichobothria and the

*Corresponding author.
E-mail address: holger.frick@gmx.li

exceptional type of modification of the carapace". Unfortunately, Lehtinen (1967) did not specify what kind of "exceptional modifications of the carapace" he used to define the subfamily. A quick look at the carapace of any known mynoglenine reveals that it cannot be anything but the very characteristic cephalic pits with which all mynoglenines are equipped—males as well as females, and juveniles—just below the anterior lateral eyes (subocular sulci; Figs 14b and 15c: SOS). This is still the best morphological character to distinguish between mynoglenines and members of all other linyphiid subfamilies (Blest, 1979: 96). Members of the subfamily are otherwise rather indistinct, being small to medium in size (2–10 mm) and without any other cephalic modifications or characteristic abdominal markings (Fig. 13e and 15a).

The first mynoglenine was described by Urquhart (1886) and placed in the well known European genus *Linyphia*. Simon described the genera *Haplinis* (1894) and *Mynoglenes* (1905), but neither Simon nor Urquhart mentions the special cephalic pits in their descriptions. Today we know that most members of this subfamily occur in the Southern Hemisphere, and that they have a disjunct distribution pattern with centres of diversity in tropical Africa (33 species) and New Zealand (90 species; including the South Pacific islands) and in Australia (one species; Tasmania). More species undoubtedly remain to be discovered, especially in Africa where the mynoglenine fauna is still very poorly surveyed, but even if more species should turn up in Africa, the subfamily is still small compared to the Erigoninae, another well defined sub-

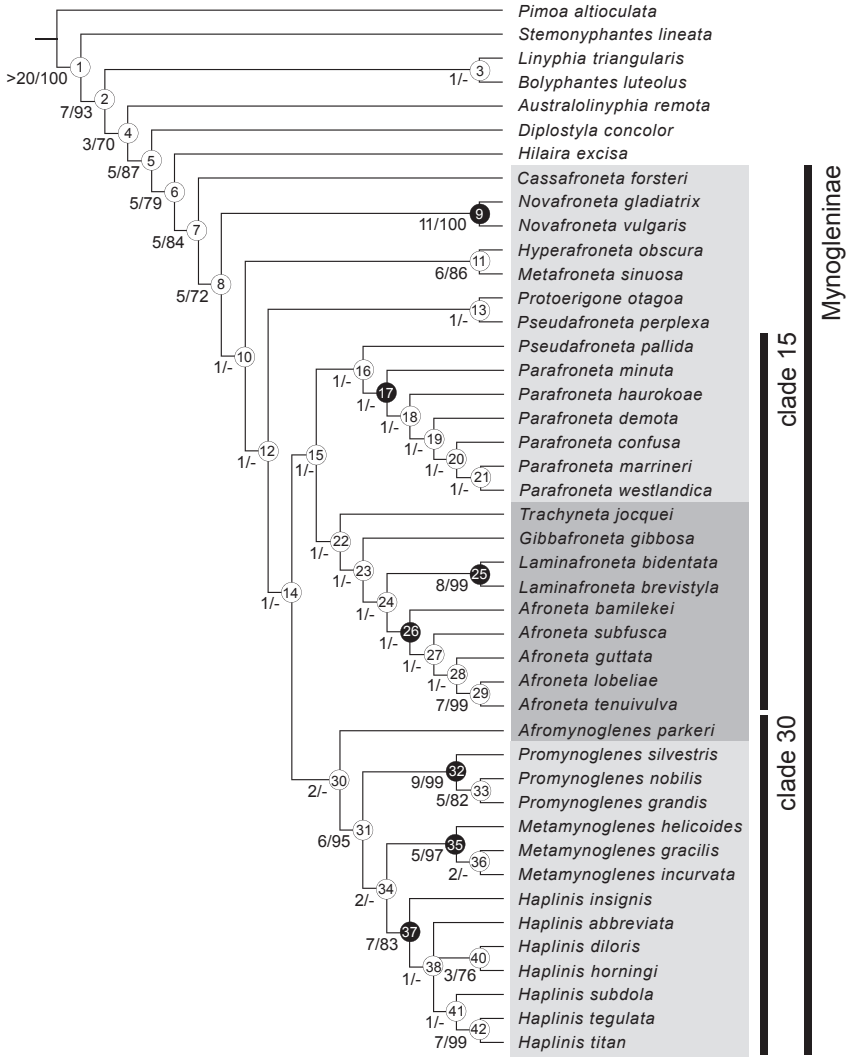

Fig. 1. Strict consensus tree of three most parsimonious trees found using equal weights (L = 873, CI = 0.28, RI = 0.62) including support values (Bremer before and Jackknife after the slash). Node numbers in circles (monophyletic genera in black). The recent distribution is indicated for Africa (dark grey) and Oceania (light grey). Note that node 39 collapses and is not depicted in the consensus tree.

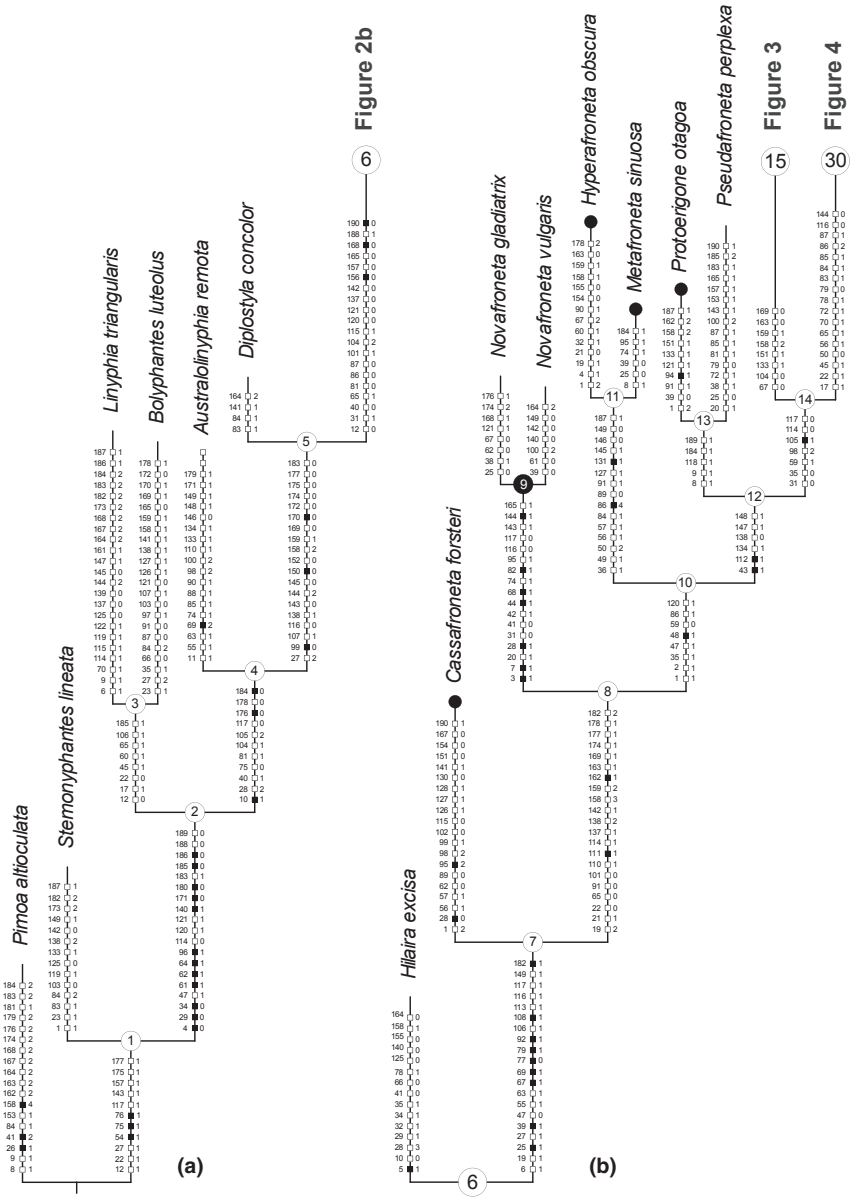

Fig. 2. Equal weights tree showing ACCTRAN character optimizations. Squares show synapomorphic (black) and homoplastic (white) character-state changes. Numbers to the left of squares correspond to character numbers, those to the right to character-state changes. Node numbers are given in circles (black, monophyletic genera). (a) Outgroups; (b) continuation of (a) showing clade 6.

family of Linyphiidae, with more than 1000 described species (Miller, 2007).

The first major attempts to understand the evolution of linyphiids was based on the male palpal conformation (Millidge, 1977) and tracheae and epigynes (Millidge, 1984, 1993), but none of these studies was done in a modern phylogenetic framework. The first quantitative phylogenetic analysis of linyphiid interrelationships was published by Hormiga (1993) and was based on a combined datasets of somatic and genital morphology. Characters and taxa have been added to this dataset over the years and have resulted in more detailed understanding of the phylogenetic structure of the family (Hormiga, 1994b, 2000; Miller and Hormiga, 2004; Arnedo et al., 2009; Frick et al., 2010). Most of these studies focused on the circumscription and phylogenetic interrelationship of the linyphiid subfamily Erigoninae, with limited representation of other recognized subfamilies. Most recently, Arnedo et al. (2009) have published phylogenies based on both morphology and molecules and with a broader representation of all subfamilies, and this study is currently the most comprehensive in terms of data and taxa for a family level phylogeny of Linyphiidae. The monophyly of the family Linyphiidae is well supported by morphological data (Miller and Hormiga, 2004) and

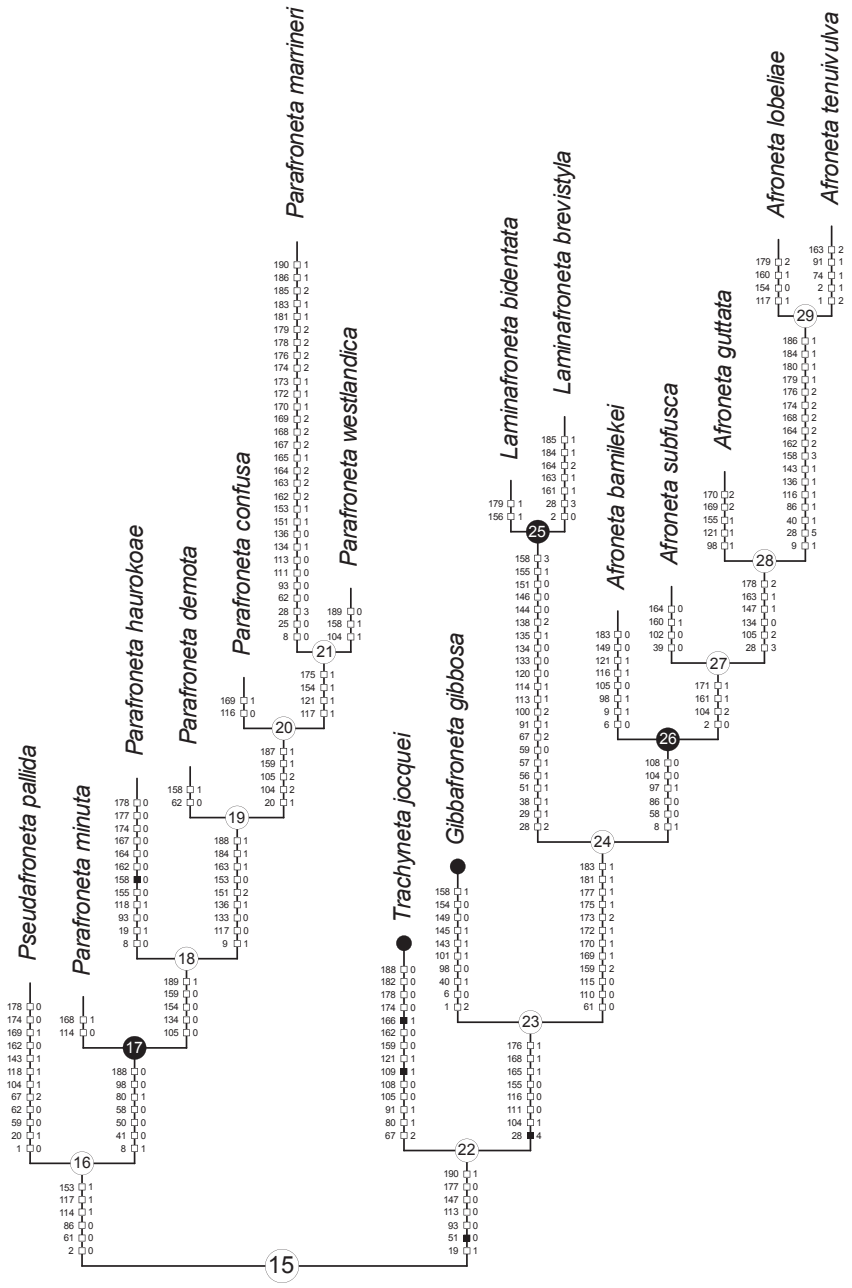

Fig. 3. Continuation of Fig. 2b showing clade 15.

almost all combined analyses (morphology and molecules) of Arnedo et al. (2009). However, when molecular data are analysed separately, they do not support monophyly of Linyphiidae (Arnedo et al., 2009).

Within Linyphiidae, the monophyly of the subfamily Mynogleninae is uncontroversial and supported by all recent analyses of morphological as well as molecular data (Miller and Hormiga, 2004; Arnedo et al., 2009). However, the relationship of the subfamily Mynogleninae to other subfamilies is not clear. A sister-group relationship to the subfamily Erigoninae has been recovered in several studies (Miller and Hormiga, 2004), but the latest study by Arnedo et al. (2009) suggests a sister-group relationship between Mynogleninae and a clade containing the genera *Bathyphantes*, *Diplostyla*, *Laetesia*, and *Australolinyphia*.

Members of the subfamily Mynogleninae occur in New Zealand, in tropical Africa, on Tasmania and on some Pacific islands. This distribution pattern has puzzled arachnologists working with African and New Zealand linyphiid faunas. Like many other groups of organisms with high degrees of endemism

and disjunct distribution in the Southern Hemisphere, mynoglenines have been suggested to be of Gondwana age and thereby relicts of an old fauna that was living on the supercontinent Gondwana some 170 Ma ago (Blest, 1979; Merrett and Russell-Smith, 1996; Merrett, 2004; Ledoux and Attié, 2008). This scenario suggests that the mynoglenine fauna of New Zealand is a result of old vicariance events, including the rifting that caused New Zealand to break away from Antarctica and Australia some 80 Ma ago (Waters and Craw, 2006; Boyer and Giribet, 2009). Many other groups of organisms in New Zealand exhibit an extraordinary high degree of endemism and disjunct distributions, and there is an ongoing debate whether such patterns are caused by old vicariance or more recent dispersal events (Pole, 1994; Waters and Craw, 2006; Knapp et al., 2007; Boyer and Giribet, 2009). Based on palynological evidence, Pole (1994) suggested that the entire forest-flora of New Zealand arrived by long-distance dispersal, and Waters and Craw (2006) have recently questioned the vicariant origin, and thereby possible Gondwanan age, of several key New Zealand Gondwana taxa such as the flightless birds (ratites), ancient reptiles (Tuatara, *Sphenodon*), and southern beeches (*Nothofagus*). To date, there is no evidence to support the old Gondwana age of mynoglenines, as there are no fossils or phylogeny that could help us deduce the distribution patterns observed. The main goal of this study is to produce a genus-level phylogeny for the subfamily. We discuss the evolution of male copulatory organs as well as the biogeography of the subfamily.

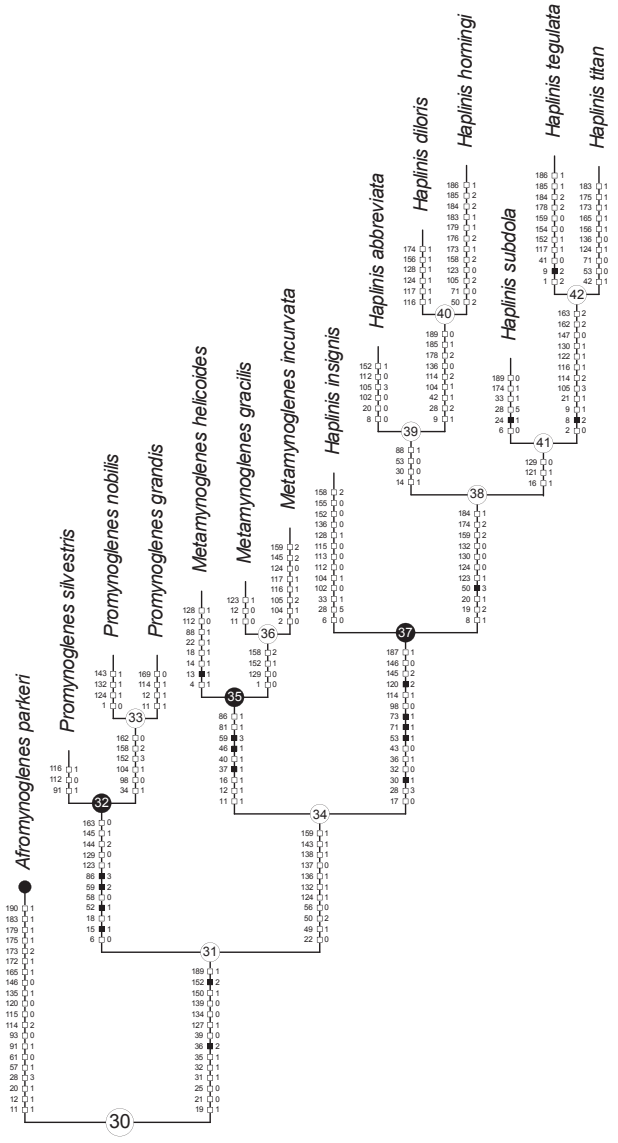

Fig. 4. Continuation of Fig. 2b showing clade 30.

Methods

Taxon sampling

All previous studies have supported the monophyly of Mynogleninae (Hormiga, 1994b, 2000; Miller and Hormiga, 2004; Arnedo et al., 2009; Dimitrov et al., 2012), but no more than three mynoglenine genera have ever been tested for monophyly and there is no consensus as to the sister-group relationship to other linyphiid subfamilies. The position of Mynogleninae as sister to all other linyphiids (except *Stemonyphantes*) was suggested by Hormiga (1994b) in a very early phylogenetic study with nine linyphiid taxa represented. A sister-group relationship between mynoglenines and *Stemonyphantes* was suggested by Hormiga (2000), based on a phylogenetic study including 38 linyphiid taxa. Miller and Hormiga (2004) suggested a sister-group relationship between Mynogleninae and the subfamily Erigoninae, based on a phylogenetic study including 77 linyphiid taxa, but this study and Hormiga (2000) focused on the interrelationships within erigonines and therefore had an overweight of erigonine taxa and few representatives of other subfamilies.

The study of Arnedo et al. (2009) was the first to include molecular data and a more balanced subfamily representation. This study included 35 linyphiid taxa, and both molecular and combined morphology and molecular data suggested a sister-group relationship between Mynogleninae and a clade containing the genera *Bathyphantes*, *Diplostyla*, *Australolinyphia*, and *Laetesia*. Morphology only suggested a sister-group relationship following Hormiga (1994b). None of the studies prior to Arnedo et al. (2009) included the four genera mentioned above. Given the uncertainty about the sister-group relationship between Mynogleninae

and the other subfamilies, we decided to include the following seven outgroup taxa: *Stemonyphantes* (*Stemonyphantes* group sensu Millidge (1984)), *Linyphia triangularis*, *Diplostyla concolor*, and *Australolinyphia remota* (Linyphiinae sensu Millidge (1984)), *Bolyphantes luteolus* (Micronetinae sensu Millidge (1984)), and *Hilaria excisa* (Erigoninae sensu Millidge (1984)). The genus *Hilaria* came out as a rather early lineage in the most recent study focusing on the phylogeny of the subfamily Erigoninae (Miller and Hormiga, 2004). Finally, we used *Pimoa altioculata* (Pimoidae) to root the phylogenetic tree.

As ingroup, we scored representatives from 15 of 17 known mynoglenine genera. Exceptions were *Megafroneta* (three species) and *Poecilafroneta* (monotypic), both from New Zealand, for which no material was available for scoring. From genera with eight or fewer species, we scored ca. 30% of the taxa and five to seven of the more species-rich genera (see Appendix 2 for a detailed list of species and author names included in this study). Where possible, the type species of the genus was scored (marked with an asterisk). In total, the character matrix includes 44 taxa: 37 mynoglenines (of 124 described mynoglenine species).

For the ingroup (Mynogleninae), we scored:

African representatives: ***Afromynoglenes*** (monotypic): **Afromynoglenes parkeri*; ***Afroneta*** (five out of 26 species): *Afroneta bamilekei*, *Afroneta guttata*, *Afroneta lobeliae*, *Afroneta subfusca*, *Afroneta tenuivulva*; ***Gibbafroneta*** (monotypic): **Gibbafroneta gibbosa*; ***Laminafroneta*** (two out of three species): **Laminafroneta bidentata*, *Laminafroneta brevistyla*; ***Trachyneta*** (one out of two species): *Trachyneta jocquei*.

New Zealand representatives: ***Cassafroneta*** (monotypic): **Cassafroneta forsteri*; ***Haplinis*** (seven out of 39 species): *Haplinis abbreviata*, *Haplinis diloris*, *Haplinis horningi*, *Haplinis insignis*, *Haplinis subdola*, *Haplinis tegulata*, *Haplinis titan*; ***Hyperafroneta*** (monotypic): **Hyperafroneta obscura*; ***Metafroneta*** (one out of three species): **Metafroneta sinuosa*; ***Metamynoglenes*** (three out of eight species): *Metamynoglenes gracilis*, *Metamynoglenes helicoides*, **Metamynoglenes incurvata*; ***Novafroneta*** (two out of six species): *Novafroneta gladiatrix*, **Novafroneta vulgaris*; ***Parafroneta*** (six out of 14 species): *Parafroneta confusa*, *Parafroneta demota*, *Parafroneta haurokoae*, **Parafroneta marrineri*, *Parafroneta minuta*, *Parafroneta westlandica*; ***Promynoglenes*** (three out of six species): *Promynoglenes grandis*, **Promynoglenes nobilis*, *Promynoglenes silvestris*; ***Protoerigone*** (one out of two species): **Protoerigone otagoa*; ***Pseudafroneta*** (two out of seven species): *Pseudafroneta pallida*, *Pseudafroneta perplexa*.

Character scoring

Characters were scored using a Leica MZ16A (Planapo 1.0× objective) stereomicroscope and based on examination of specimens as well as photographs taken with a Leica M205A (Planapo 1.0× objective) stereomicroscope. Pictures were taken using a Leica DFC 420 and Leica Application Suite v.3.7.0, and stacked with Helicon Focus v.4.60.2 Pro. For character illustrations, some pictures were edited using Adobe Creative Suite 4.

Altogether we scored 190 characters (see Appendix 3 for character descriptions) for 44 taxa: more than four times more characters than species and altogether 8360 homology statements. 147 characters used in this analysis are new and defined to account for detailed similarities of the scored taxa. Some characters defined here are based on Blest's (1979) original genus and species descriptions. A few characters from Miller and Hormiga (2004) and Arnedo et al. (2009) also turned out to be informative for mynoglenine phylogeny and were therefore adopted. The data matrix was compiled and managed in Mesquite v.2.74 (Maddison and Maddison, 2010).

It would be desirable to add more data, such as molecular sequences, behaviour, biology, anatomy, and microstructures (SEM), but very little is known about the biology and behaviour of mynoglenines, and the study of anatomy and microstructures was impossible to include given the lack of suitable material for SEM preparation. Instead of scoring existing anatomical and microstructural characters for mynoglenines, we concentrated on generating new morphological characters from the male and female genitalia—characters that have not been used in previous studies. As for molecules, suitable tissue is available for only seven of the 17 genera. Generating molecular data for the mynoglenines will be particularly interesting as a molecular phylogeny will represent an independent test of the phylogenetic hypothesis presented here.

Phylogenetic analysis

The parsimony analyses were performed in TNT v.1.1 (Goloboff et al., 2008), using heuristic methods ("traditional search") under both equal and implied weights.

Equal weight analyses (ew). The traditional searches used tree bisection–reconnection (TBR) and the standard setting for starting trees (commands: *mult = tbr replic 1000 hold 1000;*). Branches with no possible support were collapsed (collapsing "rule 3") during and after the tree search (commands: *collapse 1; collapse [;*). All characters were unordered and the

43 multistate characters were treated as non-additive (Fitch, 1971). If the most parsimonious resolutions (MPR) were found in only a few replications, we broadened the search to include more replications and to hold more trees per replication. To further broaden the search, we also applied TBR-ratchet (Nixon, 1999; commands: *ratchet: iter 1000; mult=ratchet replic 1000 tbr hold 1000;*). See Ojanguren-Affilastro and Ramirez (2009) for a detailed discussion of the significance of the ratchet. The resulting trees were checked for zero-length branches (Coddington and Scharff, 1994).

Implied weighting (iw). Implied weighting in TNT weights the characters according to a concave function of homoplasy (Goloboff, 1993). The concavity function (k) is set by the user and negatively correlates with how strongly homoplasious characters are downweighted. The implied weights analyses were run with the same search parameters as used for the equal weights analysis (commands: *piwe=1; mult=tbr replic 1000 hold 1000;*), and with the concavity constant (k) set to 1–50. Above k = 42, trees were effectively equivalent to equal weights (tree length 871).

Optimization, support and resampling

We used WinClada v.1.00.08 (Nixon, 2002) to study character optimizations on the preferred tree. Ambiguous character optimizations were resolved so as to favour reversal or secondary loss over convergence (ACCTRAN or Fast Optimization in WinClada). Mesquite was used to calculate the ensemble consistency index (CI) and ensemble retention index (RI). Appendix 4 lists character statistics (steps, ci and ri) for the preferred topology (equal weights).

TNT was also used to calculate support values for the preferred tree (equal weights, Fig. 1). For the Bremer support values (BS; Bremer, 1988, 1994) a rough precedent search setting suboptimal to 50 was made to find the upper limit of supports. The more thorough search was based on the original equal weights trees. Subsequently, the suboptimal was increased stepwise by 1 up to 20 and so was the tree buffer by 5000 for 20 cycles (commands: *mult 50; sub 1; hold 5000; bbreak=fillonly; sub 2; hold 10000; bbreak=fillonly; sub 3; hold 15000; bbreak=fillonly;…; sub 30; hold 100000; bbreak=fillonly; bsupport;*).

For the jackknife support (JK; Farris et al., 1996), we performed 1000 jackknife pseudoreplicates of 100 random sequence additions, keeping 10 trees each using TBR as swapping algorithm (commands: *mult: noratchet repl 100 tbr hold 10; resample jak repl 1000 freq from 0 [mult];*). Values above 50% threshold are given for the preferred tree (equal weights, Fig. 1).

Distribution patterns

The worldwide distribution of mynoglenines is shown in Fig. 7. It is based on 1293 published records (Urquhart, 1886, 1888, 1894; Hogg, 1911; Rainbow, 1917; Berland, 1925, 1931; Bryant, 1935; Hickman, 1939; Berland, 1942; Holm, 1968; Blest and Pomeroy, 1978; Blest, 1979; Bosmans, 1988; Scharff, 1989; Merrett and Russell-Smith, 1996; Blest and Vink, 2002, 2003; Blest, 2004; Merrett, 2004; Ledoux and Attié, 2008) and unpublished museum collection data: Natural History Museum, London (BMNH), Entomology Research Museum, Lincoln University, New Zealand (LUNZ), Museum of New Zealand (MoNZ), Musée Royal de l'Afrique centrale (MRAC), Uppsala Universitet, Zoologiska Museum (ZIUU), Natural History Museum of Denmark, Zoological Museum (ZMUC), as well as unpublished personal information (presence of mynoglenines on the Fiji Islands, G. Hormiga). The distribution of genera on the two continents is mapped on the strict consensus of the three equally weighted trees (Fig. 1).

Results

Mynoglenine relationships at the genus level are presented for the first time. The monophyly of all genera except *Pseudafroneta* were recovered using equal weights. The support values are given in Fig. 1, and a detailed discussion of the clades and their support is given in Appendix 5.

Phylogenetic analysis

Equal weights. Heuristic searches in TNT with 1000 replications, holding 1000 trees during each replication, generated three trees of length 871 (CI = 0.28, RI = 0.62). Excluding uninformative/autapomorphic characters (5, 13, 24, 26, 54, 76, 94, 109, and 166) reduced tree length to 862 (CI = 0.27, RI = 0.62). No zero-length branches were discovered (Coddington and Scharff, 1994). As optimal trees were found only 113 times out of 1000 replications, we broadened the search to include more replications and to hold more trees per replication. Various combinations, including extremes such as 10 000 replications, holding 100 trees per replication, and 100 replications, holding 10 000 trees per replication, resulted in the same three trees of length 871. Additional analyses carried out with TNT using the parsimony ratchet (Nixon, 1999) increased the number of hits to 100% (using 1000 reps and holding 1000 trees during each replication), and resulted in the same three trees of length 871. The three trees are fully resolved and differ only in the position of

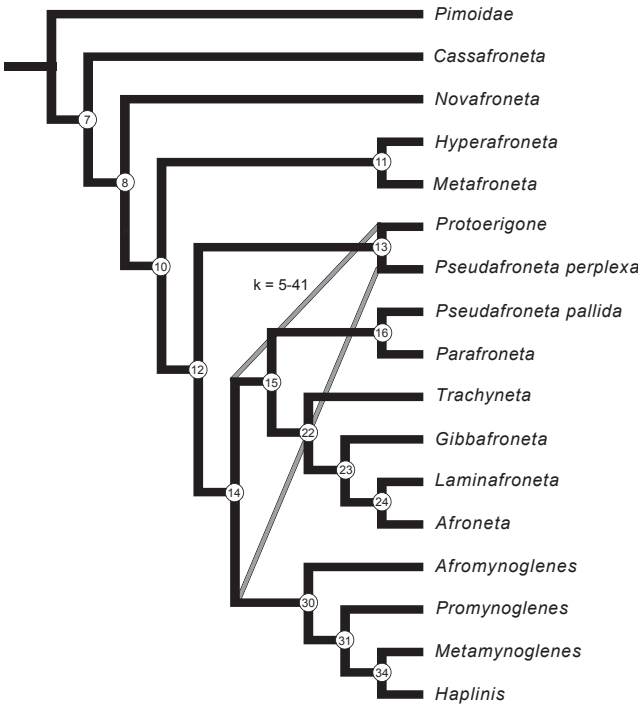

Fig. 5. Summary of the generic interrelationships independent of the weighting scheme above $k = 5$. The basic tree shows the topology found with implied weights of $k = 42$ and above (including equal weights). Differences found with k values of 5–41 are marked with shorter grey branches. Differences found with k values of 1–4 and differences within genera have been omitted. Node numbers in circles correspond to the preferred equally weighted tree.

Haplinis abbreviata within the monophyletic genus *Haplinis*. The equally weighted analysis supports the monophyly of the subfamily Mynogleninae and the genera *Novafroneta*, *Promynoglenes*, *Metamynoglenes*, *Parafroneta*, *Laminafroneta*, *Haplinis*, and *Afroneta*. The genus *Pseudafroneta* is paraphyletic. The remaining genera are either monotypic (*Cassafroneta*, *Hyperafroneta*, *Gibbafroneta*, *Afromynoglenes*) or not represented in this analysis with more than one species (*Metafroneta*, *Protoerigone*, *Trachyneta*). One of the three trees was also found with implied weighting using k values of 42 and above. This is our preferred tree (Figs 2–4) on which characters have been mapped.

Implied weights. Heuristic searches in TNT resulted in one tree regardless of the k value used, but the tree topology varied with k values. At $k = 42$ and above, implied weights analysis resulted in a tree equal to one of the three trees found with equal weights (Figs 2–4, preferred tree). The other trees found using equal weights were not discovered in any of the implied weights analyses.

Regardless of the weighting scheme used (Fig. 5; k values <5 omitted), the overall genus-level topology recovered was essentially the same. Only k values of 1–4 led to different topologies. With $k = 2$–4 (strong weights), *Australolinyphia* is sister to all mynoglenines. The early lineages within mynoglenines are (*Trachyneta* (*Afroneta* (*Gibbafroneta*))). *Gibbafroneta* is sister to a clade including two large sister clades: (*Novafroneta* (*Laminafroneta* (*Cassafroneta* (*Hyperafroneta*, *Metafroneta*)))) and (*Parafroneta* (*Pseudafroneta pallida* (*Protoerigone* (*Pseudafroneta perplexa* (*Afromynoglenes* (*Promynoglenes* (*Metamynoglenes*, *Haplinis*))))))). At species level, different k values generate different interrelationships within genera, especially within *Haplinis* and *Parafroneta*.

Support and optimization. The support values are given on the strict consensus of the equally weighted topologies (Fig. 1). The average Bremer support is 3.1 for the ingroups and 3.3 for all scored taxa. The relatively high average Bremer support might be related to the high number of characters in this matrix (over four times as many characters as species). Jackknife support values are given if higher than 50% (Fig. 1). Lower values correspond to nodes with Bremer values of 2 and below.

Most clades are supported by at least one unreversed synapomorphy. Within clade 15, only terminal nodes 25 and 29 are well supported; the other nodes are supported by homoplasious character-state changes only (Fig. 3). The (unaltered) synapomorphies supporting the genera are discussed in Appendix 5.

Distribution pattern

Based on the available distributional data, mynoglenines are restricted to tropical Africa, New Zealand, and Tasmania (Fig. 7). They have also been recorded on the Fiji islands (G. Hormiga, unpublished data). The distribution in Africa covers Cameroon in West Africa and Central East Africa from Ethiopia in the north to Malawi in the south. They also occur on the island of La Réunion east of Africa. Most records are from the Democratic Republic of Congo followed by Ethiopia and Kenya. The African findings are restricted to mountains at higher altitudes, the lowest for which elevational data are available is 1700 m a.s.l. in the highlands of the Sidamo province, Ethiopia, to the highest at 3800 m a.s.l. on Mount Ruwenzori in the Democratic Republic of Congo. Most records are from 2000 to 3200 m a.s.l. The single species known from La Réunion, *Afroneta longipalpis*, occurs above 800 m a.s.l.

Afromynoglenes is endemic to the Ethiopian highlands and *Gibbafroneta* to the volcanoes at the border between the Democratic Republic of Congo and Rwanda. *Afroneta* and *Laminafroneta* are more widespread. *Afroneta* is

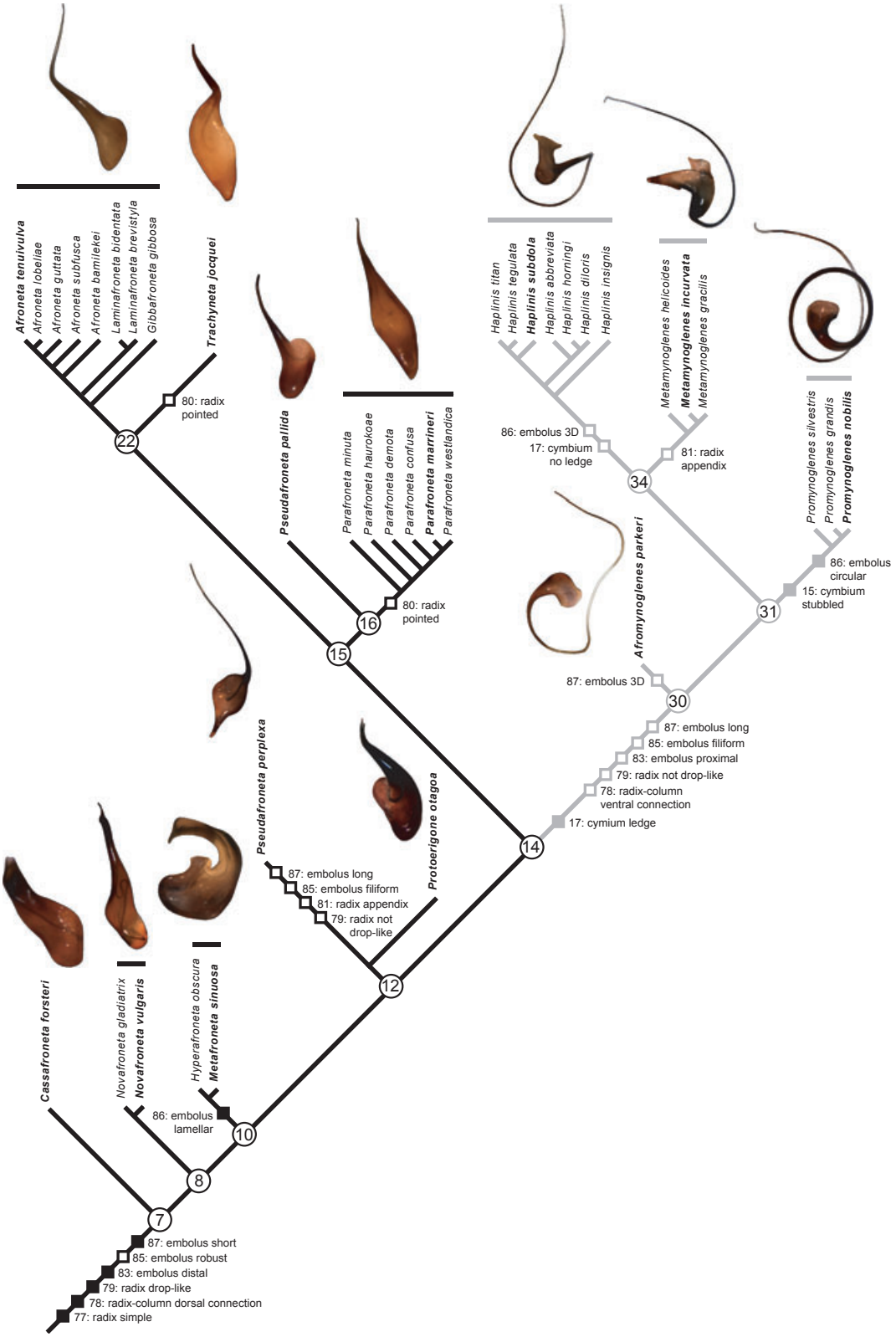

Fig. 6. Preferred tree including illustrations of the embolic division. The pictures show the radical sclerite in ventral to prolateral view (sizes not relative) of the species marked in bold. Branch colours correspond to simple (clades 1–29, black) and more complex embolic divisions in terms of additional appendices and longer emboli (clades 30–42, grey). Boxes on branches show selected characters (filled) and their modifications (unfilled).

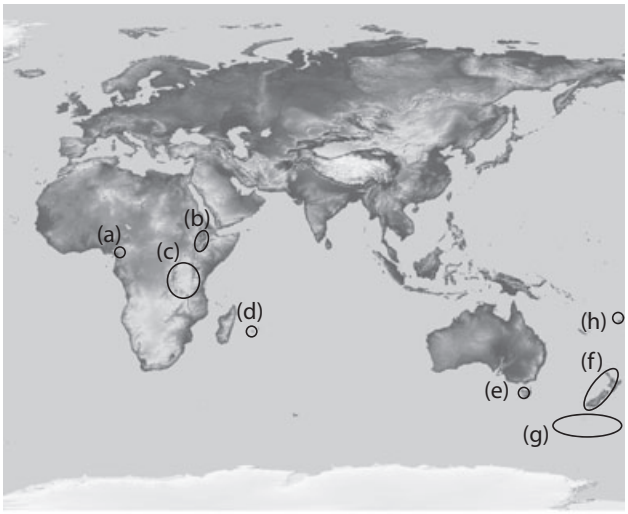

Fig. 7. Worldwide distribution of mynoglenines including genus and species numbers (genus/species). (a) Cameroon: 2/2; (b) Ethiopia: 2/5; (c) Central East Africa: 4/26; (d) La Réunion: 1/1; (e) Tasmania: 1/1; (f) New Zealand: 12/77; (g) South Pacific islands including Chatham Island: 6/15; (h) Fiji: unknown number of species.

known from Cameroon, Ethiopia, Democratic Republic of Congo, Tanzania, Uganda, and La Réunion; *Laminafroneta* from Ethiopia, Kenya, Tanzania, Burundi, and Rwanda. *Trachyneta* is found in the Democratic Republic of Congo and Malawi.

The fauna of Oceania is more diverse. One species, *Haplinis australis*, is endemic to Tasmania (Australia); several species of the genus *Haplinis* and *Parafroneta* are found on six South Pacific islands (not counting Stewart Island) belonging to New Zealand. Most species, however, are found on the two largest islands of New Zealand (North and South Islands) and Stewart Island, and can be found from the coastline to the alpine areas covering altitudinal ranges from sea level to 4500 m a.s.l. on Mount Egmont. *Cassafroneta* is endemic to the North Island; *Hyperafroneta*, *Megafroneta*, *Metafroneta*, *Protoerigone*, and *Poecilafroneta* are endemic to the South Island. *Haplinis*, *Promynoglenes*, *Metamynoglenes*, *Novafroneta* (also on Chatham Island), *Parafroneta*, and *Pseudafroneta* are more widespread, occurring on both North and South Island of New Zealand and beyond. Mynoglenines are also known from Fiji (G. Hormiga, unpublished data), but their identity is unknown.

Discussion

Morphological changes of the embolic division

The evolution of the complex linyphiid copulatory organs has been the object of several studies and includes both descriptive and analytical work

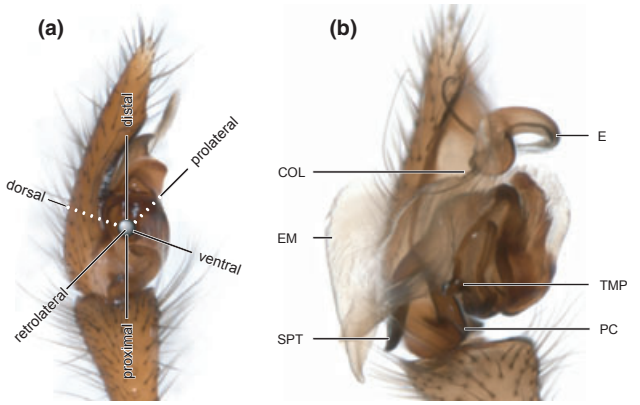

Fig. 8. Directions used in character descriptions showing the male palp of *Pseudafroneta perplexa* in retrolateral view (a). Expanded palp of *Haplinis diloris*, in retrolateral view (b).

(Merrett, 1963; Millidge, 1977, 1984; Hormiga, 1994b, 2000). Merrett (1963) divided linyphiid copulatory organs into "simple" and "complex" types, but as pointed out by Hormiga (2000), it does not make sense to talk about complex and simple copulatory organs as they consist of a number of homologous morphological structures, each of which may be more or less complex. Comparisons should be restricted to specific sclerites/structures. Here we focus on the male palp of mynoglenines. Like all other linyphiids, it consists of cymbium, paracymbium, subtegulum, tegulum, suprategulum, and an embolic division. The latter is connected to the tegulum via a membraneous column, and the tegular insertion of the column on mynoglenines is unusual within linyphiids, where the column normally inserts on the suprategulum. An embolic membrane inserts broadly on the column and the tegulum of mynoglenines (Blest, 1979: fig. 366). In other linyphiids, the embolic membrane inserts on the column or the suprategulum. The embolic division of mynoglenines consist of only two parts, the radix and the embolus.

Within mynoglenines, the early lineages of the tree (Fig. 6, clades 7–9; clade 9 not shown in Fig. 6) contain taxa that have rather similar unmodified genitalia, and no major changes to the male genitalia can be detected in clade 15. Most morphological changes emerge in clade 30. Here we see changes in the morphology of the paracymbium, the tegular mynoglenine process, the embolic membrane, and the embolic division. A similar trend is also seen in the female copulatory organs within clade 30. Here we restrict our discussion to the most striking example, the embolic division of the male palp (Fig. 6) and the embolic membrane.

Early lineages. The first branch within the monophyletic Mynogleninae contains the monotypic

genus *Cassafroneta*. Like all other mynoglenines, *Cassafroneta* has a simple and relatively small radix compared with other linyphiids (ch77, Fig. 6). It is connected dorsally to the tegulum (ch78, see also *Novafroneta*, Fig. 13a) without the column being twisted (Fig. 12b). The dorsal connection of the column can be seen in all mynoglenines except clade 30 (Fig. 6). The embolus of *Cassafroneta* is straight to curved and emerges from the distal part of the radix (Blest, 1979: fig. 584). This radix, shaped like a teardrop (ch79), is present in all mynoglenines except *Pseudafroneta perplexa* and clade 30 (Fig. 6). This type of radix is also found in *Novafroneta*.

The embolic division deviates in *Hyperafroneta* and *Metafroneta*, where the embolus is semicircularly elongated and lamellar (ch86; Fig. 12c,e) instead of straight. In *Hyperafroneta* an additional apophysis emerges from the embolus (Fig. 12c). The teardrop-like form of the radix with the straight to curved embolus is retained in all taxa (except *Pseudafroneta perplexa*) outside clade 30 and there are no additional apophyses emerging from the radix.

Protoerigone and *Pseudafroneta perplexa* occupy a special position in the cladogram. They emerge as sister to two large clades including taxa with the least modified embolic divisions (clade 15) and the most modified embolic divisions (clade 30; Fig. 2b). Their emboli are somewhat intermediate between those found in clades 15 and 30.

Protoerigone and clade 15. The embolic division of *Protoerigone* resembles that of the earliest mynoglenine lineages and that seen in clade 15, a short curved embolus and an unmodified radix. The radix of the species in clade 15 has a simple teardrop-like radix with a straight to curved short distal pointing embolus (Fig. 6) and lacking any other appendices. The only slight change can be found in *Parafroneta* and in *Trachyneta*, where the proximal side of the radix (opposing the embolus) is pointed rather than round (ch80). This structure is potentially homologous to the retrolateral radical appendix of *Pseudafroneta perplexa* and *Metamynoglenes* (ch81, Fig. 12f: RRA) and even to the radical tailpiece in erigonines. However, if homologous, it would have evolved independently four times within mynoglenines. Clade 15 includes *Pseudafroneta pallida* and *Parafroneta* (clade 16) from New Zealand and some South Pacific islands. They are sister to clade 22 including four genera endemic to Central Africa (Fig. 1).

Pseudafroneta perplexa and clade 30. A modification towards a more complex morphology of the embolic division is found in *Pseudafroneta perplexa* and becomes more distinct in clade 30. The embolus of *P. perplexa* is filiform (ch85, Fig. 6) and elongated but still two-dimensional (ch86, Fig. 6). The embolus of all species outside clade 30 emerges distally from the radix (ch83, Fig. 6). Instead, the embolic division of *P. perplexa* appears to be slightly twisted prolaterally. Moreover, the proximal side of the radix is elongated and forms an appendix-like apophysis (Fig. 6). Due to a more distinct prolateral turn (ca. 90°) of the radix, this structure is called the "retrolateral appendix" and is found only in *P. perplexa* and in *Metamynoglenes* (ch81, Figs 6 and 12f: RRA).

These modifications of the embolic division become more distinct in clade 30. The radix of *Afromynoglenes* is turned in a clockwise direction by more than 180° and the length of the embolus increased correspondingly (Merrett and Russell-Smith, 1996: fig. 16). Furthermore, the connection to the tegulum changes from a dorsal attachment to a ventral one (ch78, synapomorphy of clade 30, Fig. 2b).

The embolic division of *Promynoglenes* develops further. The 180° twist of the column may be at the upper physical limit of possible rotations in mynoglenines. In order to elongate the embolus further, the embolus starts to encircle the radix, first by only slightly more than one turn in *P. silvestris* (Blest, 1979: fig. 472) to nearly two turns in *P. nobilis* (Fig. 6; Blest, 1979: fig. 466). Presumably to avoid the embolus getting entangled in the cymbial setae, the cymbium of *Promynoglenes* is flattened ventrally at its prolateral side and carries only short bristles (ch15, Fig. 11d).

The next change within clade 30 occurs at clade 34, where *Metamynoglenes* branches off as sister to *Haplinis* (Fig. 1). This node is not well supported (BS: 2, JK: <50%). The embolic division of *Metamynoglenes* (Fig. 11c) resembles that of *Pseudafroneta perplexa* (Blest, 1979: fig. 598) and in particular that of *Afromynoglenes* (Merrett and Russell-Smith, 1996: fig. 16). The embolus of *Metamynoglenes* (e.g. Fig. 11c) is not circular as in *Promynoglenes* and *Haplinis* (Fig. 11a,d). The embolus of *Metamynoglenes gracilis* (Fig. 11c) in particular is very similar to *Pseudafroneta perplexa* (Blest, 1979: fig. 598). The radix is turned prolaterally by 90° and the embolus is of about equal length. In the other scored taxa of *Metamynoglenes*, the embolus is longer and more curved and the radix may be twisted up to 180°. This is very similar to what is seen in *Afromynoglenes* (Fig. 6). Like *Pseudafroneta perplexa* (Fig. 6), *Metamynoglenes* also has a retrolateral appendix emerging from the radix. However, the preferred cladogram leads to the conclusion that the common ancestor of node 31 had an embolic division similar to *Afromynoglenes* and *P. perplexa*. From this common ancestor, *Promynoglenes* and *Metamynoglenes* both developed longer emboli but solved the problem in different ways: *Promynoglenes* by rolling up the embolus; *Metamynoglenes* by continuing a development similar to that seen in *Afromynoglenes* (Fig. 6).

Metamynoglenes also has a modified proximal section of the prolateral side of the cymbium to avoid the long embolus becoming entangled in the cymbial setae (ch16, Fig. 11c: CPD). Here the cymbium is also slightly flattened ventrally and the setae are restricted to a hirsute area at its most proximal tip (ch16, Fig. 11c: CPD). To keep the embolus in place, *Afromynoglenes*, *Promynoglenes*, and *Metamynoglenes* developed a ledge at the proximal margin of the prolateral side of the cymbium (ch17, Fig. 12f: CPL). This ledge has been enlarged to a sclerotized apophysis in *Promynoglenes* and *Metamynoglenes helicoides* (ch18, Fig. 11d) but is entirely reduced in *Haplinis* (Fig. 11b).

The embolic division of *Haplinis* is also more or less twisted depending on the species (Fig. 11a,b). The embolus is of the same type as in *Metamynoglenes* but elongated further. Instead of rolling up the embolus, it is curved in one more dimensions towards the prolateral side (ch86, Fig. 11a). This led to the same risk of the embolus becoming entangled in the cymbial setae, and to avoid this some species of *Haplinis* (and *Metamynoglenes helicoides*) have developed a glabrous area at the proximal side of the cymbium (ch14, Fig. 11a: CPG).

Morphological changes of the embolic membrane

The shape and size of the embolic membrane correlates with the elongation of the embolus in mynoglenines. In the early lineages of the mynoglenine tree, we find taxa with relatively short emboli that are protected by short, membraneous embolic membranes. This is found in *Cassafroneta* (Blest, 1979: fig. 584), *Novafroneta* (slightly longer and narrower embolic membrane, Fig. 13a: EM), *Metafroneta* (Fig. 12a: EM), *Protoerigone*, and most taxa of clade 15, i.e. *Parafroneta*, *Afroneta* and *Gibbafroneta* (e.g. Fig. 13b: EM). However, in some cases the short embolic membrane is fully and strongly sclerotized. The strongly sclerotized embolic membrane (ch67) evolved four times independently within mynoglenines, in *Hyperafroneta* (Fig. 12c: EM), *Trachyneta*, *Laminafroneta*, and *Pseudafroneta pallida* (all outside clade 30).

However, in *Pseudafroneta perplexa* and especially in clade 30 the embolus becomes elongated, which correlates with an enlarged embolic membrane. For example, the embolic membrane of *Pseudafroneta perplexa* has an ectal outward fold (ch72; Blest, 1979: fig. 598) that is more distinct in clade 30. The size of the ectal outwards fold increases in size within clade 30. It is relatively small and narrow in *Afromynoglenes*, *Promynoglenes*, and *Metamynoglenes* (Fig. 13c: EME) and becomes distinctly larger in *Haplinis* (ch72, Fig. 12b: EME). All taxa within clade 30 have a highly enlarged embolic membrane that encloses the embolus laterally and ventrally (ch70, e.g. Fig. 12b: EM).

Distribution and diversity patterns

Gondwana origin and recent distribution. A Gondwana origin of Mynogleninae has been proposed by several authors (Blest, 1979; Merrett and Russell-Smith, 1996; Merrett, 2004; Ledoux and Attié, 2008). However, the current distribution pattern (Fig. 7) of the subfamily with the majority of species in New Zealand and tropical Africa, and their total absence from South America, southern Africa, and most of Australia, does not fit the traditional Gondwana distribution patterns. The lack of mynoglenines in the southern parts of South America, Africa, and most of Australia is considered real, and not an undersampling issue, as these areas have been sampled quite extensively over the past 30 years. This includes general sampling as well as sampling of leaf litter that has revealed other Gondwana suspects, such as representatives of Orsolobidae (South America, South Africa, Australia), Synotaxidae (South America, South Africa, Australia), and Malkaridae (South America and Australia), but no mynoglenines. Furthermore, modern revisionary work on South American linyphiids (Millidge, 1985, 1991; Miller, 2007) has not revealed mynoglenines in museum collections. Usher (1983) described *Falklandoglenes* and *Beauchenia* from the Falkland Islands and assigned them to Mynogleninae based on the overall similarity of the male and female genital organs, despite the lack of subocular sulci. Based on different lines of evidence, including genitalia and the lack of subocular sulci, Millidge (1985) rejected the placement of *Falklandoglenes* in the Mynogleninae and suggested a closer relationship to Linyphiinae. Miller (2007) synonymized *Beauchenia* with the erigonine genus *Notioscopus* Banks, 1914. In other parts of the world, mynoglenines have been searched for in Madagascar, where the California Academy of Sciences has carried out extensive spider surveys over the past 15 years; and in Sri Lanka, where David Blest (unpublished data) has searched appropriate habitats without finding mynoglenines. Given this, we find it highly unlikely that mynoglenines should turn up in South America or Southern Africa, even though the lack of collected specimens is not the same as proof of absence. In Australia, one species of mynoglenines (*Haplinis australis*) is known from Tasmania, but mynoglenines are not known from mainland Australia. No mynoglenines are known from New Guinea and New Caledonia, areas that are otherwise known to harbour old remnants of Gondwana flora and fauna, but very little fieldwork focusing on linyphiids has been carried out in these areas. However, there are records of mynoglenines from the geographically close Fiji

islands (G. Hormiga, unpublished data). We can conclude that the current distribution of Mynogleninae, with its centres of distribution in tropical Africa and New Zealand, does not point directly to an old Gondwana connection for Mynogleninae.

Based on the distribution patterns mentioned above, Millidge (1991) suggested a Gondwana origin for Mynogleninae, and more specifically suggested that mynoglenines would have been "restricted to the northern and eastern fringes of Gondwanaland". If correct, this would suggest that mynoglenines were much more widespread until 130 Ma ago when Gondwana started to break up (Gibbs, 2006).

Climatic data suggest that Antarctica was ice-free at that time and was populated with cool to temperate forests (Gibbs, 2006). This coincides with the present environmental preference of the subfamily in Africa, where mynoglenines are restricted to higher elevations such as mountaintops in tropical Africa and the highlands of Ethiopia (between 1700 and 3800 m a.s.l.). Presumably, the African mynoglenines did not adapt to warmer climates when Africa moved north after breaking off from Gondwana at around 170 Ma ago. Therefore the mountaintops would represent climatic relict distributions. This would not, however, explain why there are no mynoglenines on the high mountains of South Africa, where climate and vegetation seems favourable. However, besides the highland of Ethiopia which began to rise about 75 Ma ago (Kingdon, 1989), most African mynoglenines are found on relatively young volcanoes such as Mount Cameroon (Bosmans, 1988), Mount Kenya (unpublished records of R. Bosmans from the Belgian Mount Kenya expedition 1975, stored at MRAC) and Mount Kilimanjaro (Holm, 1968). Interestingly, mynoglenines have not been found on the old mountain ranges of Eastern Arc, although they are high enough and neighbours to Mount Kilimanjaro and Mount Kenya. This suggests that until the rise of these young volcanoes some million years ago, mynoglenines must have had other refuges, or perhaps been more widespread or adapted to a wider range of climatic conditions.

A second possibility is that Africa has been colonized by mynoglenines much later. The preferred phylogeny (Fig. 1) suggests a New Zealand origin for Mynogleninae, and two later dispersals to Africa: once for clade 22 (*Trachyneta*, *Gibbafroneta*, *Laminafroneta*, and *Afroneta*) and once again for *Afromynoglenes*.

Unfortunately, we cannot provide divergence estimates for morphology-based phylogenies, but the relationships and the branching patterns of the various taxa can be determined and compared with dated phylogenies. Dimitrov et al. (2012) recently published a dated molecular phylogeny of all orb weavers including a large selection of linyphiids, including mynoglenines. The chronogram of Dimitrov et al. (2012: fig. 2) has a monophyletic Mynogleninae, including the genera *Haplinis*, *Pseudafroneta*, and *Novafroneta*, sister to *Australolinyphia*. The estimated age for the mynoglenine clade is 8–20 Ma and the estimated age for the clade including the sister-group *Australolinyphia* is 48–80 Ma (D. Dimitrov, unpublished data).

It is generally agreed that New Zealand separated from Australia when the Tasman sea opened some 80 Ma ago (Waters and Craw, 2006) and that New Zealand has been isolated from other major land masses for at least 60 Ma (Gibbs, 2006). Separation from Africa came much earlier, ca. 160 Ma ago, so if the current occurrence of mynoglenines in Africa is the result of an old Gondwana vicariance event, mynoglenines should be at least 160 Ma old. Unfortunately, Dimitrov et al. (2012) did not include any African mynoglenines, but the clade including mynoglenines and its sister-group *Australolinyphia* (currently only known from Australia) are much younger (48–80 Ma) and therefore suggest that Mynoglenines evolved around the time when New Zealand separated from Australia (ca. 80 Ma ago) and perhaps as a result of this event. Given the preferred phylogeny (Fig. 1), this would suggest that the African mynoglenines are the result of two dispersal events and that the African mynoglenines cannot be older than ca. 80 Ma.

Although dispersal over such long distances seem unlikely, we know that many linyphiids use aerial dispersal (ballooning; Greenstone et al., 1987) to move into new areas, and Forster and Forster (1999, p. 36) observed ballooning juveniles of mynoglenines on New Zealand. Aerial dispersal also seems the most likely explanation for mynoglenines on the South Pacific Islands.

Oligocene drowning of New Zealand (26–38 Ma) has been proposed (Waters and Craw, 2006; Knapp et al., 2007; see review in Gibbs, 2006) but recent molecular phylogenetic studies of the New Zealand fauna and flora provide divergence data (molecular dating) that suggest pre-Oligocene presence of certain lineages of plants and animals (Knapp et al., 2007) and thus that New Zealand was not completely submerged during Oligocene. A "surviving" land area of 18% has been suggested (Cooper and Millene, 1993), but the issue of an Oligocene complete drowning of New Zealand is still much debated (Boyer and Giribet, 2009). If New Zealand has been totally submerged during the Oligocene, this suggests that all of its fauna and flora must have arrived through dispersal after the reappearance of land, and that many groups of organisms should show repeated sister-group relationships with taxa on nearby land areas such as Australia (Boyer and Giribet, 2009), demarcating repeated dispersals to New Zealand. How does the Oligocene drowning theory fit with our knowledge of mynoglenine phylogeny and clade ages?

The preferred phylogeny presented in Fig. 1 supports a monophyletic Mynogleninae and thus a single origin caused by vicariance or dispersal. All 12 genera and 90 species (except one species of *Haplinis*) known from New Zealand are also endemic to New Zealand. *Haplinis australis* is endemic to Tasmania and is the only know Australian mynoglenine. The high degree of endemism among species and genera suggests old age, but without a molecular dated phylogeny we cannot determine the age of the early mynoglenine clades. Dimitrov (unpublished data) estimate a minimum age of 140–174 Ma for Linyphiidae (which corresponds to the dating of the earliest linyphiid fossils in Penney and Selden, 2002) and 48–80 Ma for the clade containing *Australolinyphia* and its sister-group, including Mynogleninae. The only age estimations we have for clades within mynoglenines is an estimate of 8–20 Ma for a clade including the genera (*Haplinis* (*Novafroneta*, *Pseudafroneta*)). On the preferred tree, *Novafroneta* represents an early lineage whereas *Haplinis* represents a relatively recent lineage. Given the preferred tree, and the age estimates at hand, one could argue that mynoglenines represent a single post-drowning (post-Oligocene) dispersal and subsequent radiation in New Zealand.

If true, mynoglenines can be considered phantoms of Gondwana, but before we completely disregard the old Gondwana connections it would be good to test the two hypotheses, dispersal and vicariance, through the generation of a larger and more comprehensive molecular dataset with more mynoglenine genera represented.

Acknowledgements

For the kind loan of specimens (and/or collection data) we are very grateful to the following individuals and institutions: Phil Sirvid (Wellington, NZ; MoNZ), Rudy Jocqué (Tervuren, BE; MRAC), Hans Mejlon (Uppsala, SE; ZIUU), Janet Beccaloni (London, GB; BMNH), Cor Vink and Jagoba Malumbres-Olarte (Canterbury, NZ; LUNZ), Julia Altmann (Frankfurt, DE; Senckenberg Museum, SMF), and Christian Kropf (Bern, CH; Naturhistorisches Museum, NMBE). David Blest (Canberra, AU), Cody Fraser (Otago, NZ), Seppo Kopponen and Pekka Lehtinen (Turku, FI) kindly helped with data and information on collected material. We would like to thank Rudy Jocqué (Tervuren, BE) for translations, Dimitar Dimitrov, Efrat Gavish-Regev, Thomas Pape (all Copenhagen, DK) for fruitful discussions, and Ole Karsholt, Jan Pedersen, and Dimitar Dimitrov (all Copenhagen, DK) for their helping hands solving various problems. We are also most grateful to Gustavo Hormiga (Washington, US), and one anonymous reviewer for their efforts to improve the manuscript and the editors James M. Carpenter, Lorenzo Prendini, Ian Kitching and Reidin Vaughan for their editorial work.

N.S. acknowledges the Danish National Research Foundation for support to the Center for Macroecology, Evolution and Climate. Funding for this research was also provided by grants from the Danish Agency for Science, Technology and Innovation (project 272-08-0480) and the Carlsberg Foundation (project 2010-01-0186) to N.S.

H.F. acknowledges the Swiss National Science Foundation for the fellowship grant for prospective researchers (grant PBBEP3_130176).

We dedicate this paper to the memory of Dr A.D. Blest (1931–2012) (Canberra, Australia), whose extensive work on mynoglenines and generous help inspired us and made our own work possible.

References

Arnedo, M. A., Hormiga, G., Scharff, N., 2009. Higher-level phylogenetics of linyphiid spiders (Araneae, Linyphiidae) based on morphological and molecular evidence. Cladistics 25, 231–262.

Berland, L., 1925. Spiders of the Chatham Islands. Rec. Canterbury Mus. 2, 295–300.

Berland, L., 1931. Araignées des Iles Auckland et Campbell. Rec. Canterbury Mus. 3, 357–365.

Berland, L., 1942. Polynesian Spiders. Occ. Pap. Bernice P. Bishop Mus. Honolulu, Hawaii 17, 1–24.

Blackledge, T., Scharff, N., Coddington, J. A., Szüts, T., Wenzel, J. W., Hayashi, C. Y., Agnarsson, I., 2009. Reconstructing web evolution and spider diversification in the molecular era. Proc. Natl Acad. Sci. USA 106, 5229–5234.

Blest, A. D., 1979. The spiders of New Zealand. Part V. Linyphiidae-Mynogleninae. Otago Mus. Bull. 5, 95–173.

Blest, A. D., 2004. New Zealand spiders: the implications of current information concerning Stiphidiidae and Linyphiidae for biodiversity studies. Canterbury Mus. Bull. 10, 1–14.

Blest, A. D., Pomeroy, G., 1978. The sexual behaviour and genital mechanics of three species of *Mynoglenes* (Araneae: Linyphiidae). J. Zool. Lond. 185, 319–340.

Blest, A. D., Vink, C. J., 2002. New Zealand spiders: Linyphiidae, Mynogleninae. Rec. Canterbury Mus. 16 (Suppl.), 1–31.

Blest, A. D., Vink, C. J., 2003. New Zealand spiders: Linyphiidae, Mynogleninae, Linyphiinae Rec. Canterbury Mus. 17 (Suppl.), 1–30.

Bosmans, R., 1988. Scientific report of the Belgian Cameroon expeditions 1981 and 1983. No. 18. Further Erigoninae and Mynogleninae (Araneae: Linyphiidae) from Cameroonian highlands. Revue Zool. Afr. 102, 5–32.

Boyer, S. L., Giribet, G., 2009. Welcome back New Zealand: regional biogeography and Gondwanan origin of three endemic genera of mite harvestmen (Arachnida, Opiliones, Cyphophthalmi). J. Biogeog. 36, 1084–1099.

Bremer, K., 1988. The limits of amino acid sequence data in angiosperm phylogenetic reconstruction. Evolution 42, 795–803.

Bremer, K., 1994. Branch support and tree stability. Cladistics 10, 295–304.

Bryant, E. B., 1935. Some new and little known species of New Zealand spiders. Rec. Canterbury Mus. 4, 71–94.

Coddington, J., Scharff, N., 1994. Problems with zero-length branches. Cladistics 10, 415–423.

Cooper, R. A., Millener, P. R., 1993. The New Zealand biota: historical background and new research. Trends Ecol. Evol. 8, 429–433.
Dimitrov, D., Lopardo, L., Giribet, G., Arnedo, M. A., Alvarez-Padilla, F., Hormiga, G., 2012. Tangled in a sparse spider web: single origin of orb weavers and their spinning work unravelled by denser taxonomic sampling. Proc. R. Soc. Lond. B 279, 1341–1350.
Farris, J. S., Albert, V. A., Källersjö, M., Lipscomb, D., Kluge, A. G., 1996. Parsimony jackknifing outperforms neighbor-joining. Cladistics 12, 99–124.
Fitch, W. M., 1971. Toward defining course of evolution—minimum change for a specific tree topology. System. Zool. 20, 406–416.
Forster, R., Forster, L., 1999. Spiders of New Zealand and their Worldwide Kin. University of Otago Press, Dunedin, NZ.
Frick, H., Nentwig, W., Kropf, C., 2010. Progress in erigonine spider phylogeny—the *Savignia*-group is not monophyletic (Araneae: Linyphiidae). Org. Divers. Evol. 10, 297–310.
Gibbs, G., 2006. Ghosts of Gondwana—The history of life in New Zealand. Craig Potton Publishing, Nelson, NZ.
Goloboff, P. A., 1993. Estimating character weights during tree search. Cladistics 9, 83–91.
Goloboff, P. A., Farris, J. S., Nixon, K. C., 2008. TNT, a free program for phylogenetic analysis. Cladistics 24, 774–786.
Greenstone, M. H., Morgan, C. E., Hultsch, A. L., Farrow, R. A., Dowse, J. E., 1987. Ballooning spiders in Missouri, USA, and New South Wales, Australia: family and mass distributions. J. Arachnol. 15, 163–170.
Helsdingen, P. J. v., Thaler, K., Deltshev, C., 2001. The European species of *Bolyphantes* with an attempt of a phylogenetic analysis (Araneae Linyphiidae). Mem. Soc. Entomol. Ital. 80, 3–35.
Hickman, V. V. 1939. Opiliones and Araneae. B.A. New Zealand Antarctic Research Expedition 1929–1931. Reports—Series B. Adelaide, pp. 157–188.
Hogg, H. R., 1911. On some New Zealand spiders. Proc. Zool. Soc. Lond. 1911, 297–313.
Holm, Å., 1968. Spiders of the families Erigonidae and Linyphiidae from East and Central Africa. Ann. Mus. R. Afr. Cent. 171, 1–49.
Holm, Å., 1979. A taxonomic study of European and East-African species of the genera *Pelecopsis* and *Trichopterna* (Araneae, Linyphiidae), with descriptions of a new genus and two new species of *Pelecopsis* from Kenya. Zool. Scr. 8, 255–278.
Hormiga, G., 1993. Implications of the phylogeny of Pimoidae for the systematics of linyphiid spiders (Araneae, Araneoidea, Linyphiidae). Mem. Queensland Mus. 33, 533–542.
Hormiga, G., 1994a. A revision and cladistic analysis of the spider family Pimoidae (Araneoidea: Araneae). Smithson. Contrib. Zool. 549, 1–104.
Hormiga, G., 1994b. Cladistics and the comparative morphology of linyphiid spiders and their relatives (Araneae, Araneoidea, Linyphiidae). Zool. J. Linn. Soc. 111, 1–71.
Hormiga, G., 2000. Higher level phylogenetics of ergonine spiders (Araneae, Linyphiidae, Erigoninae). Smithson. Contrib. Zool. 609, 1–160.
Kingdon, J., 1989. Island Africa—The Evolution of Africa's Rare Animals and Plants. Princeton University Press, Princeton, NJ.
Knapp, M., Mudaliar, R., Havell, D., Wagstaff, S. J., Lockhart, P.J., 2007. The drowning of New Zealand and the problem of *Agathis*. Syst. Biol. 56, 862–870.
Ledoux, J.-C., Attié, M., 2008. Un nouveau Mynogleninae de l'île de La Réunion et sa signification biogéographique (Araneae, Linyphiidae). Revue Arachnol. 17, 35–42.
Ledoux, J.-C., Hallé, N., 1995. Araignées de l'île Rapa (îles Australes, Polynésie). Revue Arachnol. 11, 1–15.
Lehtinen, P. T., 1967. Classification of the cribellate spiders and some allied families, with notes on the evolution of the suborder Araneomorpha. Ann. Zool. Fenn. 4, 199–468.
Maddison, W. P., Maddison, D. R. 2010. Mesquite: A Modular System for Evolutionary Analysis version 2.74. Available from http://mesquiteproject.org.
Merrett, P. 1963. The palpus of male spiders of the family Linyphiidae. Proc. Zool. Soc. London 40, 347–467.
Merrett, P., 2004. A revision of African mynoglenines (Araneae: Linyphiidae: Mynogleninae). Bull. Br. Arachnol. Soc. 13, 1–30.
Merrett, P., Russell-Smith, A., 1996. New mynoglenine spiders from Ethiopia (Araneae: Linyphiidae: Mynogleninae). Bull. Br. Arachnol. Soc. 10, 218–224.
Miller, J. A., 2007. Review of erigonine spider genera in the Neotropics (Araneae: Linyphiidae, Erigoninae). Zool. J. Linn. Soc. 149, 1–272.
Miller, J. A., Hormiga, G., 2004. Clade stability and the addition of data: a case study from erigonine spiders (Araneae: Linyphiidae, Erigoninae). Cladistics 20, 385–442.
Millidge, A. F., 1977. The conformation of the male palpal organs of linyphiid spiders, and its application to the taxonomic and phylogenetic analysis of the family (Araneae: Linyphiidae). Bull. Br. Arachnol. Soc. 4, 1–60.
Millidge, A. F., 1984. The taxonomy of the Linyphiidae, based chiefly on the epigynal and tracheal characters (Araneae: Linyphiidae). Bull. Br. Arachnol. Soc. 6, 229–267.
Millidge, A. F., 1985. Some Linyphiid spiders from South America (Araneae, Linyphiidae). Am. Mus. Novit. 2836, 1–78.
Millidge, A. F., 1991. Further Linyphiid spiders (Araneae) from South America. Bull. Am. Mus. Nat. Hist. 205, 1–204.
Millidge, A. F., 1993. Further remarks on the taxonomy and relationships of the Linyphiidae, based on the epigynal duct conformations and other characters (Araneae). Bull. Br. Arachnol. Soc. 9, 145–156.
Nixon, K. C., 1999. The parsimony ratchet, a new method for rapid parsimony analysis. Cladistics 15, 407–414.
Nixon, K. 2002. WinClada version 1.00.08. Published by the author, Ithaca, NY. Available from http://www.cladistics.com.
Ojanguren-Affilastro, A. A., Ramirez, M. J., 2009. Phylogenetic analysis of the scorpion genus *Brachistosternus* (Arachnida, Scorpiones, Bothriuridae). Zool. Scr. 38, 183–198.
Penney, D., Selden, P. A., 2002. The oldest linyphiid spider, in lower cretacious Lebanese amber (Araneae, Linyphiidae, Linyphiinae). J. Arachnol. 30, 487–493.
Platnick, N. I. 2013. The World Spider Catalog, version 13.5. Am. Mus. Nat. Hist., online at http://research.amnh.org/iz/spiders/catalog. doi: 10.5531/db.iz.0001.
Pole, M., 1994. The New Zealand flora—entirely long-distance dispersal? J. Biogeog. 21, 625–635.
Rainbow, W. J., 1917. Arachnida from Macquarie Island. In Australasian Antarctic expedition 1911–1914. Scientific Reports, Ser. C5, 1–13.
Roberts, M. J., 1987. The Spiders of Britain and Northern Ireland. Volume II. Linyphiidae. Harley Books, Colchester, UK.
Scharff, N., 1989. New species and records of Afrotropical Linyphiidae (Araneae). Bull. Br. Arachnol. Soc. 8, 13–20.
Scharff, N., 1992. The linyphiid fauna of Eastern Africa (Araneae, Linyphiidae)—distribution patterns, diversity and endemism. Biol. J. Linn. Soc. 45, 117–154.
Scharff, N. 1993. The linyphiid spider fauna (Araneae, Linyphiidae) of mountain forests in the Eastern Arc mountains. In: Lovett, J., Wasser, S. K. (Eds.), Biogeography and Ecology of the Rain Forests of Eastern Africa. Cambridge University Press, Cambridge, pp. 115–132.
Scharff, N., Gudik-Sørensen, O., 2006. Katalog over Danmarks edderkopper (Araneae)/Catalogue of the Spiders of Denmark (Araneae). Ent Meddelelser 74, 3–71.
Simon, E., 1894. Histoire naturelle des araignées. Paris, 1. 489–760.
Simon, E., 1905. Arachnides des îles Chatham (Ergebnisse einer Reise nach dem Pacific. Schauinsland 1896–1897). Zool. Jahrb. Syst. 21, 415–424.

Sørensen, L., Coddington, J. A., Scharff, N., 2002. Inventorying and estimating spider diversity using semi-quantitative sampling methods in an afrotropical montane forest. Environ. Entomol. 31, 319–330.
Urquhart, A. T., 1886. On the spiders of New Zealand. Trans. NZ Inst. 18, 184–205.
Urquhart, A. T., 1888. On new species of Araneida. Trans. NZ Inst. 20, 109–125.
Urquhart, A. T., 1894. Description of new species of Araneae. Trans. NZ Inst. 26, 204–218.
Usher, M. B. 1983. Two spiders in subfamily Mynogleninae (Araneae: Linyphiidae) from the Falkland Islands, South Atlantic. J. Zool. Lond. 200, 549–560.
Waters, J. M., Craw, D., 2006. Goodbye Gondwana? New Zealand biogeography, geology, and the problem of circularity. Syst. Biol. 55, 251–356.
Wunderlich, J., 1986. Spinnenfauna gestern und heute: fossile Spinnen in Bernstein und ihre heute lebenden Verwandten. Erich Bauer Verlag bei Quelle & Meyer, Wiesbaden.

Appendix 1

Abbreviations used in the figures

The letters of the abbreviations correspond where possible to the sclerite (first), its position (second), and its name (third).

Male palp

C	cymbium
CDM	cymbial dorsal macroseta (ch20)
COL	column (ch78)
CPA	cymbial prolateral apophysis (ch18)
CPD	cymbial prolateral hair density (ch16)
CPH	cymbial prolateral hirsute bump (ch13)
CPF	cymbial prolateral flat area (ch15)
CPG	cymbial prolateral glabrous area (ch14)
CPL	cymbial prolateral ledge (ch17)
CPM	cymbial prolateral macrosetae (ch19)
CRH	cymbium retrolateral proximal hump (ch24)
CRM	cymbial retrolateral membraneous area (ch25)
CRT	cymbium retrobasal thin apophysis (ch22)
CVM	cymbium ventral macroseta (ch21)
E	embolus
EBA	embolic bifurcated apophysis (ch90)
EM	embolic membrane (ch64)
EME	embolic membrane ectal outwards fold (ch72)
EMM	embolic membrane mesal inwards fold (ch71)
F	foramen (ch63)
PC	paracymbium
PDS	paracymbium basal membraneous area (ch33)
PDE	paracymbium longitudinal prominence distal extension (ch32)
PIC	paracymbium inner connection (ch38)
PLP	paracymbium longitudinal prominence (ch31)
PMB	paracymbium mesally broadened (ch37)
PRL	paracymbium retrolateral long setae (ch34)
R	radix (ch76)
RRA	radix retrolateral appendix (ch81)
SD	sperm duct
SDP	subtegular distal sclerotized protrusion (ch40)
SPT	suprategulum (ch54)
ST	subtegulum
T	tegulum
TDE	tibial distal dorsal expansion (ch4)
TFP	tegular flange-like process (ch53)
TME	tibial thin marginal expansion (ch7)
TMK	tegular mynoglenine knob (ch52)
TMP	tegular mynoglenine process (ch48)
TPT	tibial prolateral trichobothrium (ch8)
TRI	tibial retrolateral invagination (ch6)
TRL	tegular retrolateral lobe (ch45)
TRT	tibial retrolateral trichobothrium (ch9)

Epigyne

CD	copulatory duct (ch148)
CO	copulatory opening (ch139)
DP	dorsal plate
DPS	dorsal plate scape (ch142)
ECM	epigyne central margin (ch123)
ECT	epigyne posterior to central thickened (ch124)
ELA	epigyne lateral glabrous area (ch125)
ELM	epigyne anterior to lateral margin (ch121)
ELS	epigyne lateral side ventral extension (ch126)
EME	epigyne lateral side median extension (ch127)
EPM	epigyne posterior margin (ch122)
EVE	epigyne ventrally protruding median edge (ch132)
EVD	epigyne ventral plate depression (ch120)
SO	socket (ch140)
VAD	ventral plate anterior depression (ch134)
VAS	ventral plate anterior margin sclerotization (ch135)
VMR	ventral plate median narrow ridge (ch146)
VP	ventral plate
VPS	ventral plate scape (ch141)
VTT	ventral plate transverse tube (ch133)

Somatic morphology

AB	abdomen
ALE	anterior lateral eyes
AME	anterior median eyes
CL	clypeus
CPB	cheliceral posterior side hirsute bump (ch107)
CPS	cheliceral posterior side freestanding seta (ch108)
CPT	chelicera promarginal teeth (ch104)
CRD	chelicera retromarginal denticles (ch105)
FRT	male femur retrolateral proximal scales (ch118)
MS	macroseta
PBC	pedicel sternite bifid prolongation connection (ch112)
PBP	pedicel sternite bifid prolongation (ch111)
PLE	posterior lateral eyes
PME	posterior median eyes
PMP	pedicel sternite median pouch (ch113)
PS	pedicel sternite
SOS	subocular sulci (ch92)

STR	sternum
TEM	palpal tibia ectal macroseta (ch160)
TET	palpal tibia dorsoectal trichobothria (ch163)
TFD	thorax foveal double setae (ch153)
TH	thorax
TMT	palpal tibia dorsomesal trichobothria (ch162)
TPP	tibial ventral proximal prolateral macrosetae (ch171)
TPR	tibial ventral proximal retrolateral macrosetae (ch172)
TVD	tibial ventral distal macrosetae (ch173)

Appendix 2

Scored specimens

Outgroups

Pimoidae, ***Pimoa altioculata*** (Keyserling, 1886): USA, California, Siskiyou Co, O'Neill Creek, nr Ntl For. Campground, 6.0 km W of Hamburg, Klamath National Forest [41.96970N, 123.10525W], 31.VII.1990, leg. Hormiga, G., Garcia de Mendoza L., coll. ZMUC. 1f.—USA, Washington, King Co. Seattle, Ravenna Park, 30 m [47.673N, 122.307W], 18.XI.1987, leg. Crawford R., coll. ZMUC. 1m.

Linyphiidae, Linyphiinae, Linyphinini, ***Linyphia triangularis*** (Clerck, 1757). Denmark, Bornholm, Rø Plantage [55.18N, 14.90E], 16.IX.2005, leg. and det. Langemark S., coll. ZMUC (ZMUC00011572). 1m1f.

Diplostyla concolor (Wider, 1834). Austria, North Tyrol, Innauen, Langenkampfen [47.54N, 12.10E], 28.VI.1988, leg. and det. Thaler K., coll. NMBE (AR7101). 1m1f.

Linyphiidae, Linyphiinae, ***Australolinyphia remota*** Wunderlich, 1976. Australia, Queensland, Lamington National park close to Brisbane [28.21N, 153.15E], VIII. 1975, leg. and det. Wunderlich J., coll. SMF (SMF 29075). 1m (holotype).—same location, coll. SMF (SMF 29066). 1f (paratype).

Linyphiidae, Linyphiinae, Micronetini, ***Bolyphantes luteolus*** (Blackwall, 1833). Denmark, North East Zealand, Melby Overdrev [56.01755N, 11.97756E], 11.IX.2003, leg, and det. Langemark S., coll. ZMUC (ZMUC00009742). 1m1f.

Linyphiidae, Erigoninae, ***Hilaira excisa*** (O. P.-Cambridge, 1871). Germany, Mecklenburg-Hither Pomerania, Poppendorf [54.13N, 12.28E], 16.VI.1984, leg. and det. von Broen B., coll. NMBE (AR1097). 1m.—Austria, Styria, Oppenberg [47.48N, 14.27E], 12.VII.1995, leg. and det. Kropf C., coll. NMBE (AR1265). 1f.

Linyphiidae, Stemonyphantinae, ***Stemonyphantes lineatus*** (Linnaeus, 1758): Denmark, North East Zealand, Melby Overdrev, [56.01755N, 11.97756E], 11.IX.2003, leg. and det. Schmidt J.B., coll. ZMUC (ZMUC00008656). 1f.—Denmark, North West Zealand, Ellinge Lyng [55.90N, 11.50E], 15.I.2005, leg. Liljehult H., det. Gudik-Sørensen O., coll. ZMUC (ZMUC00009627). 1m.

Ingroups (Linyphiidae, Mynogleninae)

Afromynoglenes parkeri Merrett and Russell-Smith, 1996: Ethiopia, Shewa province, Djemdjem forest, north of Ginchi, 2600 m [9.05000N, 38.13333E], in grass and herbs, mixed *Juniperus*/deciduous forest, 22.IX.1987, leg. Russell-Smith A., coll. BMNH, 1m1f (paratype).

Afroneta bamilekei Bosmans, 1988: Cameroon, Bambouto mountains, 2700 m [5.73333N, 10.06667E], 24.I.1983, leg. Van Stalle J., det. Bosmans R., coll. MRAC (165098). 1m (paratype).—Cameroon, Mount Manengouba, 2250 m [5.00000N, 9.83333E], 25.II.1983, leg. and det. Bosmans R., coll. MRAC (165107). 1f.

Afroneta guttata Holm, 1968: D.R. Congo, Uvira, Mount Kambekulu, 2450 m [3.55000S, 29.15000E], VI.1955, leg. Leleup N., coll. MRAC (81512). 1m1f.

Afroneta lobeliae Merrett, 2004: D.R. Congo, North side of Ruwenzori, Camp of Kanzuiri, ridge of Karibumba, 3800 m [0.41667N, 29.90000E], VII–VIII.1974, leg. Lejeune M., coll. MRAC (154983). 1m1f (paratype).

Afroneta subfusca Holm, 1968: D.R. Congo, North side of Ruwenzori, Kilindera, 2750 m [0.38333N, 29.91667E], VII–VIII.1974, leg. Lejeune M., det. Merrett P., coll. MRAC (155396). 1m1f.

Afroneta tenuivulva Merrett, 2004: D.R. Congo, North side of Ruwenzori, Camp of Kanzuiri, Karibumba, 3700 m [0.41667N, 29.90000E], VII–VIII.1974, leg. Lejeune M., det. Merrett P., coll. MRAC (214287). 1m1f (paratype).

Cassafroneta forsteri Blest, 1979: New Zealand, Te Ponanga, Lake Rotoaira, [39.05800S, 175.70500E], 24.XI.1982, leg. and det. Blest A.D., coll. MoNZ (AS.000280). 1m1f.

Gibbafroneta gibbosa Merrett, 2004: D.R. Congo, Kivu, Nyiragongo volcano, shaheru, 2700 m [1.46667S, 29.41667E], 18.VIII.1970, leg. Lejeune M., det. Merrett P., coll. MRAC (222862). 1m1f (paratype).

Haplinis abbreviata (Blest, 1979): New Zealand, Mount Te Aroha, 610 m [37.53333S, 175.73333E], 30.XI.1982, leg. and det. Blest A.D., coll. MoNZ (AS.000753). 1m1f.

Haplinis diloris (Urquhart, 1886): New Zealand, Dunedin, Kaikorai Estuary, [45.92592S, 170.39333E], 07.V.1994, leg. and det. Blest A.D., coll. MoNZ (AS.000749). 1m1f.

Haplinis horningi (Blest, 1979): New Zealand, Antipodes Island, Reef Point, [49.67333S, 178.81250E], 03.XI.1995, leg. Marris J., McIntosh A., det. Blest A.D., coll. MoNZ (AS.000736). 1m1f.

Haplinis insignis (Blest, 1979): New Zealand, Canterbury, Christchurch, Riccarton Bush (Dean's Bush), [43.52783S, 172.59583E], 15.IV.1994, leg. and det. Blest A.D., coll. MoNZ (AS.000682). 1m1f.

Haplinis subdola (O. P-Cambridge, 1879): New Zealand, Banks Peninsula, Lake Forsyth, [43.80500S, 172.74067E], 15.V.1994, leg. and det. Blest A.D., coll. MoNZ (AS.000350). 1m1f.

Haplinis tegulata (Blest, 1979): New Zealand, Chatham Island, Ocean Mail Scenic Reserve, [43.74715S, 176.40050W], 11.XI.2005, leg. Curtis N., McIntosh M., det. Sirvid P., coll. MoNZ (AS.000953). 1m1f.

Haplinis titan (Blest, 1979): New Zealand, Kaikoura, Mount Fyffe, 457 m [42.35000S, 173.58333E], 03.XII.1995, leg. and det. Blest A.D., coll. MoNZ (AS.000802). 1m1f.

Hyperafroneta obscura Blest, 1979: New Zealand, Te Papanui Conservation Park, [45.66657S, 169.77683E], 16.III.2008, leg. and det. Malumbres-Olarte J., coll. LUNZ (17231). 1m1f.

Laminafroneta bidentata (Holm, 1968): Kenya, Mount Kenya, 3050 m [0.16667S, 37.33333E], 30.VII.1975, leg. and det. Bosmans R., coll. MRAC (150267). 1m1f.

Laminafroneta brevistyla (Holm, 1968): D.R. Congo, Bikara, 18 km south of Lubero, Lubéro-Goma road, 2100 m [0.25000S, 29.20000E], XII.1976, leg. Lejeune M., coll. MRAC (159765). 1m1f.

Metafroneta sinuosa Blest, 1979: New Zealand, Dunedin, Saddle Hill, [45.91222S, 170.35533E], 08.V.1994, leg. and det. Blest A.D., coll. MoNZ (AS.000303). 1m1f.

Metamynoglenes gracilis Blest, 1979: New Zealand, Nelson, Motueka, Brooklyn Valley Road, third bridge, [41.09942S, 172.97017E], 04.XII.1994, leg. Vink C.J., det. Blest A.D., coll. MoNZ (AS.000227). 1m1f.

Metamynoglenes helicoides Blest, 1979: New Zealand, Mount Egmont, Dawson Falls, [39.33333S, 174.10000E], 12.XI.1994, leg. and det. Blest A.D., coll. MoNZ (AS.000208). 1m1f.

Metamynoglenes incurvata Blest, 1979: New Zealand, Nelson, Motueka, Brooklyn Valley Road, third bridge, [41.09942S, 172.97017E], 03.XII.1994, leg. Blest A.D. and Vink C.J., det. Blest A.D., coll. MoNZ (AS.000234). 1f.—New Zealand, Mount Stokes Scenic Reserve, Titirangi road X Anakoha road, 566 m [41.08669S, 174.13816E], 11.III.2010, leg. Scharff N. and Hormiga G., det. Frick H., coll. ZMUC. 1m.

Novafroneta gladiatrix Blest, 1979: New Zealand, Mount Egmont, Dawson Falls, [39.33333S, 174.10000E], 12.XI.1994, leg. and det. Blest A.D., coll. MoNZ (AS.000473). 1f—New Zealand, Arthur's Pass, Klondyke Corner, [43.01100S, 171.58100E], 19.XII.1994, leg. and det. Blest A.D., coll. MoNZ (AS.000475). 1m.

Novafroneta vulgaris Blest, 1979: New Zealand, Arthur's Pass, Klondyke Corner, [43.01100S, 171.58100E], 23.I.1998, leg. and det. Blest A.D., coll. MoNZ (AS.000455). 1m1f.

Parafroneta confusa Blest, 1979: New Zealand, Arthur's Pass, Greyney's lay-by, [42.95000S, 171.56667E], 17.XII.2002, leg. Blest A.D. and Vink C.J., det. Blest A.D., coll. MoNZ (AS.000587, as *Parafroneta westlandica* Blest and Vink, 2002). 1m1f.

Parafroneta demota Blest and Vink, 2002: New Zealand, Turangi, Stump Bay, swamp, [38.95000S, 175.81667E], 09.XI.1994, leg. Blest A.D. and Vink C.J., det. Blest A.D., coll. MoNZ (AS.000611). 1m1f.

Parafroneta haurokoae Blest and Vink, 2002: New Zealand, Lake Hauroko, [45.94700S, 167.30219E], 20.I.1992, leg. Forster R.R., det. Blest A.D., coll. MoNZ (AS.000592). 1m1f (paratype).

Parafroneta marrineri (Hogg, 1909): New Zealand, Antipodes Island, [49.67167S, 178.80667E], 12.XI.1995, leg. Marris J., McIntosh A., det. Blest A.D., coll. MoNZ (AS.000563). 1f.—New Zealand, Antipodes Island, Mount Galloway, 360 m [49.69167S, 178.78667E], 04.XI.1995, leg. Marris J., McIntosh A., det. Vink C.J., coll. MoNZ (AS.000571). 1m.

Parafroneta minuta Blest, 1979: New Zealand, Te Papanui Conservation Park, [45.66476S, 169.78406E], 22.I.2008, leg. and det. Malumbres-Olarte J., coll. LUNZ (22143). 1f.—New Zealand, Banks Peninsula, Summit Road, [43.73812S, 173.02450E], 29.V.1994, leg. and det. Blest A.D., coll. MoNZ (AS.000526). 1m.

Parafroneta westlandica Blest and Vink, 2002: New Zealand, South Island, Peel Forest, [43.91667S, 171.26667E], 28.IV.2002, leg. Blest A.D. and Vink C.J., det. Blest A.D., coll. MoNZ (AS.000406, as *Pseudafroneta incerta* (Bryant, 1935)). 1m1f.

Promynoglenes grandis Blest, 1979: New Zealand, Fiordland, Mavora Lakes, [45.25167S, 168.15000E], 09.IV.1993, leg. Forster R.R., det. Blest A.D., coll. MoNZ (AS.000242). 1m.—New Zealand, Westland, Fox Glacier, Creek at ca. 1895 feet marker, 580 m [43.51667S, 170.11667E], 13.XII.1994, leg. and det. Blest A.D., coll. MoNZ (AS.000244). 1f.

Promynoglenes nobilis Blest, 1979: New Zealand, Haast, Hapuka Estuary, [43.90000S, 168.90000E], 17.XI.1995, leg. and det. Blest A.D., coll. MoNZ (AS.000261). 1m1f.

Promynoglenes silvestris Blest, 1979: New Zealand, Arthur's pass National Park, nr Greyneys Shelter, 670 m [42.98438S, 171.59047E], 4.III.2010, leg. Scharff N. and Hormiga G., det. Frick H., coll. ZMUC. 1m1f.

Protoerigone otagoa Blest, 1979: New Zealand, Te Papanui Conservation Park, [45.66657S, 169.77683E], 22.I.2008, leg. and det. Malumbres-Olarte J., coll. LUNZ (22211). 1m.—New Zealand, Te Papanui Conservation Park, [45.66657S, 169.77683E], 22.I.2008, leg. and det. Malumbres-Olarte J., coll. LUNZ (22212). 1f.

Pseudafroneta pallida Blest, 1979: New Zealand, Nelson, Lake Rotoiti, [41.82450S, 172.83817E], 27.III.1994, leg. Forster R.R., det. Blest A.D., coll. MoNZ (AS.000360). 1m1f.

Pseudafroneta perplexa Blest, 1979: New Zealand, Southland, Invercargill, Otatara Scenic Reserve, [46.43333S, 168.28333E], 21.XI.2000, leg. Blest A.D., Vink C.J., det. Blest A.D., coll. MoNZ (AS.000414). 1m1f.

Trachyneta jocquei Merrett, 2004: Malawi, Nyika plateau, Chelinda, small swamp by dam no. 1, 2300 m [10.31667S, 33.80000E], 7.XII.1981, leg. Jocqué R., det. Merrett P., coll. MRAC (156827). 1f (paratype).—Malawi, Nyika plateau, Dambo, langs circular drive, 500 m S of the exit to Dembo-bridge, 2350 m [10.66667S, 33.83333E], 12.XII.1981, leg. Jocqué R., det. Merrett P., coll. MRAC (156848). 1m (paratype).

Appendix 3

Character descriptions

Illustrations of male and female copulatory organs are given only if characters are new (all underlined characters) or were not illustrated originally. Illustrations of many characters can be found elsewhere (Blest, 1979; Hormiga, 1994a; Merrett and Russell-Smith, 1996; Hormiga, 2000; Merrett, 2004; Miller and Hormiga, 2004). Illustrations of expanded palps and cleared vulvae of eight New Zealand genera are previously published (Blest, 1979: figs 596–603; Blest and Vink, 2002, 2003). We have added a figure with the expanded palp of *Haplinis diloris* (Fig. 8b). A total of 147 characters are described here for the first time; 43 have been described and discussed in detail in other papers (Hormiga, 2000; Miller and Hormiga, 2004; Arnedo et al., 2009). For those characters, we added the reference to its most recent usage including its definition. References are abbreviated as follows: A09 (Arnedo et al., 2009), MH04 (Miller and Hormiga, 2004), M04 (Merrett, 2004), H00 (Hormiga, 2000). The abbreviation is followed by the character number in the cited reference. For example, H00-28 refers to character 28 in the matrix of Hormiga (2000). Reference to a character of which a state has been deleted, added, or modified is indicated with an asterisk (*).

Directions are used as defined in Fig. 8a. The number and size of the macrosetae are variable within species, sexes, and even in single specimens. In rare cases the number of macrosetae differed between right and left legs. In these cases we scored the highest number. They range from similar to a leg seta to very thick and distinct macrosetae. When scoring, presence of the character was preferred over absence in another specimen.

Male copulatory organs

1 Palpal tibia, dorsal length. 0: less than 2.3 times as long as proximally wide (Fig. 11c, *Metamynoglenes gracilis*). 1: between 2.4 and 4.0 times longer than proximally wide (Fig. 11a, *Haplinis diloris*). 2: more than 4.1 times longer than proximally wide (Fig. 10e, *Haplinis tegulata*). This character accounts for the tibia length and is corrected for body size by dividing the dorsal maximum length by the proximal diameter. State limits were set to the largest gaps in the measurements. This character is inapplicable for taxa with distinct tibial apophyses, e.g. erigonines.

2 Palpal tibia, distal width. 0: less than 1.9 times proximal width (Fig. 10e, *Haplinis tegulata*). 1: more than 2.0 times proximal width (Fig. 12f, *Metamynoglenes gracilis*). This character accounts for the distal width of the tibia and was corrected for the body size by dividing the distal maximum width by the proximal diameter. The state limits were set to the largest gaps in the measurements.

3 Palpal tibia, form. 0: straight (Fig. 9c, *Haplinis diloris*). 1: dorsally bent (Fig. 10b, *Novafroneta gladiatrix*). The tibia of *Novafroneta* is typically bent.

4 Palpal tibia, distal dorsal expansion (TDE). 0: absent, tibia uniformly thin (Fig. 9c, *Haplinis diloris*). 1: fleshy dorsal expansion present (Fig. 10a, *Metamynoglenes helicoides*).

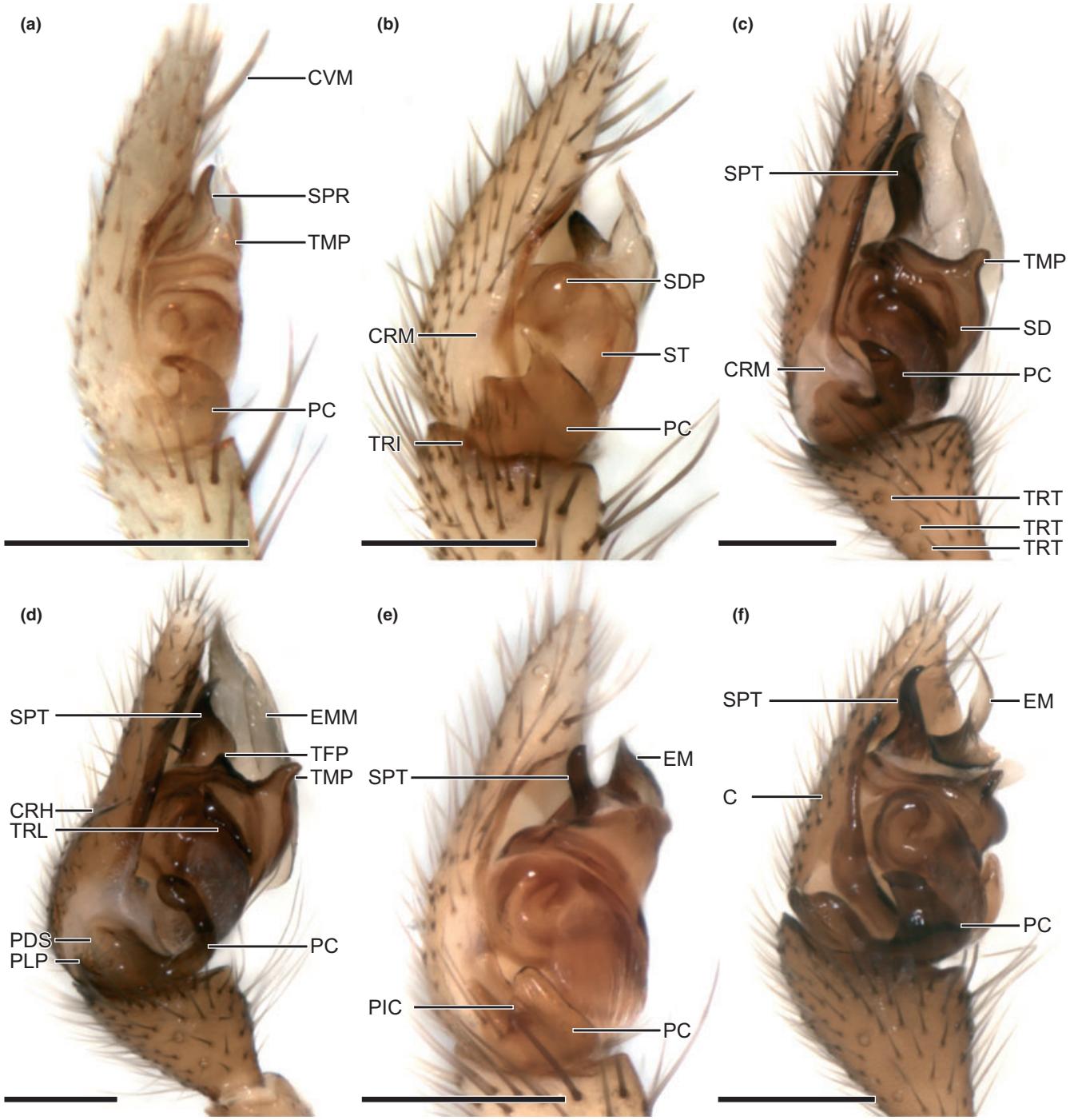

Fig. 9. Male palps, retrolateral view, scale 200 μm. (a) *Afroneta subfusca*; (b) *Afroneta tenuivulva*; (c) *Haplinis diloris*; (d) *Haplinis subdola*; (e) *Laminafroneta bidentata*; (f) *Metafroneta sinuosa*.

5 Palpal tibia, prolateral tibial apophysis. 0: absent (Fig. 9c, *Haplinis diloris*). 1: present (Hormiga, 2000: fig. 14A, *Hilaira excisa*). A09-57, MH04-67, H00-28.

6 Palpal tibia, retrolateral invagination (TRI). 0: absent (Fig. 9c, *Haplinis diloris*). 1: present (Fig. 9b, *Afroneta tenuivulva*). The retrolateral distal margin of the tibia has a distinct invagination in some taxa.

7 Palpal tibia, retrolateral thin marginal expansion (TME). 0: distal margin of tibia continuous (Fig. 9b, *Afroneta tenuivulva*). 1: distal margin of tibia retrolaterally expanded (Fig. 10b, *Novafroneta gladiatrix*). In *Novafroneta*, a pronounced sclerotized expansion arises from the retrolateral distal margin of the tibia. This structure is similar to the retrolateral sclerotized band but more pronounced and restricted to a narrow area.

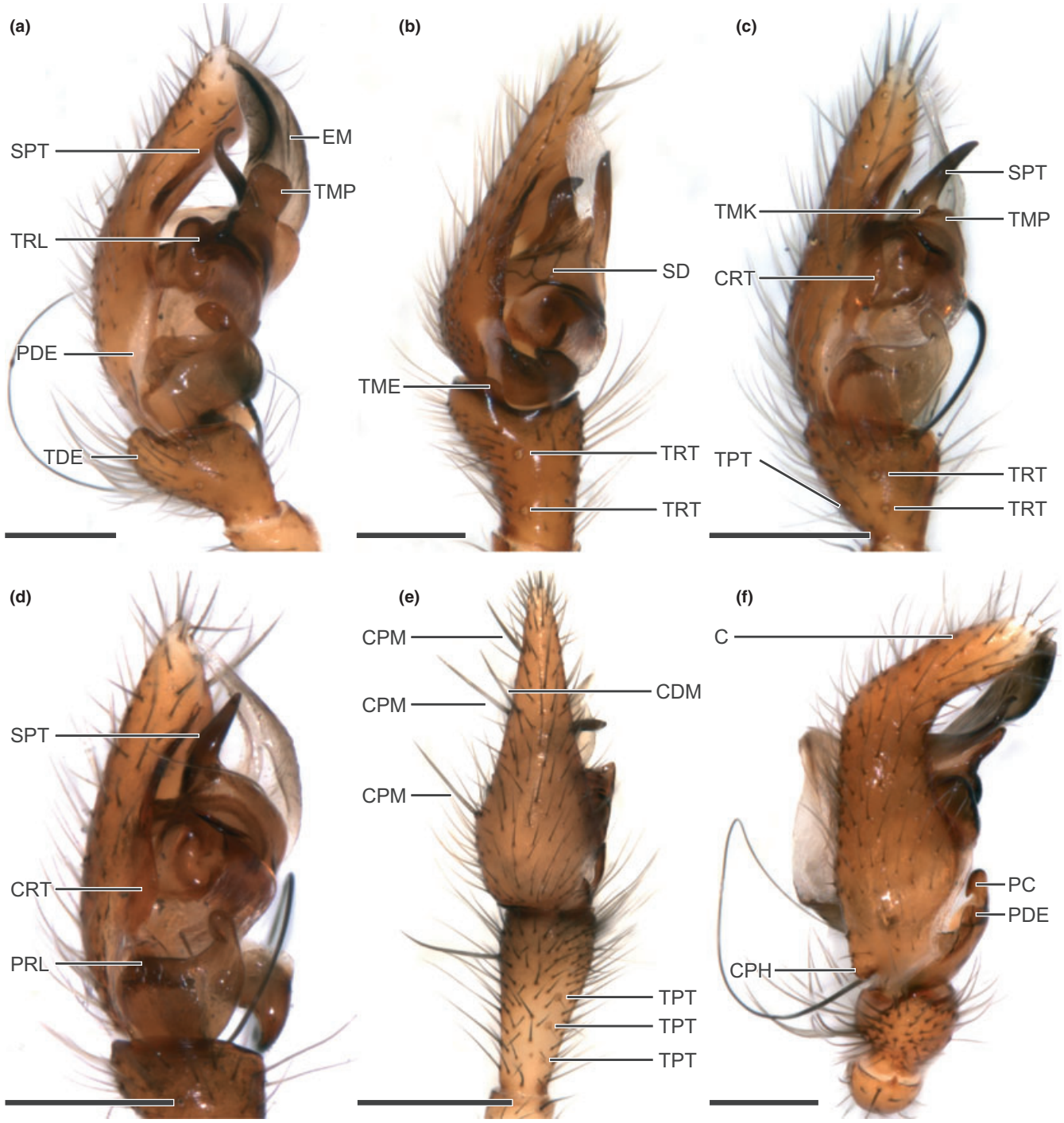

Fig. 10. Male palps, retrolateral (a–d) and dorsal (e–f) view, scale 200 μm. (a) *Metamynoglenes helicoides*; (b) *Novafroneta gladiatrix* (mirrored); (c) *Promynoglenes silvestris* (mirrored); (d) *Promynoglenes nobilis*; (e) *Haplinis tegulata*, dorsal (mirrored); (f) *Metamynoglenes helicoides*.

8 Palpal tibia, prolateral trichobothria (TPT). 0: one (Fig. 10c, *Promynoglenes silvestris*). 1: two (*Haplinis diloris*). 2: three (Fig. 10e, *Haplinis tegulata*). A09-61*, MH04-73*, H00-30*.

9 Palpal tibia, retrolateral trichobothria (TRT). 0: two (Fig. 10b, *Novafroneta gladiatrix*). 1: three (Fig. 9c, *Haplinis diloris*). 2: four (*Haplinis tegulata*). A09-62*, MH04-74*, H00-31*.

10 Alveolus. 0: nearly as long as cymbium (Hormiga, 2000: plate 33A, *Hilaira excisa*). 1: much shorter than cymbium (Fig. 10b, *Novafroneta gladiatrix*). MH04-6. The cymbium is either as long as the alveolus (state 0) or exceeds it (state 1).

11 Cymbium, distal shape. 0: in line with cymbium (Fig. 10e, *Haplinis tegulata*). 1: distal section bent retrolaterally, as seen in dorsal view (Fig. 10f, *Metamynoglenes helicoides*).

12 Cymbium, width. 0: pear-shaped, like most linyphiids (Fig. 10e, *Haplinis tegulata*). 1: narrowed, almost parallel-sided (Fig. 10f, *Metamynoglenes helicoides*).

Fig. 11. Male palps, prolateral view, scale 200 μm. (a) *Haplinis diloris*; (b) *Haplinis tegulata* (mirrored); (c) *Metamynoglenes gracilis*; (d) *Promynoglenes nobilis*; (e) *Pseudafroneta pallida*; (f) *Trachyneta jocquei*.

13 Cymbium, prolateral hirsute bump proximally (CPH). 0: absent (Fig. 10e, *Haplinis tegulata*). 1: present (Fig. 10f, *Metamynoglenes helicoides*). An autapomorphy for *Metamynoglenes helicoides* but might be a useful character in another context.

14 Cymbium, prolateral glabrous area proximally (CPG). 0: hairy as cymbium (Fig. 11f, *Trachyneta jocquei*). 1: glabrous area present prolaterally (Fig. 11a, *Haplinis diloris*). This is a proximal setae-free area on the prolateral side of the cymbium that could be functionally related to the embolus, which rests upon this area in the unexpanded palp. The area can be more sclerotized than the remaining part of cymbium and includes a small depression.

15 Cymbium, prolateral flat area (CPF). 0: surface as cymbium (Fig. 11a, *Haplinis diloris*). 1: area ventrally flattened with short thick setae (Fig. 11d, *Promynoglenes nobilis*). The proximal part of

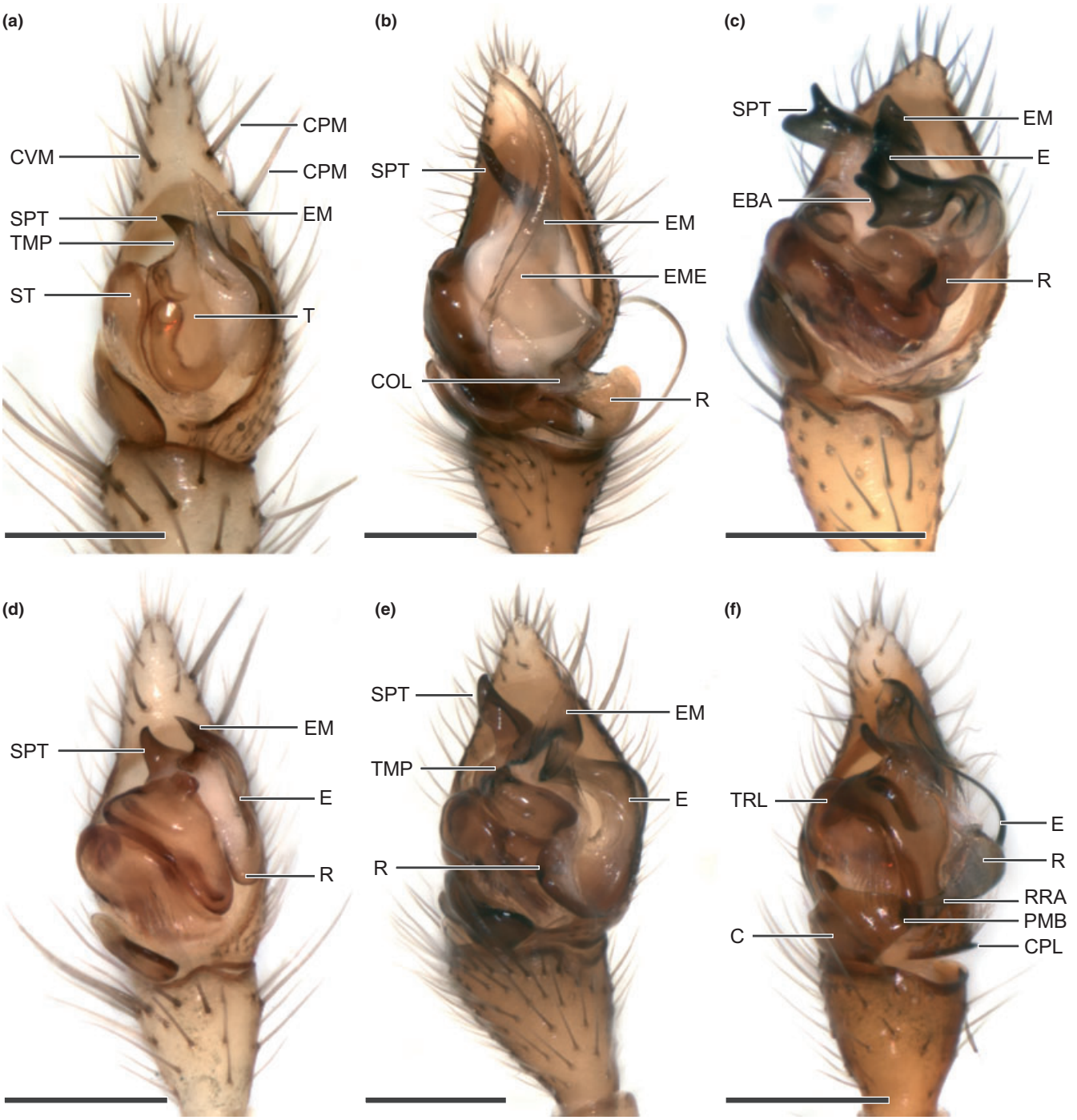

Fig. 12. Male palps, ventral view, scale 200 μm. (a) *Afroneta tenuivulva*; (b) *Haplinis horningi*; (c) *Hyperafroneta obscura* (mirrored); (d) *Laminafroneta bidentata*; (e) *Metafroneta sinuosa*; (f) *Metamynoglenes gracilis*.

the cymbium of *Promynoglenes* is flattened ventrally. The short setae on the ventral flattened area might be functionally related to the circular filiform embolus that rests upon this area.

16 Cymbium, prolateral hair density (CPD). 0: hair density as cymbium (Fig. 11a, *Haplinis diloris*). 1: hirsute area proximally (Fig. 11b, *Haplinis tegulata*). The prolateral side of the cymbium is prolonged proximally and very hirsute.

17 Cymbium, prolateral ledge (CPL). 0: proximal margin unmodified (Fig. 11a, *Haplinis diloris*). 1: proximal margin with ledge (Fig. 12f, *Metamynoglenes gracilis*). This ledge emerges at the prolateral and proximal margin of the cymbium and can form a distinct apophysis in some species (ch18).

18 Cymbium, prolateral sclerotized apophysis (CPA). 0: proximal margin unmodified or at most with ledge (Fig. 11a, *Haplinis diloris*).

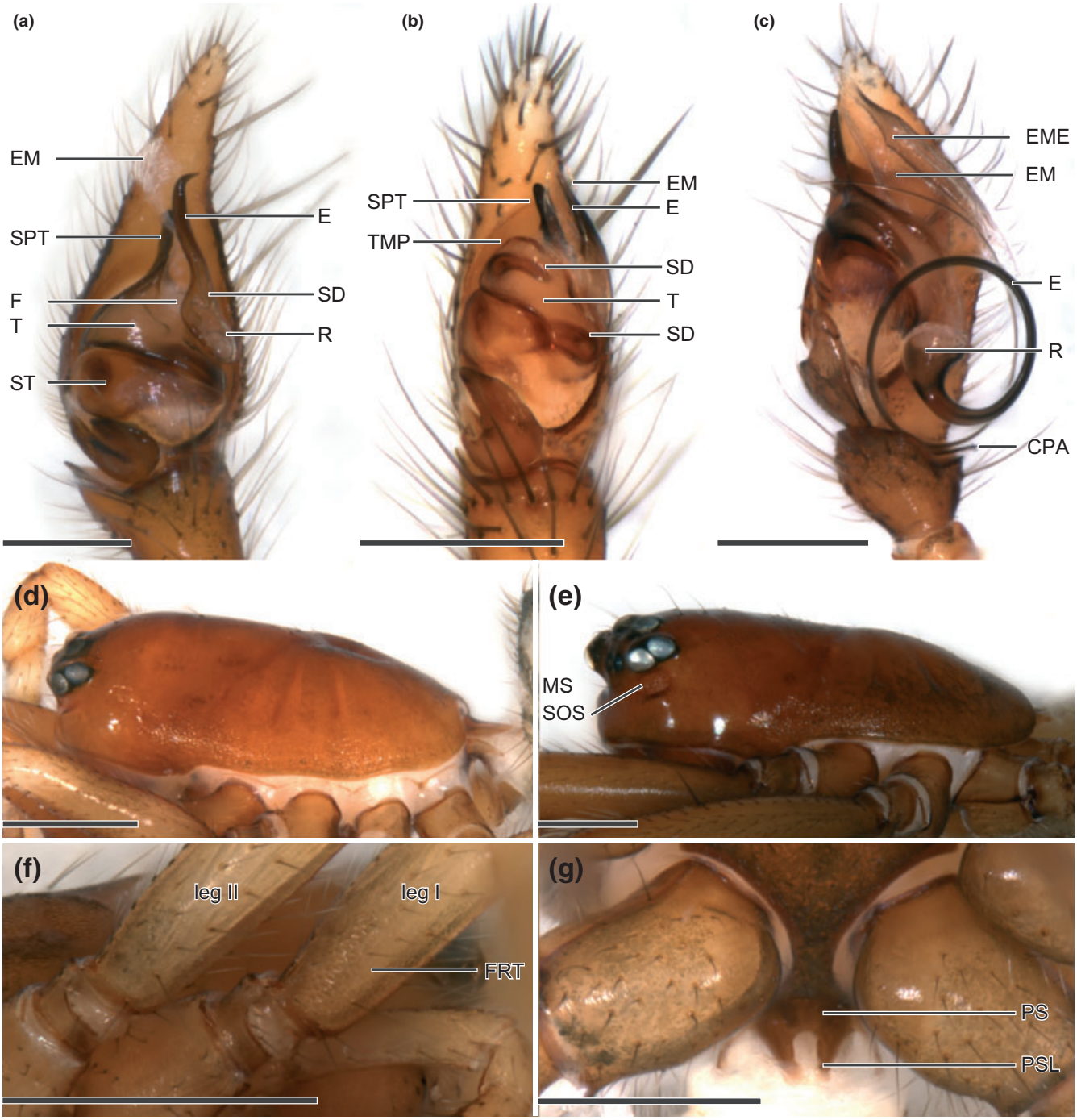

Fig. 13. Male palps, ventral (a–c), scale 200 μm; male prosoma, lateral (d–e), male femora I–II, ventral (f) and male petiolus, ventral (g), scale 500 μm. (a) *Novafroneta gladiatrix* (mirrored); (b) *Parafroneta westlandica*; (c) *Promynoglenes nobilis*; (d) *Parafroneta haurokoae*; (e) *Novafroneta vulgaris*; (f) *Pseudafroneta pallida*; (g) *Novafroneta vulgaris*.

1: proximal margin with sclerotized apophysis (Fig. 11d, *Promynoglenes nobilis*). See character 17.

19 Cymbium, prolateral macrosetae (CPM). 0: absent (Hormiga, 2000: plate 33B, *Hilaira excisa*). 1: two (Fig. 11f, *Trachyneta jocquei*). 2: three or more (Fig. 9e, *Haplinis tegulata*). Some species have three very distinct macroseta along the prolateral margin of the cymbium. The dorsal one is considered in character 20. The most proximal one is absent in rare cases (e.g. *Parafroneta minuta*, three on right and two on left palp).

20 Cymbium, prolateral to dorsal macrosetae (CDM). 0: absent (Fig. 11a, *Haplinis diloris*). 1: one or two present (Fig. 10e, *Haplinis tegulata*).

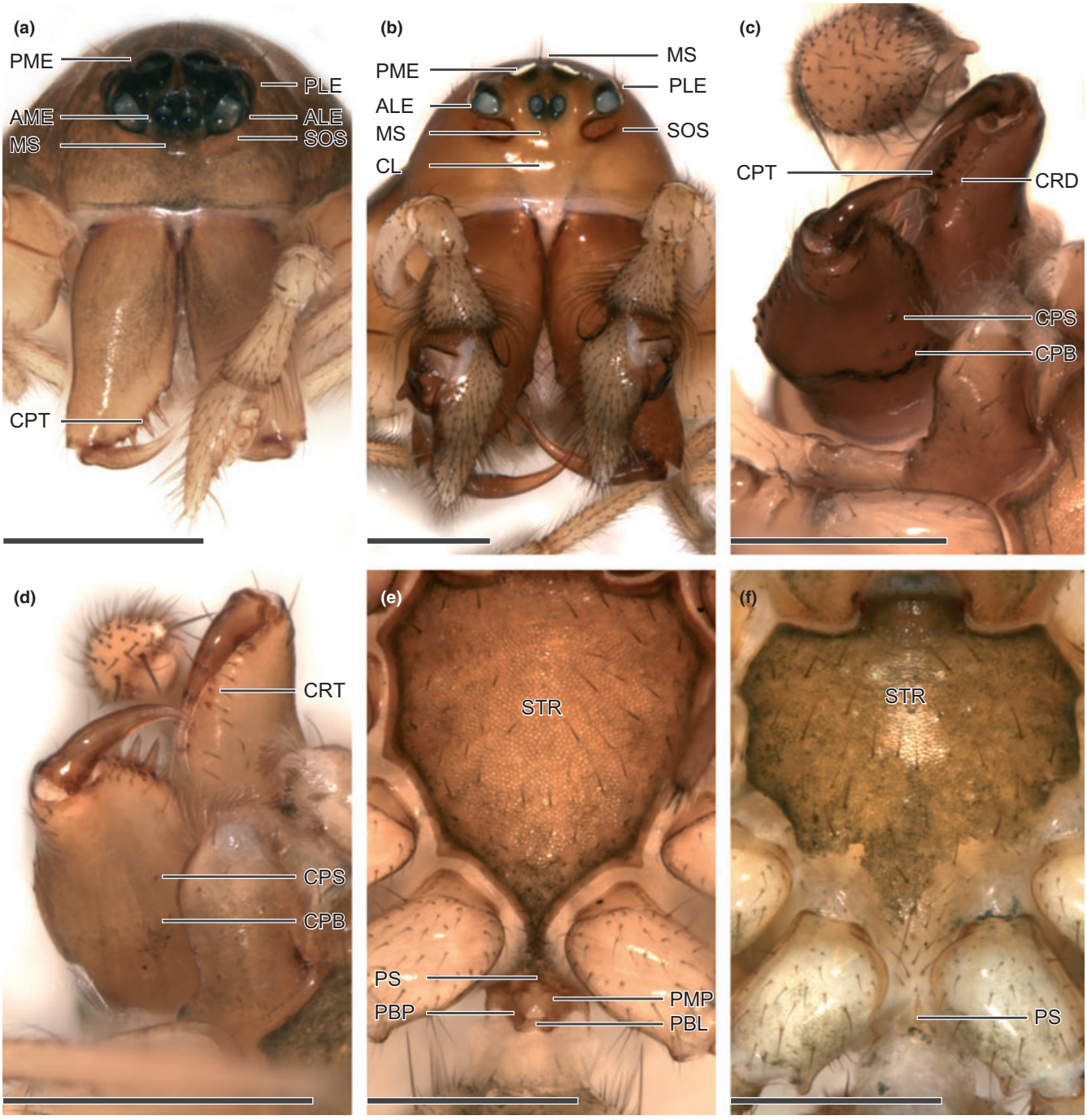

Fig. 14. Male prosoma, frontal (a, b), male chelicera, ventral (c, d) and male sternum, ventral (e, f), scale 500 μm. (a) *Afroneta guttata*; (b) *Haplinis diloris*; (c) *Haplinis diloris*; (d) *Afroneta guttata*; (e) *Haplinis diloris*; (f) *Afroneta tenuivulva.*

21 Cymbium, distal ventral macrosetae (CVM). 0: absent (Fig. 9c, *Haplinis diloris*). 1: present (Fig. 12a, *Afroneta tenuivulva*). Tip of cymbium with ventral macrosetae in some species. In most species shifted more retrolaterally than prolaterally.

22 Cymbium, retrobasal thin apophysis (CRT). 0: absent (Fig. 9c, *Haplinis diloris*). 1: present (Fig. 10c, *Promynoglenes silvestris*). Sclerotized thin protrusion of the retrolateral margin of the cymbium. Might be homologous with the cymbial retrobasal process (MH04-04).

23 Cymbium, retrolateral setae rich bump proximally. 0: absent (Fig. 9c, *Haplinis diloris*). 1: present (Hormiga, 2000: plate 1A, *Bolyphantes luteolus*).

24 Cymbial retrolateral hump proximally (CRH). 0: absent (Fig. 9c, *Haplinis diloris*). 1: present (Fig. 9d, *Haplinis subdola*). An

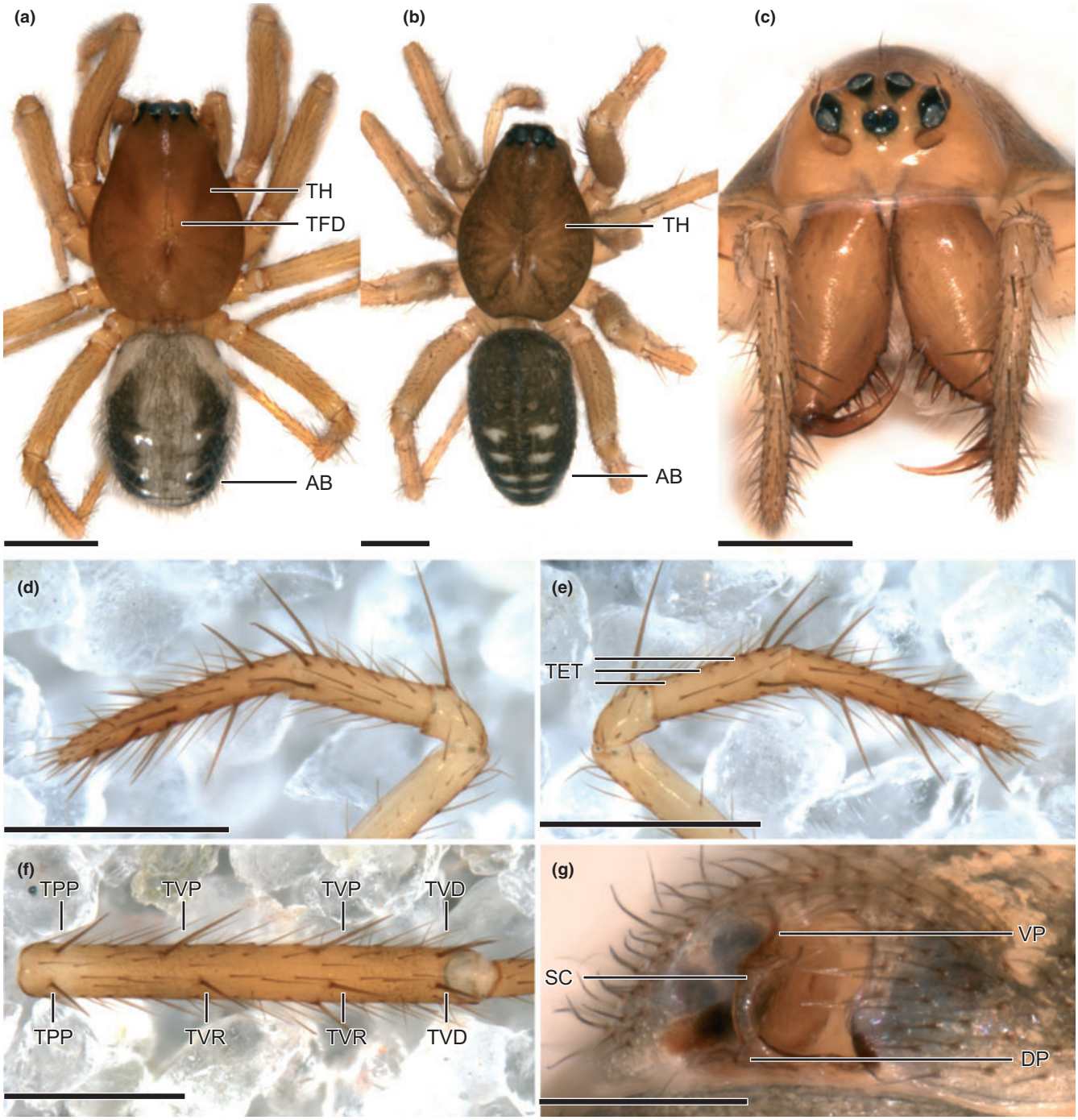

Fig. 15. Male habitus, dorsal (a, b), female prosoma, frontal (c), female right palp (d, e) and female left tibia I, ventral (f), scale 500 μm; female epigyne, aboral to lateral (g), scale 200 μm. (a) *Pseudafroneta pallida*; (b) *Afroneta guttata*; (c) *Haplinis diloris*; (d) *Afroneta guttata*, prolateral; (e) *Afroneta guttata*, retrolateral; (f) *Afroneta guttata*; (g) *Novafroneta gladiatrix*.

autapomorphy for *Haplinis subdola* in the current study but defines Blest's (1979) group I of *Haplinis*.

25 Cymbium, retrolateral membraneous area proximally (CRM). 0: restricted to small area around paracymbium (Fig. 9c, *Haplinis diloris*). 1: expanding distally, covering about half of the alveolus (Fig. 9b, *Afroneta tenuivulva*). The membraneous area, i.e. intersegmental connection of paracymbium to cymbium, can either be restricted to the direct surrounding of the paracymbium or expand distally to cover about half of the retrolateral side of the alveolus.

26 Paracymbium, attachment. 0: intersegmental (Fig. 9c, *Haplinis diloris*). 1: integral (Hormiga, 1994b: figs 303, 304, *Pimoa altioculata*). A09-11*, MH04-11, H00-4. The integral attachment is an autapomorphy of *Pimoa altioculata* in this study.

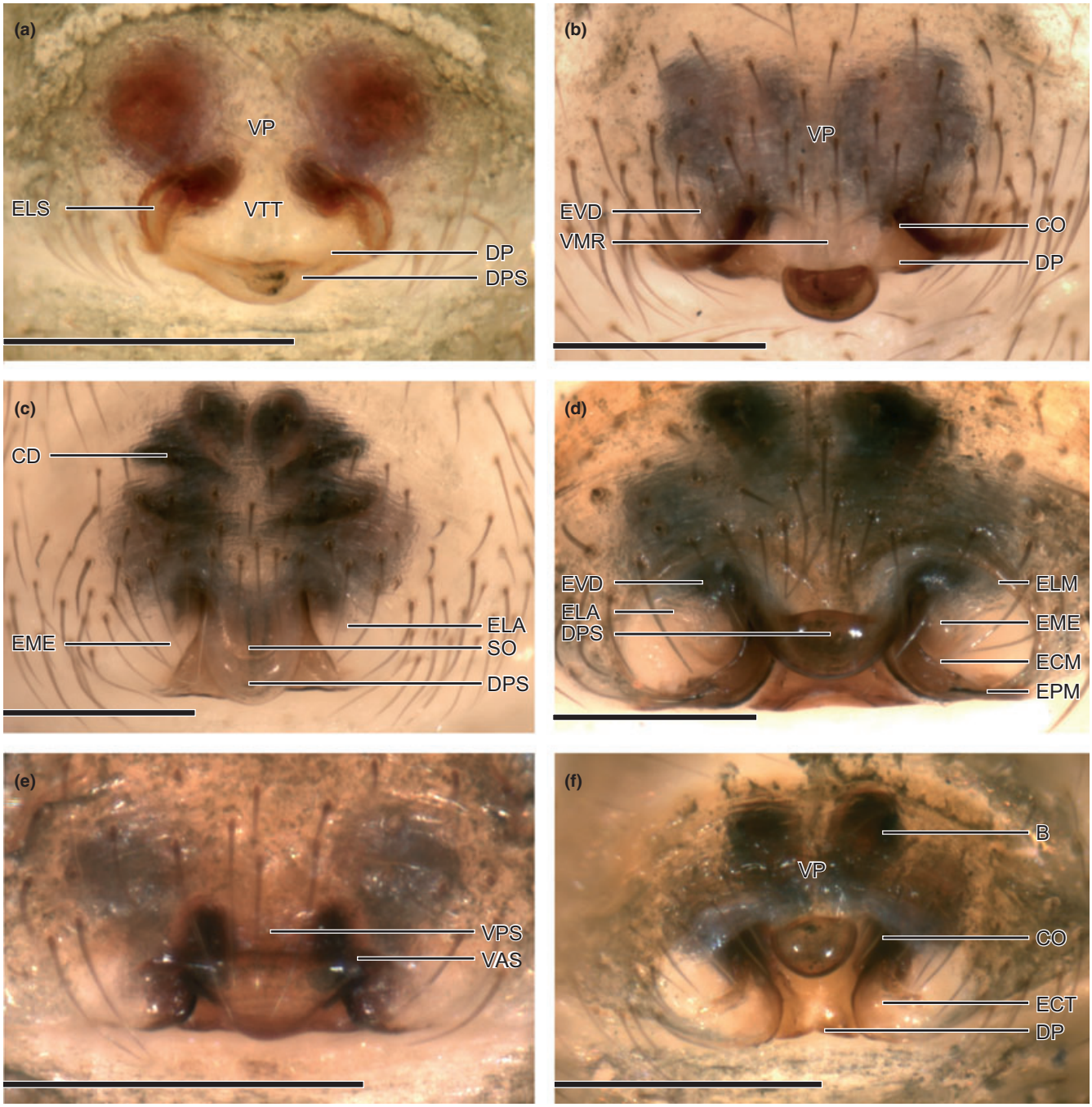

Fig. 16. Female epigyne, ventral, scale 200 µm. (a) *Afroneta bamilekei*; (b) *Afroneta lobeliae*; (c) *Haplinis diloris*; (d) *Haplinis tegulata*; (e) *Laminafroneta brevistyla*; (f) *Metamynoglenes gracilis*.

27 Paracymbium, morphology. 0: triangular (Hormiga, 1994b: figs 303, 304, *Pimoa altioculata*). 1: straight hook (Fig. 9d, *Haplinis subdola*). 2: spiral (Hormiga, 2000: fig. 14C, *Hilaira excisa*). A09-12*, MH04-12*, H00-5*.

28 Paracymbium base, number of setae. 0: glabrous, no setae (*Cassafroneta forsteri*). 1: one seta (Fig. 10b, *Novafroneta gladiatrix*). 2: two setae (Fig. 9c, *Haplinis diloris*). 3: three setae. 4: four setae (Fig. 9a, *Afroneta subfusca*). 5: eight or more setae (Fig. 9b, *Afroneta tenuivulva*). A09-14*, MH04-14*. This character accounts for the different number of setae found at the base of the paracymbium.

29 Paracymbium, proximal setae, length. 0: shorter than cymbial setae (Fig. 9b, *Afroneta tenuivulva*). 1: as long as cymbial setae (Fig. 9e, *Laminafroneta bidentata*).

30 Paracymbium, proximal setae, expansion. 0: restricted to sclerotized area (Fig. 9c, *Haplinis diloris*). 1: extending from sclerotized area to membraneous part (Fig. 9d, *Haplinis subdola*).

31 Paracymbium, proximal part, longitudinal prominence (PLP). 0: absent (Fig. 9b, *Afroneta tenuivulva*). 1: present (Fig. 9d, *Haplinis subdola*). The proximal part of the paracymbium forms a longitudinal prominance from which the proximal setae emerge. The prominence is

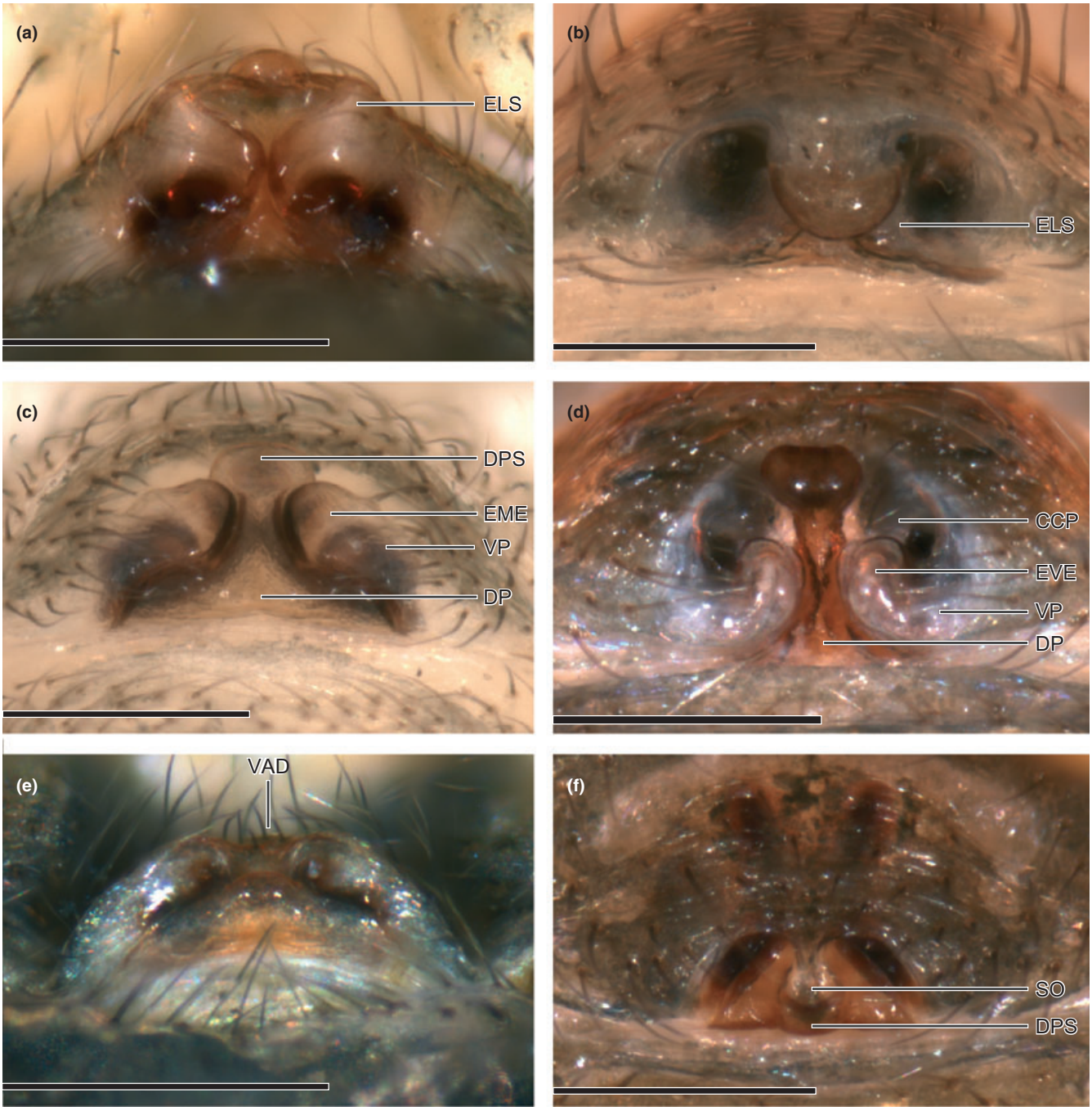

Fig. 17. Female epigyne, aboral (a–e) and ventral (f), scale 200 μm. (a) *Cassafroneta forsteri*; (b) *Haplinis horningi*; (c) *Metafroneta sinuosa*; (d) *Metamynoglenes helicoides*; (e) *Parafroneta minuta*; (f) *Parafroneta westlandica*.

nearly right-angled to the remaining retrolateral surface of the paracymbium. Shallower longitudinal indentations from which setae emerge are also found in most other mynoglenines, such as *Parafroneta*.

32 Paracymbium, proximal part, distal extension (PDE). 0: absent (Fig. 9d, *Haplinis subdola*). 1: present (Fig. 10a, *Metamynoglenes helicoides*). In some species, a sclerotized semitransparent glabrous outgrowth extends distally from the prominance.

33 Paracymbium, proximal part degree of sclerotization (PDS). 0: sclerotized (Fig. 9c, *Haplinis diloris*). 1: membraneous (Fig. 9d, *Haplinis subdola*). The central part of the base of the paracymbium is membraneous in some species of *Haplinis*. This membraneous area is delimited towards the membrane connecting the paracymbium with the cymbium.

34 Paracymbium, long retrolateral surface setae (PRL). 0: absent (Fig. 10c, *Promynoglenes silvestris*). 1: present (Fig. 10d, *Promynoglenes nobilis*). *Promynoglenes nobilis* has two short setae behind the extension (ch32) of the longitudinal prominance (ch31). These are homologous with setae found in most other mynoglenines. Additionally, it has many long setae on the outer retrolateral surface of the paracymbium, for which this character accounts.

35 Paracymbium, proximal part, connection with cymbium. 0: angular, with gradient to membraneous part (Fig. 9b, *Afroneta tenuivulva*). 1: round to oval, with clear delimitation to membraneous part (Fig. 9c, *Haplinis diloris*). The distal side of the base of state 0 is often pointy. The round to oval shape can be broken by a membraneous tissue (e.g. Fig. 9d, *Haplinis subdola*) but is always more or less oval.

36 Paracymbium, types. 0: edgy hook (Fig. 9b, *Afroneta tenuivulva*). 1: oval hook (Fig. 9c, *Haplinis diloris*). 2: large base with small tip (Fig. 10c, *Promynoglenes silvestris*). The edgy hook is found in many genera including *Afroneta*, *Laminafroneta* and *Parafroneta*. It has a broad proximal and median section and a more delicate distal part. The oval hook is mainly found in *Haplinis* and defined by an oval proximal part and a more delicate median and distal part. It is somewhat more stretched than the compact edgy hook. State 2 is found in *Metamynoglenes* and *Promynoglenes*. It has broad proximal and median parts and a small roundish distal part. In addition, the proximal part is rebordered by a distal extending protrusion of the longitudinal prominence (ch31).

37 Paracymbium, mesal broadening (PMB). 0: unmodified (Fig. 10c, *Promynoglenes silvestris*). 1: with mesal broadening (Fig. 12f, *Metamynoglenes gracilis*). In *Metamynoglenes* the median part is considerably extended towards the mesal side of the palp.

38 Paracymbium, inner connection (PIC). 0: absent (Fig. 9b, *Afroneta tenuivulva*). 1: present (Fig. 9e, *Laminafroneta bidentata*). In *Laminafroneta*, the distal part is connected with the proximal part and forms a triangle.

39 Paracymbium, inner margin form. 0: round (Fig. 9d, *Haplinis subdola*). 1: angular, straight (Fig. 9b, *Afroneta tenuivulva*). The paracymbium of mynoglenines looks more or less like an arch. This character accounts for the form of its inner margin.

40 Subtegulum distal sclerotized protrusion (SDP). 0: absent (Fig. 9c, *Haplinis diloris*). 1: present (Fig. 9b, *Afroneta tenuivulva*). In *Afroneta tenuivulva* the subtegulum protrudes further distally than the tegulum (excluding appendages). In distal view, this protrusion looks like a sclerotized round bulb.

41 Tegulum to subtegulum orientation in unexpanded palp. 0: tegulum distal to subtegulum (Fig. 13a, *Novafroneta gladiatrix*). 1: tegulum mesal to subtegulum (Fig. 12a, *Afroneta tenuivulva*). 2: tegulum ventral to subtegulum (Hormiga, 1994b: fig. 9, *Pimoa altioculata*). A09-21, MH04-21.

42 Tegulum, distal expansion. 0: expanded, covering most of alveolus (Fig. 13b, *Parafroneta westlandica*). 1: restricted, covering only proximal half of alveolus (Fig. 13a, *Novafroneta gladiatrix*).

43 Tegulum, number of sperm duct turns in tegulum. 0: single turn (Fig. 9c, *Haplinis diloris*). 1: double turn (Fig. 13b, *Parafroneta westlandica*).

44 Tegulum, sperm duct diameter. 0: thick (Fig. 9c, *Haplinis diloris*). 1: very thin (Fig. 10b, *Novafroneta gladiatrix*). The spermduct of most linyphiids narrows considerably before entering the suprategulum or embolic division (Fig. 11f). State 0 accounts for diameters seen before the constriction, state 1 for diameters after the constriction.

45 Tegular retrolateral lobe (TRL). 0: absent (Fig. 10b, *Novafroneta gladiatrix*). 1: present (Fig. 9d, *Haplinis subdola*). A small lobe emerging from the retrolateral side of the tegulum.

46 Tegular retrolateral lobe, form. 0: round (Fig. 9d, *Haplinis subdola*). 1: pointed (Fig. 10a, *Metamynoglenes helicoides*).

47 Tegulum, protegular process. 0: absent (Fig. 13b, *Parafroneta westlandica*). 1: present (Hormiga, 2000: plate 33A, *Hilaira excisa*). A09-16*, MH04-16*, H00-8*. Instead of scoring the "protegulum" (A09-16), which would be autapomorphic for *Hilaira excisa* in the current taxon sampling (see MH04-16 for details), we prefer to score presence/absence of protegular apophyses. Miller and Hormiga (2004) mention that many linyphiid taxa have one or the other structure arising from the tegulum at roughly the same position. We agree that a character should be introduced to summarize these structures, assuming they are homologous. See also discussion on the tegular mynoglenine process (ch48).

48 Tegular mynoglenine process (TMP). 0: absent (Fig. 13a, *Novafroneta gladiatrix*). 1: present (Fig. 9c, *Haplinis diloris*). Blest (1979) used the term "tegular prominence" for this structure. The two scored species of *Novafroneta* have a ridge connecting the tegulum and the suprategulum, which might also be considered a special type of mynoglenine tegular process. This structure is mentioned in the abbreviations section of Hormiga (1994) as "mynoglenine tegular process" (MTB). Hormiga (2000) lists this structure in the section on the "tegular sac" (character 10) with reference to Holm (1979: 256), who suggested a correspondence between the protegulum and the "tegular prominence" of *Mynoglenes* (described by Blest and Pomeroy, 1978: 328). It is mentioned as a potential homologue of the erigonine protegulum (Hormiga, 2000; Miller and Hormiga, 2004).

49 Tegular mynoglenine process, general conformation. 0: fleshy broad (Fig. 13b, *Parafroneta westlandica*). 1: thin appendix (Fig. 9c, *Haplinis diloris*). The broad type lacks distinct delimitations and is usually a fleshy, weakly sclerotized outgrowth of the tegulum. It is either ridge-like or a more or less pointy fleshy triangular structure. The appendix-like type has clear delimitations and is either longer than broad, or broader than long. The different forms are coded in character 50.

50 Tegular mynoglenine process, form. 0: ridge-like (Fig. 13b, *Parafroneta westlandica*). 1: triangular (Fig. 12a, *Afroneta tenuivulva*). 2: appendix as long as broad. 3: appendix longer than broad. The ridge-like form accounts for a fleshy rather than thin ridge along the distal part of the tegulum and the triangular type for a nearly equilateral, usually carnous triangle emerging from the distal side of the tegulum. States 2 and 3 account for appendix-like processes of which state 3 is usually much larger than state 2.

51 Tegular mynoglenine process, sclerotization. 0: whitish, soft (Fig. 9b, *Afroneta tenuivulva*). 1: brownish, sclerotized (Fig. 9c, *Haplinis diloris*).

52 Tegular mynoglenine process, additional small retrolateral knob (TMK). 0: absent (Fig. 9c, *Haplinis diloris*). 1: present (Fig. 10c, *Promynoglenes silvestris*). In *Promynoglenes* the mynoglenine tegular processes is accompanied by a small knob at its retrolateral side.

53 Tegular flange-like process (TFP). 0: absent (Fig. 9c, *Haplinis diloris*). 1: present (Fig. 9d, *Haplinis subdola*). An additional flange-like process emerges retrolateral to the mynoglenine tegular process in some *Haplinis* species.

54 Suprategulum (SPT). 0: absent (Hormiga, 1994b: fig. 301, *Pimoa altioculata*). 1: present (Fig. 9c, *Haplinis diloris*). A09-23, MH04-24, H00-7 + 11. Following Miller and Hormiga (2004) the mynoglenine tegular apophysis (MTA; character 7 in Hormiga, 2000) is considered homologous with the suprategulum. The suprategulum of mynoglenines varies considerably in form. Different conformations are accounted for in characters 58 and 59.

55 Suprategulum, position on tegulum. 0: proximal (Hormiga, 2000: fig. 14D, *Hilaira excisa*). 1: distal (Fig. 9e, *Laminafroneta bidentata*). In most linyphiids the suprategulum emerges from the proximal part of the tegulum, while in mynoglenines it emerges more distally.

56 Suprategulum, origin. 0: prolateral (Fig. 13b, *Parafroneta westlandica*). 1: retrolateral (Fig. 11e, *Metafroneta sinuosa*).

57 Suprategulum, proximal part orientation. 0: in line with tegulum, pointing distally (Fig. 9c, *Haplinis diloris*). 1: emerging in right angle from tegulum, pointing dorsally (Fig. 9e, *Laminafroneta bidentata*).

58 Suprategulum, form in retrolateral view. 0: straight (Fig. 9a, *Afroneta subfusca*). 1: curved to sigmoid (Fig. 9c, *Haplinis diloris*). In retrolateral view, the dorsal side of the suprategulum can either be straight, narrowing constantly towards its tip or else is curved to the ventral side or even sigmoid.

59 Suprategulum, form in ventral view. 0: broad triangular (12 d, *Laminafroneta bidentata*). 1: narrow finger-like (Fig. 13b, *Parafroneta westlandica*). 2: dagger-like (Fig. 10c, *Promynoglenes silvestris*). 3:

thin long hook (Fig. 10a, *Metamynoglenes helicoides*). A triangular suprategulum is about as long as its proximal diameter. The finger-like suprateguli are longer than broad. *Promynoglenes* has a straight, dagger-like suprategulum pointing distal to ventral. They are more robust than the finger-like suprateguli and have a triangular diameter. Long thin hook-like suprateguli are only found in *Metamynoglenes*. They are very narrow from base to tip.

60 Suprategulum, distal section. 0: entire (Fig. 9a, *Haplinis diloris*). 1: bifid (Fig. 12c, *Hyperafroneta obscura*). The distal section of the suprategular apophysis is bifid in some taxa, i.e. split into the distal suprategular apophysis plus an additional smaller process.

61 Suprategulum, tip coronal direction. 0: none, distal (Fig. 9b, *Afroneta tenuivulva*). 1: ventral (Fig. 10c, *Promynoglenes silvestris*).

62 Suprategulum, tip sagittal direction. 0: none, distal (Fig. 13a, *Novafroneta gladiatrix*). 1: retrolateral (Fig. 12a, *Afroneta tenuivulva*).

63 Foramen (F). 0: in suprategulum (Hormiga, 2000: fig. 14D, *Hilaira excisa*). 1: in tegulum (Fig. 13a, *Novafroneta gladiatrix*). A09-26, MH04-28.

64 Embolic membrane (EM). 0: absent (Hormiga, 1994b: fig. 301, *Pimoa altioculata*). 1: present (Fig. 13a, *Novafroneta gladiatrix*). A09-34, MH04-40, H00-18.

65 Embolic membrane, shape. 0: slender, long and narrow (Fig. 12a, *Afroneta tenuivulva*). 1: broad (Fig. 12b, *Haplinis horningi*). Blest (1979) mentions that the shape of the conductor and its folds can be species-specific (at least in combination with other characters).

66 Embolic membrane, size. 0: hidden below radix (Hormiga, 2000: fig. 14E, *Hilaira excisa*). 1: visible in ventral or prolateral view (Fig. 11a, *Haplinis diloris*).

67 Embolic membrane, sclerotization. 0: membraneous (Fig. 13b, *Parafroneta westlandica*). 1: partially and weakly sclerotized (Fig. 12b, *Haplinis horningi*). 2: fully and strongly sclerotized (Fig. 12d, *Laminafroneta bidentata*).

68 Embolic membrane, tip modification. 0: not modified (Fig. 12a, *Afroneta tenuivulva*). 1: membraneous broadened bundle (Fig. 13a, *Novafroneta gladiatrix*). The tip is particularly broad and modified in *Novafroneta gladiatrix* and supposedly also in *N. truncata* (Blest and Vink, 2003: fig. 23), a species not scored here.

69 Embolic membrane, attachment. 0: attached to column (Hormiga, 2000: fig. 14E, *Hilaira excisa*). 1: attached to tegulum (Fig. 12a, pale area right to the tegulum, *Afroneta tenuivulva*). 2: attached to radix (Blest, 1979: fig. 592: *Australolinyphia remota*). If present, the embolic membrane is attached to the tegulum in mynoglenines, while it emerges from the column in other linyphiids.

70 Embolic membrane, wrapping the embolus. 0: absent (Fig. 12a, *Afroneta tenuivulva*). 1: present (Fig. 12b, *Haplinis horningi*).

71 Embolic membrane, ventral, mesal inwards fold (EMM). 0: absent (Fig. 12b, *Novafroneta gladiatrix*). 1: present (Fig. 9d, *Haplinis subdola*). This is a fold emerging from the retrolateral side of the embolic membrane and turned inwards.

72 Embolic membrane, ventral, ectal outwards fold (EME). 0: absent (Fig. 12a, *Afroneta tenuivulva*). 1: present (Fig. 12b, *Haplinis horningi*). This fold emerges from the prolateral side of the embolic membrane and turns retrolateral, covering the embolus.

73 Embolic membrane, ventral, ectal outwards fold, size. 0: narrow (Fig. 12f, *Metamynoglenes gracilis*). 1: broad lobe (Fig. 12b, *Haplinis horningi*). The size of the embolic membrane can vary considerably from a narrow fold in *Metamynoglenes helicoides* and *Afromynoglenes parkeri* to broad lobes in *Haplinis*.

74 Embolic membrane, distal twist. 0: absent (Fig. 9e, *Laminafroneta bidentata*). 1: present (Fig. 12e, *Metafroneta sinuosa*). The embolic membrane of a few taxa is twisted distally.

75 Terminal apophysis. 0: absent (Fig. 13b, *Parafroneta westlandica*). 1: present (Hormiga, 2000: plate 1B, *Bolyphantes luteolus*). A09-46, MH04-65, H00-26.

76 Radix (R). 0: absent (Hormiga, 1994b: fig. 9, *Pimoa altioculata*). 1: present (Fig. 11d, *Promynoglenes nobilis*). A09-40, MH04-50, H00-20. The presence of a radix supports the monophyly of Linyphiidae (Hormiga, 1993, 1994a, 1994b, Miller and Hormiga, 2004).

77 Radix, size. 0: indistinct, simple with embolus only (Fig. 11d, *Promynoglenes nobilis*). 1: distinct with additional apophyses (Hormiga, 2000: plate 33C, *Hilaira excisa*). State 1 is only found in mynoglenines.

78 Radix, attachment to column (COL). 0: dorsal connection to column (Fig. 13a, *Novafroneta gladiatrix*). 1: ventral connection to column (Fig. 12b, *Haplinis horningi*). The column of *Haplinis* and others is bent proximally, revealing the membraneous tissue of the column in ventral view. Instead, the radix covers the column in taxa with a dorsal connection (e.g. *Afroneta*).

79 Radix plus embolus, proximal part of radix teardrop-shaped. 0: absent (Fig. 11d, *Promynoglenes nobilis*). 1: present (Fig. 11e, *Pseudafroneta pallida*). The radix of some taxa is teardrop-shaped, at least if the distal pointing steadily narrowing embolus is also taken into account. *Hyperafroneta* and *Metafroneta* were also scored as having this character.

80 Radix plus embolus, teardrop-shaped, proximal end. 0: round (Fig. 11e, *Pseudafroneta pallida*). 1: triangular (Fig. 11f, *Trachyneta jocquei*). In some taxa the proximal side of the radix is drawn-out and more or less triangular.

81 Radix, retrolateral appendix (RRA). 0: absent (Fig. 12b, *Haplinis horningi*). 1: present (Fig. 12f, *Metamynoglenes gracilis*). This is a narrowing and easily visible appendix emerging from the radix, pointing retrolaterally. *Pseudafroneta perplexa* also has this appendix, but pointing proximally. The embolic divisions of *Pseudafroneta perplexa* and *Metamynoglenes gracilis* (and other *Metamynoglenes*) are very similar but rotated 90° prolaterally in *Metamynoglenes*. This structure might be homologous to the radical tailpiece (A09-42, MH04-52, H00-21).

82 Sperm duct in radix. 0: not convoluted (Fig. 11f, *Trachyneta jocquei*). 1: convoluted (Fig. 13a, *Novafroneta gladiatrix*).

83 Embolus, origin. 0: distal (Hormiga, 2000: plate 33A, *Hilaira excisa*). 1: proximal (Fig. 11a, *Haplinis diloris*). MH04-42.

84 Embolus, initial orientation. 0: distal (Fig. 11e, *Pseudafroneta pallida*). 1: proximal to prolateral (Fig. 11a, *Haplinis diloris*). 2: retrolateral to ventral (*Bolyphantes luteolus*).

85 Embolus, apical half. 0: robust (Fig. 10e, *Pseudafroneta pallida*). 1: filiform (Fig. 11a, *Haplinis diloris*). A09-38*. The robust embolus has a broad apical half (about as broad as the radix in mynoglenines). It narrows towards the tip in most taxa. The filiform embolus is very narrow in its apical half (and already very narrow when emerging from the radix in mynoglenines).

86 Embolus, form. 0: straight (Fig. 11e, *Pseudafroneta pallida*). 1: curved two-dimensional (Fig. 11c, *Metamynoglenes gracilis*; Fig. 11f, *Trachyneta jocquei*). 2: curved three-dimensional (Fig. 11a, *Haplinis diloris*). 3: circular two-dimensional (Fig. 13c, *Promynoglenes nobilis*). 4: lamellar (Fig. 12e, *Metafroneta sinuosa*). Straight emboli are mostly found in mynoglenines with simple, robust emboli emerging distally from the radix. The two-dimensionally curved embolus either emerges distally from the radix and is somewhat curved (Fig. 11f, *Trachyneta jocquei*), or emerges prolaterally from the radix, continues prolaterally, and finally curves distally (Fig. 11c, *Metamynoglenes gracilis*). In contrast, the three-dimensionally curved embolus additionally turns distal, ventral, retrolateral, and finally in a distal direction. The circular two-dimensionally curved embolus forms a circle around the radix on a coronal plane before turning in a distal direction. The lamellar type is found only in *Hyperafroneta* and *Metafroneta* within the mynoglenines. It is very broad and supposedly more closely related to different robust emboli rather than filiform ones, according to our analysis.

87 Embolus, length. 0: short (Fig. 11f, *Trachyneta jocquei*). 1: long (Fig. 13c, *Promynoglenes nobilis*). MH04-43, H00-17. A long embolus is defined as being at least one-third of cymbial length.

88 Embolus, prolaterally extended above cymbium. 0: positioned entirely ventral to the cymbium (Fig. 11b, *Haplinis tegulata*). 1: extending prolaterally above cymbium (Fig. 11a, *Haplinis diloris*).

89 Embolus, tip. 0: blunt (Fig. 12e, *Metafroneta sinuosa*). 1: pointed (Fig. 11e, *Pseudafroneta pallida*).

90 Embolus, bifurcated apophysis (EBA). 0: absent (Fig. 12e, *Metafroneta sinuosa*). 1: present (Fig. 12c, *Hyperafroneta obscura*). This large and highly sclerotized apophysis emerges from the embolus and is an autapomorphy for *Hyperafroneta obscura* within the mynoglenines. *Australolinyphia remota* also has a bifurcated apophysis emerging from the embolus.

Male somatic characters

91 Clypeus, texture. 0: smooth (Fig. 14b, *Haplinis diloris*). 1: rough, reticulate, or rugose (Hormiga, 2000: plate 8A, C, *Linyphia triangularis*). A09-86, MH04-112.

92 Subocular sulci (SOS). 0: absent (Hormiga, 2000: plate 34B, *Hilaira excisa*). 1: present (Fig. 14b, *Haplinis diloris*). A09-83, MH04-107, H00-47. Subocular sulci are a synapomorphy of Mynogleninae.

93 Subocular sulci, demarcation. 0: continuous with clypeus (Fig. 14a, *Afroneta guttata*). 1: clearly demarcated (Fig. 14b, *Haplinis diloris*). The missing margins are more obvious in females than in males.

94 Subocular sulci, depth. 0: shallow, evenly deep (Fig. 14b; Hormiga, 2000: plate 4A,B *Haplinis diloris*). 1: anteriorly more deeply invaginated (Blest, 1979: fig. 609, *Protoerigone otagoa*). The deeply invaginated sacs are an autapomorphy of *Protoerigone obtusa* in the current analysis but synapomorphic for the genus *Protoerigone*.

95 Subocular sulci, form. 0: longer than broad (Fig. 14b, *Haplinis diloris*). 1: nearly as broad as long (Fig. 13e, *Novafroneta vulgaris*). 2: circular (Blest, 1979: fig. 582, *Cassafroneta forsteri*).

96 Eye-field, AME-size. 0: ≥ other eyes (Hormiga, 1994: fig. 22, *Pimoa rupicola*). 1: < other eyes (Fig. 14b, *Haplinis diloris*).

97 Eye-field, PME-size. 0: ≤ PLE (Fig. 14b; Blest, 1979: fig. 405, *Haplinis diloris*). 1: > PLE (Fig. 14a, *Afroneta guttata*).

98 Eye-field, PME-PLE eye distances. 0: ≥ than PME (Fig. 14b, *Haplinis diloris*). 1: juxtaposed (Fig. 14a, *Afroneta guttata*). 2: < PME (*Afroneta lobelia*).

99 Eye-field, macrosetae and setae on clypeus. 0: one macrosetae (Fig. 14b, *Haplinis diloris*). 1: one macroseta plus many setae (Blest, 1979: figs 583, *Cassafroneta forsteri*). A09-87*, MH04-113*. We scored females instead of males.

100 Eye-field, post-PME macroseta. 0: one (Fig. 14b, *Haplinis diloris*). 1: two (Fig. 13e, *Novafroneta vulgaris*). Most species have a row of setae along the back of the cephalothorax running from the PME to the fovea. The first one behind the PME is considerably thicker and longer than the other setae and is considered here as a macroseta. Some species have two macrosetae behind the PME.

101 Cephalothorax, post PME-lobe. 0: absent (Fig. 13d, *Parafroneta haurokoae*). 1: present (Blest, 1979: fig. 582, *Cassafroneta forsteri*). A09-82, MH04-103, H00-43. Only distinct lobes have been considered.

102 Chelicerae, lateral face. 0: smooth (*Haplinis abbreviata*). 1: stridulatory striae (Hormiga, 2000: plate 3E, *Haplinis diloris*). A09-90, MH04-116, H00-55.

103 Chelicerae, stridulatory striae rows. 0: widely and evenly spaced (Hormiga, 2000: plate 1E, *Bolyphantes luteolus*). 1: compressed and evenly spaced (Hormiga, 2000: plate 3E, *Haplinis diloris*). A09-92*, MH04-118*.

104 Chelicerae, promarginal teeth (CPT). 0: three (*Bolyphantes luteolus*). 1: four (Fig. 14c, *Haplinis diloris*). 2: five or more (Fig. 14a, *Afroneta guttata*). A09-96*. Males showed many characters on the chelicerae that were not present in the females, therefore the chelicerae teeth were scored for the males. Previous analyses on linyphids used females instead (Hormiga, 2000; Miller and Hormiga, 2004).

105 Chelicerae, retromarginal denticles (CRD). 0: two or three (*Bolyphantes luteolus*). 1: four (Fig. 14c, *Haplinis diloris*). 2: five or six (*Haplinis horningi*). 3: nine or more (*Haplinis abbreviata*). A09-97*, MH04-123*, H00-58*. We scored males instead of females.

106 Chelicerae, retrolateral denticles, position. 0: separated from prolateral row (Hormiga, 2000: plate 60C, *Sciastes truncatus*). 1: distal teeth adjacent to prolateral row (Fig. 14c, *Haplinis diloris*).

107 Chelicerae, posterior side, proximal hirsute field on bump (CPB). 0: hirsute field without bump (Hormiga, 2000: fig. 7E, *Linyphia triangularis*). 1: hirsute field on bump (Fig. 14c; Hormiga, 2000: plate 78A, *Haplinis diloris*). Posterior side of chelicera bears a hirsute bump proximally.

108 Chelicerae, posterior central free standing seta (CPS). 0: base of seta nearly flush with chelicerae to small bump (Fig. 14d, *Afroneta guttata*). 1: base of seta formed into distinct bump (Fig. 14c, *Haplinis diloris*). State 0 is found in most African taxa, state 1 in most New Zealand taxa.

109 Chelicerae, posterior side, distal bump. 0: absent (Fig. 14a, *Haplinis diloris*). 1: present (*Trachyneta jocquei*; Holm, 1968: fig. 65, *Trachyneta extensa*). The posterior side of the chelicera has a distal bump in *Trachyneta jocquei*. In the current analysis, this is an autapomorphy of *T. jocquei*. It is also present in *T. extensa* (Holm, 1968: fig. 65) and therefore is a synapomorphy for the genus *Trachyneta*.

110 Pedicel sternite (PS) and pleurites. 0: separated (Miller and Hormiga, 2004: fig. 21H, *Mermessus dentiger*). 1: juxtaposed or fused (Fig. 14e, *Haplinis diloris*). A09-126, MH04-153.

111 Pedicel sternite, bifid prolongation (PBP). 0: absent (Fig. 14f, *Afroneta tenuivulva*). 1: present (Fig. 14e, *Haplinis diloris*). In some species the sternite is ventrally extended towards the abdomen. It is bifid in most species and the two "tips" are connected. A central unsclerotized area remains between the two branches and its distal connection. *Afromynoglenes parkeri* has only an inconspicuous area, visible in frontal view. The sclerotized prolongation is very distinct in other species with distinct bifid branches.

112 Pedicel sternite, bifid prolongation, connection (PBC). 0: absent (Fig. 13g, *Novafroneta vulgaris*). 1: present (Fig. 14e, *Haplinis diloris*). See ch111. *Haplinis insignis* has a branch but seems to lack the unsclerotized area in the centre; however, the tip of the branch is bifid. *Novafroneta vulgaris* has been coded as lacking the connection. It has only a slightly sclerotized section that connects both branches, whereas in other species the connection is a broad sclerotized structure.

113 Pedicel sternite, median pouch (PMP). 0: absent (Fig. 14f, *Afroneta tenuivulva*). 1: present (Fig. 4e, *Haplinis diloris*). The sternite of the pedicel is provided with a cloverleaf-shaped pouch at the junction between pedicel and sternum.

114 Pedicel-sternum connection, width. 0: broad, 0.50-1.00 times diameter of coxa IV (Fig. 14f, *Afroneta tenuivulva*). 1: intermediate, ca. 0.25 times diameter of coxa IV (Fig. 13g, *Novafroneta vulgaris*). 2: very narrow, less than 0.2 times diameter of coxa IV (Fig. 14e, *Haplinis diloris*). The width of the connection in *H. titan* is somewhat intermediate between states 1 and 2.

115 Sternum, sclerotization between coxae IV. 0: nearly not sclerotized (Fig. 14f, *Afroneta tenuivulva*). 1: strongly sclerotized (Fig. 14e, *Haplinis diloris*). This refers to the extension between the coxa IV. *Afroneta lobelia* has a slightly different type of sternite that is slightly sclerotized.

116 Abdominal pattern, transverse connection between two dorsal rows of white dots. 0: separated (Fig. 15b, *Afroneta guttata*). 1: transversely connected (Fig. 15a, *Pseudafroneta pallida*). If connected they appear nearly as white transverse lines. This applies mainly to the frontal pairs of dots as the distal ones are usually so close that they are always somewhat connected.

117 Abdominal pattern, longitudinal connection between two dorsal rows of white dots. 0: separated (Fig. 15b, *Afroneta guttata*). 1: longitudinally connected (Fig. 15a, *Pseudafroneta pallida*). If connected, dots appear nearly as white longitudinal zig-zag lines.

118 Femur I retrolateral proximal texture (FRT). 0: smooth and hirsute as the remaining femur (Fig. 13f, *Pseudafroneta pallida*, like femur leg II). 1: scaly, glabrous field adjacent to joint of trochanter (Fig. 13f, *Pseudafroneta pallida*, femur leg I).

119 Metatarsus I and II distal macroseta(e). 0: absent. 1: present (*Linyphia triangularis*).

Female copulatory organs

120 Epigyne, ventral plate, depression (EVD). 0: absent (Fig. 16e, *Laminafroneta brevistyla*). 1: one oval depression (Fig. 16b, *Afroneta lobeliae*). 2: two nearly circular depressions (Fig. 16d, *Haplinis tegulata*). The ventral plate often defines an oval depression that can also be interrupted by a septum, forming two separate atria.

121 Epigyne, ventral plate, anterior and lateral sclerotized margin (ELM). 0: absent (Fig. 16b, *Afroneta lobeliae*). 1: present (Fig. 16d, *Haplinis tegulata*). The anterior margin of the ventral plate depression is sometimes clearly defined by a ventral pointing margin. In some cases the margin continues along the lateral side of the epigyne.

122 Epigyne, ventral plate, posteriorly margined (EPM). 0: absent (Fig. 16c, *Haplinis diloris*). 1: present (Fig. 16d, *Haplinis tegulata*).

123 Epigyne, ventral plate, postero-centrally margined (ECM). 0: absent (Fig. 16b, *Afroneta lobeliae*). 1: present (Fig. 16d, *Haplinis tegulata*).

124 Epigyne, postero-central margin thickened part (ECT). 0: absent (Fig. 16d, *Haplinis tegulata*). 1: present (Fig. 16f, *Metamynoglenes gracilis*).

125 Epigyne, ventral plate, lateral glabrous area (ELA). 0: absent (Hormiga, 2000: plate 8D, *Linyphia triangularis*). 1: present (Fig. 16d, *Haplinis tegulata*). This character describes the lateral side of the depression (ch120), which is always a more or less enlarged glabrous area and always present in mynoglenines.

126 Epigyne, ventral plate, lateral side with ventral extension (ELS). 0: absent (Fig. 17b, *Haplinis horningi*). 1: present, ventral extension (Fig. 17a, *Cassafroneta forsteri*). Lateral sides of the epigynum with ventral extensions. In the current analysis observed in *Cassafroneta forsteri* and *Bolyphantes luteolus* (Helsdingen et al., 2001: fig. 67).

127 Epigyne, ventral plate, lateral side with median extension (EME). 0: absent, restricted to lateral side (Fig. 16b, *Afroneta lobeliae*). 1: present, median extension (Fig. 16d, *Haplinis tegulata*). The lateral side of the ventral plate extends medially and covers the dorsal plate in *Haplinis* and other genera. This "median extension" is always glabrous.

128 Epigyne, ventral plate, median extension, posterior edges. 0: round (Fig. 16d, *Haplinis tegulata*). 1: rectangular, angular (Fig. 16c, *Haplinis diloris*).

129 Epigyne, ventral plate, median extension, median margins. 0: not parallel (Fig. 16d, *Haplinis tegulata*). 1: parallel (Fig. 16c, *Haplinis diloris*).

130 Epigyne, ventral plate, median extension, median margins, separation. 0: juxtaposed (Fig. 16c, *Haplinis diloris*). 1: separated by ca. diameter of scape (Fig. 16d, *Haplinis tegulata*).

131 Epigyne, median extension (EME) and dorsal plate scape (DPS) are flush with abdomen. 0: absent, not flush (Fig. 17b, *Haplinis horningi*). 1: present, flush (Fig. 17c, *Metafroneta sinuosa*). Usually the dorsal plate scape and the median extension are on different levels. The median extension is dorsal to the scape, while the scape is ventral or dorsal to the surrounding tissue.

132 Epigyne, ventrally protruding thickened median edge (EVE). 0: not protruding ventrally (Fig. 17b, *Haplinis horningi*). 1: protruding ventrally, hook-like (Fig. 17d, *Metamynoglenes helicoides*).

133 Epigyne, ventral plate, anteriorly broad transverse tube (VTT). 0: absent (Fig. 16d, *Haplinis tegulata*). 1: present (Fig. 16a, *Afroneta bamilekei*).

134 Epigyne, ventral plate, anterior margin depression (VAD). 0: margin at same level as surrounding tissue (Fig. 17b, *Haplinis horningi*). 1: median section of margin with depression (Fig. 17e, *Parafroneta minuta*). The anterior margin of the epigynal depression is usually continuous. A depressed median section interrupts the anterior margin in some taxa.

135 Epigyne, ventral plate, sclerotization of anterior margin of copulatory duct (VAS). 0: absent (Fig. 16d, *Haplinis tegulata*). 1: present (Fig. 16e, *Laminafroneta brevistyla*). This character accounts for the sclerotized anterior margin of the copulatory duct in *Laminafroneta*. It marks the point where the ventral and dorsal plates fuse and is shifted posteriorly compared with other mynoglenines.

136 Epigyne, ventral plate, median section, narrow ridge (VMR). 0: absent (Fig. 16a, *Afroneta bamilekei*). 1: present (Fig. 16b, *Afroneta lobeliae*). The anterior median part of the ventral plate can have a longitudinal ventral elevation. This may arise from a transverse tube-like form (ch133) or from the base of an anterior scape.

137 Epigyne, dorsal plate, posterior margin. 0: narrow, about as broad as scape (Fig. 17d, *Metamynoglenes helicoides*). 1: broad, nearly as broad as epigyne (Fig. 17c, *Metafroneta sinuosa*).

138 Epigyne, ventral plate and dorsal plate fusion. 0: concave, U-shaped in lateral view (Fig. 16a, *Afroneta bamilekei*). 1: concave, S-shaped in lateral view (Fig. 16d, *Haplinis tegulata*). 2: convex, shaped like a "?" in lateral view (Fig. 15g, *Novafroneta gladiatrix*). State 0 accounts for simple epigynes, where no separation between plates is detectable but a small posteriorly situated scape or knob may be seen. State 1 accounts for what is seen in most *Haplinis* species, where the base of the dorsal plate is hidden behind the lateral extensions. The dorsal plate extends from its anterior side towards the posterior side and forms a cap around the scape, which emerges anteriorly from the ventral plate. State 2 accounts for the septum found in *Novafroneta gladiatrix*.

139 Epigyne, copulatory opening (CO). 0: formed by ventral plate (Fig. 16f, *Metamynoglenes gracilis*). 1: formed by ventral and dorsal plate (Fig. 16b, *Afroneta lobeliae*).

140 Epigyne, socket (SO). 0: absent (Fig. 16e, *Laminafroneta brevistyla*). 1: present (Fig. 17f, *Parafroneta westlandica*). A09-67*+70*+71*, MH04-89*+90*. We score all sockets found in mynoglenines as homologous independent of their position.

141 Epigyne, ventral plate scape (VPS). 0: absent (Fig. 16a, *Afroneta bamilekei*). 1: present (Roberts, 1987: fig. 71C, *Diplostyla concolor*). A09-66, MH04-81, H00-33.

142 Epigyne, dorsal plate scape (DPS). 0: absent (Hormiga, 2000: fig. 14G, *Hilaira excisa*). 1: present (Fig. 16c, *Haplinis diloris*). A09-65, MH04-79, H00-33. Most mynoglenines have a dorsal scape that varies in position and shape. In some taxa this scape emerges from the anterior side of the dorsal plate (see ch144). The sclerotization and the attachment seen in aboral view show that they are a part of the dorsal plate rather than the ventral plate.

143 Epigyne, dorsal plate scape type. 0: knob-like (Fig. 17f, *Parafroneta westlandica*). 1: elongated (Fig. 16c, *Haplinis diloris*).

144 Epigyne, dorsal plate scape origin. 0: anterior, i.e. ventral (Fig. 16d, *Haplinis tegulata*). 1: median, i.e. intermediate (Fig. 13g, *Novafroneta gladiatrix*). 2: posterior, i.e. dorsal (Fig. 16a, *Afroneta bamilekei*). Our definition of scape is broad and therefore also accommodates the knob-like structures seen in several genera.

145 Epigyne, dorsal plate scape, longitudinal direction. 0: no longitudinal extension (Fig. 16a, *Afroneta bamilekei*). 1: anterior (Fig. 17c, *Metafroneta sinuosa*). 2: posterior (Fig. 16c, *Haplinis diloris*).

146 Epigyne, dorsal plate scape, sagittal direction. 0: no sagittal expansion (Fig. 17b, *Haplinis horningi*). 1: ventral (Fig. 17d, *Metamynoglenes helicoides*).

147 Epigyne, copulatory opening, outer circular depression (CCP). 0: only slit to tiny depression (Fig. 16a, *Afroneta bamilekei*). 1: deep circular depression with slit (Fig. 17d, *Metamynoglenes helicoides*).

This character accounts for the shape of the openings to the vulva. It refers only to the sclerotized part where the ventral and dorsal plates are fused to form a slit.

148 Copulatory duct (CD) turning point. 0: absent (Blest, 1979: fig. 578, *Metafroneta sinuosa*). 1: present (Blest, 1979: fig. 478, *Promynoglenes nobilis*). A09-76.

149 Copulatory duct, complexity. 0: short, direct (Merrett, 2004: fig. 55, *Afroneta bamilekei*). 1: long, with loops or coils (Blest, 1979: fig. 420, *Haplinis diloris*).

150 Copulatory duct, shape of encapsulation. 0: straight to curved (Fig. 16b, *Afroneta lobeliae*). 1: coiled (Fig. 16c, *Haplinis diloris*).

151 Copulatory duct, length. 0: shorter than the receptacula (Merrett, 2004: fig. 84, *Laminafroneta bidentata*). 1: about as long as receptacula (Merrett, 2004: fig. 29, *Afroneta lobeliae*). 2: much longer than receptacula (Merrett, 2004: fig. 60, *Afroneta guttata*).

152 Copulatory duct, number of helical turns. 0: none (Merrett, 2004: fig. 84, *Laminafroneta bidentata*). 1: one (Blest, 1979: fig. 494, *Metamynoglenes gracilis*). 2: three (Blest, 1979: fig. 492, *Metamynoglenes helicoides*). 3: four to five (Blest, 1979: fig. 478, *Promynoglenes nobilis*). The number of helical turns is also diagnostic for different species groups within *Haplinis* as defined by Blest (1979: 103).

Female somatic characters

153 Thorax, foveal double setae (TFD), length. 0: short, as surrounding setae. 1: longer (Fig. 15a, *Pseudafroneta pallida*).

154 Palpal tarsus, proximal dorsomesal macrosetae. 0: absent. 1: present (Fig. 15d, *Afroneta guttata*). A09-101, MH04-127.

155 Palpal tarsus, distal dorsomesal macrosetae. 0: absent. 1: present (Fig. 15d, *Afroneta guttata*). A09-102, MH04-128.

156 Palpal tarsus, proximal dorsoectal macrosetae. 0: absent (Fig. 15e, *Afroneta guttata*). 1: present. A09-103, MH04-129.

157 Palpal tarsus, distal dorsoectal macrosetae. 0: absent (Fig. 15e, *Afroneta guttata*). 1: present. A09-104, MH04-130.

158 Palpal tarsus, ventromesal macrosetae. 0: two. 1: three (Miller and Hormiga, 2004: fig. 21D, *Triplogyna major*). 2: four (Miller and Hormiga, 2004: fig. 21F, *Neocautinella neoterica*). 3: five or six (*Linyphia triangularis*). 4: eleven or twelve (*Pimoa altioculata*). A09-105*, MH04-131*.

159 Palpal tarsus, ventroectal macrosetae. 0: one. 1: two (Miller and Hormiga, 2004: fig. 21E, *Triplogyna major*). 2: three (Fig. 15e, *Afroneta guttata*). A09-106*, MH04-132*.

160 Palpal tibia, distal dorsoectal macrosetae. 0: absent (Fig. 15e, *Afroneta guttata*). 1: present (*Afroneta lobelia*).

161 Palpal tibia, distal ectal macrosetae (TEM). 0: absent. 1: present (Fig. 15e, *Afroneta guttata*).

162 Palpal tibia, dorsomesal trichobothria (TMT). 0: one (*Linyphia triangularis*). 1: two (Fig. 15d, *Afroneta guttata*). 2: three (*Pimoa altioculata*).

163 Palpal tibia, dorsoectal trichobothria (TET). 0: two. 1: three (Fig. 15e, *Afroneta guttata*). 2: four or five (*Pimoa altioculata*).

164 Femur I, prolateral macroseta(ae). 0: absent. 1: one (*Promynoglenes*). 2: two or more (*Novafroneta vulgaris*). A09-111*, MH04-135*.

165 Femur I and II, dorsal macroseta(ae). 0: absent (*Metamynoglenes*). 1: one or more. A09-110*, MH04-134*. Blest (1979) notes that, dorsal femoral macrosetae are present or absent in various combinations and not always consistent even within species.

166 Tibial spine (macrosetae) formula. 0: 2222. 1: 2221. A09-112*-116*, MH04-136*-143*, H00-61*-64*. 2221 occurs only in *Trachyneta jocquei*.

167 Tibia I, prolateral macroseta(ae). 0: absent. 1: one. 2: two or more. A09-117*, MH04-144*.

168 Tibia I, retrolateral macroseta(ae). 0: absent. 1: one. 2: two or more. A09-118*, MH04-145*.

169 Tibia I, ventral prolateral row macroseta(e) (TVP). 0: absent. 1: one (*Haplinis diloris*). 2: two or more (Fig. 15f, *Afroneta guttata*). The formerly used character "ventral tibial macrosetae" (A09-119*, MH04-146*) was divided into more characters to create more specific homology statements for the different ventral macrosetae.

170 Tibia I, ventral retrolateral row macroseta(e) (TVR). 0: absent. 1: one. 2: two or more (Fig. 15f, *Afroneta guttata*). The second row is situated retrolaterally to the prolateral row.

171 Tibia I, ventral proximal prolateral macroseta (TPP). 0: absent. 1: one (Fig. 15f, *Afroneta guttata*).

172 Tibia I, ventral proximal retrolateral macroseta (TPR). 0: absent. 1: one (Fig. 15f, *Afroneta guttata*). One present on the right leg only of *Afromynoglenes parkeri* (none in the males)

173 Tibia I, ventral distal macroseta(e) (TVD). 0: absent. 1: one. 2: two (Fig. 15f, *Afroneta guttata*).

174 Tibia IV, prolateral macroseta(e). 0: absent. 1: one. 2: two or more.

175 Tibia IV, prolateral distal macroseta(e). 0: absent. 1: one.

176 Tibia IV, retrolateral macroseta(e). 0: absent. 1: one. 2: two or more (*Haplinis horningi*).

177 Tibia IV, retrolateral distal macroseta(e). 0: absent. 1: one (*Haplinis diloris*). These macrosetae are situated right at the distal margin to the metatarsus.

178 Tibia IV, ventral prolateral row macroseta(e). 0: absent. 1: one. 2: two or more (*Haplinis diloris*).

179 Tibia IV, ventral retrolateral row macroseta(e). 0: absent. 1: one. 2: two or more (*Haplinis diloris*).

180 Tibia IV, ventral proximal prolateral macroseta. 0: absent. 1: one.

181 Tibia IV, ventral proximal retrolateral macroseta. 0: absent. 1: one.

182 Tibia IV, ventral distal macroseta(e). 0: absent. 1: one (*Cassafroneta forsteri*). 2: two (*Haplinis diloris*). These macrosetae are situated right at the distal margin to the metatarsus.

183 Metatarsus IV, dorsal macroseta(e). 0: absent. 1: one (*Laminafroneta brevistyla*). 2: two or more.

184 Metatarsus IV, prolateral macroseta(e). 0: absent. 1: one (*Laminafroneta brevistyla*). 2: two or more (*Haplinis tegulata*).

185 Metatarsus IV, ventral macroseta(e). 0: absent. 1: one (*Laminafroneta brevistyla*). 2: two or more (*Haplinis tegulata*).

186 Metatarsus IV, retrolateral macroseta(e). 0: absent. 1: one or more.

187 Metatarsus IV, distal macroseta(e). 0: absent. 1: one or more (usually three to four).

188 Metatarsus IV, trichobothrium. 0: absent. 1: present. A09-124*, MH04-152*, H00-65*.

189 Legs, tibia coloration. 0: without annulations. 1: with annulations.

190 Legs I, II, macrosetae strength. 0: weak, reduced or almost reduced to setae. 1: well developed.

Appendix 4 Character matrix

Rows represent characters and columns taxa. The last three columns give the length (steps), consistency index (ci), and retention index (ri) assigned to the character. Calculations are based on the preferred tree from the equally weighted analysis. Tree statistics: length = 871; CI = 0.28; RI = 0.62.

Character	*Pimoa altiocalata*	*Stemonyphantes lineata*	*Linyphia triangularis*	*Bolyphantes luteolus*	*Australolinyphia remota*	*Diplostyla concolor*	*Hilaira excisa*	*Cassafroneta forsteri*	*Novafroneta gladiatrix*	*Novafroneta vulgaris*	*Hyperafroneta obscura*	*Metafroneta sinuosa*	*Protoerigone otagoa*	*Pseudafroneta perplexa*	*Pseudafroneta pallida*	*Parafroneta minuta*	*Parafroneta hauroko*ae	*Parafroneta demota*	*Parafroneta confusa*	*Parafroneta marrineri*	*Parafroneta westlandica*	*Trachyneta jocquei*	*Gibbafroneta gibbosa*	*Laminafroneta bidentata*	*Laminafroneta brevistyla*	*Afroneta hamiltekei*	*Afroneta subfusca*	*Afroneta guttata*	*Afroneta lobeliae*	*Afroneta tenuivulva*	*Afromyoglenes parkeri*	*Promyoglenes silvestris*	*Promyoglenes nobilis*	*Promyoglenes grandis*	*Metamyoglenes helicoides*	*Metamyoglenes gracilis*	*Metamyoglenes incurvata*	*Haplinis insignis*	*Haplinis abbreviata*	*Haplinis illoris*	*Haplinis hornungi*	*Haplinis subdola*	*Haplinis tegulata*	*Haplinis titan*	steps	ci	ri
1	0	1	0	0	0	0	–	2	0	0	2	1	2	1	0	1	1	1	1	1	1	1	2	1	1	1	1	1	1	2	1	1	0	1	1	0	0	1	1	1	1	1	2	1	11	0.18	0.40
2	0	0	0	0	0	0	0	–	0	0	0	1	1	1	0	0	0	0	0	0	0	0	1	1	1	0	1	0	0	0	1	1	1	1	1	1	0	1	1	1	1	1	0	0	7	0.14	0.68
3	0	0	0	0	0	0	0	0	0	1	1	0	0	0	0	0	0	0	0	0	0	0	0	0	0	0	0	0	0	0	0	0	0	0	0	0	0	0	0	0	0	0	0	0	1	1.00	1.00
4	1	1	0	0	0	0	0	0	0	0	1	0	0	0	0	0	0	0	0	0	0	0	0	0	0	0	0	0	0	0	0	0	0	0	1	0	0	0	0	0	0	0	0	0	3	0.33	0.33
5	0	0	0	0	0	0	1	0	0	0	0	0	0	0	0	0	0	0	0	0	0	0	0	0	0	0	0	0	0	0	0	0	0	0	0	0	0	0	0	0	0	0	0	0	1	1.00	0.00
6	0	0	1	0	0	0	0	1	1	1	1	1	1	1	1	1	1	1	1	1	1	1	0	1	1	0	1	1	1	1	1	0	0	0	1	1	1	0	1	1	1	0	1	1	7	0.14	0.50
7	0	0	0	0	0	0	0	0	1	1	0	0	0	0	0	0	0	0	0	0	0	0	0	0	0	0	0	0	0	0	0	0	0	0	0	0	0	0	0	0	0	0	0	0	1	1.00	1.00
8	1	0	0	0	0	0	0	0	0	0	0	1	1	1	0	1	0	1	1	0	1	0	0	0	0	1	1	1	1	1	0	0	0	0	0	0	0	0	1	1	1	2	2	10	0.20	0.50
9	1	0	1	0	0	0	0	0	0	0	0	0	1	1	0	0	0	1	1	1	1	0	0	0	0	1	0	0	1	1	0	0	0	0	0	0	0	0	1	1	0	2	1	9	0.22	0.46
10	0	0	0	0	1	1	0	1	1	1	1	1	1	1	1	1	1	1	1	1	1	1	1	1	1	1	1	1	1	1	1	1	1	1	1	1	1	1	1	1	1	1	1	1	2	0.50	0.75
11	0	0	0	0	1	0	0	0	0	0	0	0	0	0	0	0	0	0	0	0	0	0	0	0	0	0	0	0	0	0	1	0	0	1	1	0	1	0	0	0	0	0	0	0	5	0.20	0.00
12	0	1	0	0	1	1	0	0	0	0	0	0	0	0	0	0	0	0	0	0	0	0	0	0	0	0	0	0	0	0	1	0	0	1	1	0	1	0	0	0	0	0	0	0	7	0.14	0.00
13	0	0	0	0	0	0	0	0	0	0	0	0	0	0	0	0	0	0	0	0	0	0	0	0	0	0	0	0	0	0	0	0	0	0	1	0	0	0	0	0	0	0	0	0	1	1.00	0.00
14	0	0	0	0	0	0	0	0	0	0	0	0	0	0	0	0	0	0	0	0	0	0	0	0	0	0	0	0	0	0	0	0	0	0	1	0	0	0	1	1	1	0	0	0	2	0.50	0.67
15	0	0	0	0	0	0	0	0	0	0	0	0	0	0	0	0	0	0	0	0	0	0	0	0	0	0	0	0	0	0	0	1	1	1	0	0	0	0	0	0	0	0	0	0	1	1.00	1.00
16	0	0	0	0	0	0	0	0	0	0	0	0	0	0	0	0	0	0	0	0	0	0	0	0	0	0	0	0	0	0	0	0	0	0	1	1	1	0	0	0	0	1	1	1	2	0.50	0.80
17	0	0	1	1	0	0	0	0	0	0	0	0	0	0	0	0	0	0	0	0	0	0	0	0	0	0	0	0	0	0	1	1	1	1	1	1	1	0	0	0	0	0	0	0	3	0.33	0.75
18	0	0	0	0	0	0	0	0	0	0	0	0	0	0	0	0	0	0	0	0	0	0	0	0	0	0	0	0	0	0	0	1	1	1	1	0	0	0	0	0	0	0	0	0	2	0.50	0.67
19	0	0	0	0	0	0	0	1	2	2	1	2	2	2	2	2	1	2	2	2	2	1	1	1	1	1	1	1	1	1	2	1	1	1	1	1	1	2	2	2	2	2	2	2	7	0.29	0.78
20	0	0	0	0	0	0	0	0	0	1	1	0	0	0	1	1	0	0	0	1	1	1	0	0	0	0	0	0	0	0	1	0	0	0	0	0	0	0	1	1	1	1	1	7	0.14	0.50
21	0	0	0	0	0	0	0	0	0	1	1	0	1	1	1	1	1	1	1	1	1	1	1	1	1	1	1	1	1	1	1	0	0	0	0	0	0	0	0	0	0	1	1	4	0.25	0.84
22	0	1	0	0	1	1	1	1	0	0	0	0	0	0	0	0	0	0	0	0	0	0	0	0	0	0	0	0	0	0	1	1	1	1	1	0	0	0	0	0	0	0	0	0	6	0.17	0.44
23	0	1	0	1	0	0	0	0	0	0	0	0	0	0	0	0	0	0	0	0	0	0	0	0	0	0	0	0	0	0	0	0	0	0	0	0	0	0	0	0	0	0	0	0	2	0.50	0.00
24	0	0	0	0	0	0	0	0	0	0	0	0	0	0	0	0	0	0	0	0	0	0	0	0	0	0	0	0	0	0	0	0	0	0	0	0	0	0	0	0	1	0	0	1	1	1.00	0.00
25	–	0	0	0	0	0	0	1	0	1	1	0	1	0	1	1	1	1	1	0	1	1	1	1	1	1	1	1	1	1	0	0	0	0	0	0	0	0	0	0	0	0	0	0	6	0.17	0.74
26	1	0	0	0	0	0	0	0	0	0	0	0	0	0	0	0	0	0	0	0	0	0	0	0	0	0	0	0	0	0	0	0	0	0	0	0	0	0	0	0	0	0	0	0	1	1.00	0.00
27	0	1	1	2	1	2	2	1	1	1	1	1	1	1	1	1	1	1	1	1	1	1	1	1	1	1	1	1	1	1	1	1	1	1	1	1	1	1	1	1	1	1	1	1	4	0.50	0.00
28	5	5	5	5	2	2	3	0	1	1	2	2	2	2	2	2	2	2	2	3	2	2	4	2	3	4	4	3	5	5	3	2	2	2	2	2	2	5	3	2	2	5	3	3	15	0.33	0.41
29	1	1	0	0	0	0	1	–	0	0	0	0	0	0	0	0	0	0	0	0	0	0	0	0	1	1	0	0	0	0	0	0	0	0	0	0	0	0	0	0	0	0	0	0	3	0.33	0.50
30	0	0	0	0	0	0	0	0	–	0	0	0	0	0	0	0	0	0	0	0	0	0	0	0	0	0	0	0	0	0	0	0	0	0	0	0	1	0	0	0	1	1	1	2	0.50	0.67
31	0	0	0	0	0	0	1	1	0	0	1	1	1	1	0	0	0	0	0	0	0	0	0	0	0	0	0	0	0	0	1	1	1	1	1	1	1	1	1	1	1	1	1	1	4	0.25	0.83
32	0	0	0	0	0	0	1	0	0	0	1	0	0	0	0	0	0	0	0	0	0	0	0	0	0	0	0	0	0	0	1	1	1	1	1	1	0	0	0	0	0	0	0	0	4	0.25	0.57
33	0	0	0	0	0	0	0	0	0	0	0	0	0	0	0	0	0	0	0	0	0	0	0	0	0	0	0	0	0	0	0	0	0	0	0	0	0	0	1	0	0	2	0.50	0.00
34	1	1	0	0	0	0	1	0	0	0	0	0	0	0	0	0	0	0	0	0	0	0	0	0	0	0	0	0	0	0	0	1	1	0	0	0	0	0	0	0	0	0	0	0	3	0.33	0.50
35	–	0	0	1	0	–	1	0	0	0	1	1	1	1	0	0	0	0	0	0	0	0	0	0	0	0	0	0	0	0	0	1	1	1	1	1	1	1	1	1	1	1	1	1	5	0.20	0.78
36	–	–	–	–	–	–	–	–	0	0	–	1	0	0	0	0	0	0	0	0	0	0	0	0	0	0	0	0	0	0	0	2	2	2	2	2	2	1	1	1	1	1	1	1	3	0.67	0.92
37	–	0	0	0	0	0	0	0	0	0	0	0	0	0	0	0	0	0	0	0	0	0	0	0	0	0	0	0	0	0	0	0	0	0	1	1	1	0	0	0	0	0	0	0	1	1.00	1.00
38	–	0	0	0	0	0	0	0	1	0	0	0	0	1	0	0	0	0	0	0	0	0	0	1	1	0	0	0	0	0	0	0	0	0	0	0	0	0	0	0	0	0	0	0	3	0.33	0.33
39	–	0	0	0	0	0	0	1	1	0	1	0	0	1	1	1	1	1	1	1	1	1	1	1	1	1	0	1	1	1	1	0	0	0	0	0	0	0	0	0	0	0	0	0	6	0.17	0.74
40	0	0	0	0	1	1	0	0	0	0	0	0	0	0	0	0	0	0	0	0	0	0	1	0	0	0	0	0	1	1	0	0	0	0	0	1	1	1	0	0	0	0	0	0	5	0.20	0.43
41	2	1	1	1	1	1	0	1	0	0	1	1	1	1	1	0	0	0	0	0	0	1	1	1	1	1	1	1	1	1	1	1	1	1	1	1	1	1	1	1	1	0	1	5	0.40	0.67
42	0	0	0	0	0	0	0	0	1	1	0	0	0	0	0	0	0	0	0	0	0	0	0	0	0	0	0	0	0	0	0	0	0	0	0	0	0	0	1	1	0	0	1	3	0.33	0.50
43	0	0	0	0	–	0	0	0	0	0	0	0	1	1	1	1	1	1	1	1	1	1	1	1	1	1	1	1	1	1	1	1	1	1	1	1	0	0	0	0	0	0	0	2	0.50	0.94
44	0	0	0	0	–	0	0	0	1	1	0	0	0	0	0	0	0	0	0	0	0	0	0	0	0	0	0	0	0	0	0	0	0	0	0	0	0	0	0	0	0	0	0	1	1	1.00	1.00
45	0	0	1	1	0	0	0	0	0	0	0	0	0	0	0	0	0	0	0	0	0	0	0	0	0	0	0	0	0	0	1	1	1	1	1	1	1	1	1	1	1	1	1	2	2	0.50	0.93

(*Continued*)

Character	*Pimoa altioculata*	*Stemonyphantes lineata*	*Linyphia triangularis*	*Bolyphantes luteolus*	*Australolinyphia remota*	*Diplostyla concolor*	*Hilaira excisa*	*Cassafroneta forsteri*	*Novafroneta gladiatrix*	*Novafroneta vulgaris*	*Hyperafroneta obscura*	*Metafroneta sinuosa*	*Protoerigone otagoa*	*Pseudafroneta perplexa*	*Pseudafroneta pallida*	*Parafroneta minuta*	*Parafroneta haurokoae*	*Parafroneta demota*	*Parafroneta confusa*	*Parafroneta marrineri*	*Parafroneta westlandica*	*Trachyneta jocquei*	*Gibbafroneta gibbosa*	*Laminafroneta bidentata*	*Laminafroneta brevistyla*	*Afroneta bamilekei*	*Afroneta subfusca*	*Afroneta guttata*	*Afroneta lobeliae*	*Afroneta tenuivulva*	*Afromynoglenes parkeri*	*Promynoglenes silvestris*	*Promynoglenes nobilis*	*Promynoglenes grandis*	*Metamynoglenes helicoides*	*Metamynoglenes gracilis*	*Metamynoglenes incurvata*	*Haplinis insignis*	*Haplinis abbreviata*	*Haplinis diloris*	*Haplinis horningi*	*Haplinis subdola*	*Haplinis tegulata*	*Haplinis titan*	steps	ci	ri
46	–	–	0	0	–	–	–	–	–	–	–	–	–	–	–	–	–	–	–	–	–	–	–	–	–	–	–	–	–	–	0	0	0	0	1	1	1	0	0	0	0	0	0	0	1	1.00	1.00
47	0	0	1	1	1	1	1	0	0	0	1	1	1	1	1	1	1	1	1	1	1	1	1	1	1	1	1	1	1	1	1	1	1	1	1	1	1	1	1	1	1	1	1	1	3	0.33	0.50
48	0	0	0	0	0	0	0	0	0	0	1	1	1	1	1	1	1	1	1	1	1	1	1	1	1	1	1	1	1	1	1	1	1	1	1	1	1	1	1	1	1	1	1	1	1	1.00	1.00
49	–	–	–	–	–	–	–	–	–	–	1	1	0	0	0	0	0	0	0	0	0	0	0	0	0	0	0	0	0	0	0	0	0	0	1	1	1	1	1	1	1	1	1	1	2	0.50	0.91
50	–	–	–	–	–	–	–	–	–	–	2	2	1	1	1	0	0	0	0	0	0	1	1	1	1	1	1	1	1	1	0	0	0	0	2	2	2	2	3	3	2	3	3	3	6	0.50	0.84
51	–	–	–	–	–	–	–	–	–	–	1	1	1	1	1	1	1	1	1	1	1	0	0	1	1	0	0	0	0	0	1	1	1	1	1	1	1	1	1	1	1	1	1	1	2	0.50	0.83
52	0	0	0	0	0	0	0	0	0	0	0	0	0	0	0	0	0	0	0	0	0	0	0	0	0	0	0	0	0	0	0	1	1	1	0	0	0	0	0	0	0	0	0	0	1	1.00	1.00
53	0	0	0	0	0	0	0	0	0	0	0	0	0	0	0	0	0	0	0	0	0	0	0	0	0	0	0	0	0	0	0	0	0	0	0	0	0	1	0	0	0	1	1	0	3	0.33	0.00
54	0	1	1	1	1	1	1	1	1	1	1	1	1	1	1	1	1	1	1	1	1	1	1	1	1	1	1	1	1	1	1	1	1	1	1	1	1	1	1	1	1	1	1	1	1	1.00	0.00
55	–	0	0	0	1	0	0	?	1	1	1	1	1	1	1	1	1	1	1	1	1	1	1	1	1	1	1	1	1	1	1	1	1	1	1	1	1	1	1	1	1	1	1	1	2	0.50	0.75
56	–	0	0	0	–	0	0	1	0	0	1	1	0	0	0	0	0	0	0	0	0	0	0	1	1	0	0	0	0	0	1	1	1	1	0	0	0	0	0	0	0	0	0	0	5	0.20	0.50
57	–	0	0	0	0	0	0	1	0	0	1	1	0	0	0	0	0	0	0	0	0	0	0	1	1	0	0	0	0	0	1	0	0	0	0	0	0	0	0	0	0	0	0	0	4	0.25	0.40
58	–	–	–	–	1	–	–	1	1	1	1	1	1	1	1	0	0	0	0	0	0	1	1	1	1	0	0	0	0	0	1	0	0	0	1	1	1	1	1	1	1	1	1	1	3	0.33	0.85
59	–	–	–	–	1	–	–	1	1	1	0	0	0	0	0	1	1	1	1	1	1	1	1	0	0	1	1	1	1	1	1	2	2	2	3	3	3	1	1	1	1	1	1	1	6	0.50	0.70
60	–	0	1	1	0	0	0	0	0	0	1	0	0	0	0	0	0	0	0	0	0	0	0	0	0	0	0	0	0	0	0	0	0	0	0	0	0	0	0	0	0	0	0	0	2	0.50	0.50
61	–	0	1	1	1	–	1	1	1	0	1	1	1	1	0	0	0	0	0	0	0	1	1	0	0	0	0	0	0	0	0	1	1	1	1	1	1	1	1	1	1	1	1	1	5	0.20	0.75
62	–	0	1	1	1	–	1	0	0	1	1	1	1	1	0	1	1	0	1	0	1	1	1	1	1	1	1	1	1	1	1	1	1	1	1	1	1	1	1	1	1	1	1	1	6	0.17	0.00
63	–	0	0	0	1	0	0	1	1	1	1	1	1	1	1	1	1	1	1	1	1	1	1	1	1	1	1	1	1	1	1	1	1	1	1	1	1	1	1	1	1	1	1	1	2	0.50	0.75
64	0	0	1	1	1	1	1	1	1	1	1	1	1	1	1	1	1	1	1	1	1	1	1	1	1	1	1	1	1	1	1	1	1	1	1	1	1	1	1	1	1	1	1	1	1	1.00	1.00
65	–	–	1	1	0	0	1	1	0	0	0	0	0	0	0	0	0	0	0	0	0	0	0	0	0	0	0	0	0	0	1	1	1	1	1	1	1	1	1	1	1	1	1	1	4	0.25	0.82
66	–	–	1	0	1	1	0	1	1	1	1	1	1	1	1	1	1	1	1	1	1	1	1	1	1	1	1	1	1	1	1	1	1	1	1	1	1	1	1	1	1	1	1	1	2	0.50	0.00
67	–	–	0	0	0	0	0	1	0	1	2	1	1	1	2	0	0	0	0	0	0	2	0	2	2	0	0	0	0	0	1	1	1	1	1	1	1	1	1	1	1	1	1	1	7	0.29	0.76
68	–	–	0	0	0	0	0	0	1	1	0	0	0	0	0	0	0	0	0	0	0	0	0	0	0	0	0	0	0	0	0	0	0	0	0	0	0	0	0	0	0	0	0	0	1	1.00	1.00
69	–	–	0	0	2	0	0	1	1	1	1	1	1	1	1	1	1	1	1	1	1	1	1	1	1	1	1	1	1	1	1	1	1	1	1	1	1	1	1	1	1	1	1	1	2	1.00	1.00
70	–	–	1	0	0	0	0	0	0	0	0	0	0	0	0	0	0	0	0	0	0	0	0	0	0	0	0	0	0	0	1	1	1	1	1	1	1	1	1	1	1	1	1	1	2	0.50	0.93
71	–	–	0	0	0	0	0	0	0	0	0	0	0	0	0	0	0	0	0	0	0	0	0	0	0	0	0	0	0	0	0	0	0	0	0	0	0	1	1	1	0	1	1	0	3	0.33	0.50
72	–	–	0	0	0	0	0	0	0	0	0	0	0	1	0	0	0	0	0	0	0	0	0	0	0	0	0	0	0	0	1	1	1	1	1	1	1	1	1	1	1	1	1	1	2	0.50	0.93
73	–	–	–	–	–	–	–	–	–	–	–	–	–	0	–	–	–	–	–	–	–	–	–	–	–	–	–	–	–	–	0	0	0	0	0	0	0	1	1	1	1	1	1	1	1	1.00	1.00
74	–	–	0	0	1	0	0	0	1	1	0	1	0	0	0	0	0	0	0	0	0	0	0	0	0	0	0	0	0	1	0	0	0	0	0	0	0	0	0	0	0	0	0	0	4	0.25	0.25
75	0	1	1	1	0	0	0	0	0	0	0	0	0	0	0	0	0	0	0	0	0	0	0	0	0	0	0	0	0	0	0	0	0	0	0	0	0	0	0	0	0	0	0	0	2	0.50	0.50
76	0	1	1	1	1	1	1	1	1	1	1	1	1	1	1	1	1	1	1	1	1	1	1	1	1	1	1	1	1	1	1	1	1	1	1	1	1	1	1	1	1	1	1	1	1	1.00	0.00
77	–	1	1	1	1	1	1	0	0	0	0	0	0	0	0	0	0	0	0	0	0	0	0	0	0	0	0	0	0	0	0	0	0	0	0	0	0	0	0	0	0	0	0	0	1	1.00	1.00
78	–	0	0	0	0	0	1	0	0	0	0	0	0	0	0	0	0	0	0	0	0	0	0	0	0	0	0	0	0	0	1	1	1	1	1	1	1	1	1	1	1	1	1	1	2	0.50	0.93
79	–	0	0	0	0	0	0	1	1	1	1	1	1	0	1	1	1	1	1	1	1	1	1	1	1	1	1	1	1	1	0	0	0	0	0	0	0	0	0	0	0	0	0	0	3	0.33	0.90
80	–	–	–	–	–	–	–	0	0	0	0	0	0	–	0	1	1	1	1	1	1	1	0	0	0	0	0	0	0	0	–	–	–	–	–	–	–	–	–	–	–	–	–	–	2	0.50	0.83
81	–	0	0	0	1	1	0	0	0	0	0	0	0	1	0	0	0	0	0	0	0	0	0	0	0	0	0	0	0	0	0	0	0	0	1	1	1	0	0	0	0	0	0	0	4	0.25	0.40
82	–	0	0	0	0	0	0	0	1	1	0	0	0	0	0	0	0	0	0	0	0	0	0	0	0	0	0	0	0	0	0	0	0	0	0	0	0	0	0	0	0	0	0	0	1	1.00	1.00
83	0	1	0	0	0	1	0	0	0	0	0	0	0	0	0	0	0	0	0	0	0	0	0	0	0	0	0	0	0	0	1	1	1	1	1	1	1	1	1	1	1	1	1	1	3	0.33	0.87
84	1	2	0	2	0	1	0	0	0	0	1	1	0	0	0	0	0	0	0	0	0	0	0	0	0	0	0	0	0	0	1	1	1	1	1	1	1	1	1	1	1	1	1	1	6	0.33	0.78
85	–	–	–	–	1	0	0	0	0	0	0	0	0	1	0	0	0	0	0	0	0	0	0	0	0	0	0	0	0	0	1	1	1	1	1	1	1	1	1	1	1	1	1	1	3	0.33	0.87
86	–	–	–	–	2	2	–	0	0	0	4	4	1	1	0	0	0	0	0	0	0	1	1	1	1	0	0	0	1	1	2	3	3	3	1	1	1	2	2	2	2	2	2	2	9	0.44	0.77
87	1	1	1	0	1	1	0	0	0	0	0	0	0	1	0	0	0	0	0	0	0	0	0	0	0	0	0	0	0	0	1	1	1	1	1	1	1	1	1	1	1	1	1	1	4	0.25	0.84
88	0	0	0	0	1	0	0	0	0	0	0	0	0	0	0	0	0	0	0	0	0	0	0	0	0	0	0	0	0	0	0	0	0	0	1	0	0	0	1	1	1	0	0	0	4	0.25	0.25
89	1	1	1	1	1	1	1	0	1	1	0	0	1	1	1	1	1	1	1	1	1	1	1	1	1	1	1	1	1	1	1	1	1	1	1	1	1	1	1	1	1	1	1	1	2	0.50	0.50
90	0	0	0	0	1	0	0	0	0	0	1	0	0	0	0	0	0	0	0	0	0	0	0	0	0	0	0	0	0	0	0	0	0	0	0	0	0	0	0	0	0	0	0	0	2	0.50	0.00
91	1	1	1	0	1	1	1	1	0	0	1	1	1	0	0	0	0	0	0	0	0	1	0	1	1	0	0	0	0	1	1	1	0	0	0	0	0	0	0	0	0	0	0	0	9	0.11	0.47
92	0	0	0	0	0	0	0	1	1	1	1	1	1	1	1	1	1	1	1	1	1	1	1	1	1	1	1	1	1	1	1	1	1	1	1	1	1	1	1	1	1	1	1	1	1	1.00	1.00
93	–	–	–	–	–	–	–	1	1	1	1	1	1	1	1	1	0	1	1	0	1	0	0	0	0	0	0	0	0	0	0	1	1	1	1	1	1	1	1	1	1	1	1	1	4	0.25	0.73

(*Continued*)

Character	*Pimoa altioculata*	*Stemonyphantes lineata*	*Linyphia triangularis*	*Bolyphantes luteolus*	*Australolinyphia remota*	*Diplostyla concolor*	*Hilaira excisa*	*Cassafroneta forsteri*	*Novafroneta gladiatrix*	*Novafroneta vulgaris*	*Hyperafroneta obscura*	*Metafroneta sinuosa*	*Protoerigone otagoa*	*Pseudafroneta perplexa*	*Pseudafroneta pallida*	*Parafroneta minuta*	*Parafroneta haurokoae*	*Parafroneta demota*	*Parafroneta confusa*	*Parafroneta marrineri*	*Parafroneta westlandica*	*Trachyneta jocquei*	*Gibbafroneta gibbosa*	*Laminafroneta bidentata*	*Laminafroneta brevistyla*	*Afroneta bamilekei*	*Afroneta subfusca*	*Afroneta guttata*	*Afroneta lobeliae*	*Afroneta tenuivulva*	*Afromynoglenes parkeri*	*Promynoglenes silvestris*	*Promynoglenes nobilis*	*Promynoglenes grandis*	*Metamynoglenes helicoides*	*Metamynoglenes gracilis*	*Metamynoglenes incurvata*	*Haplinis insignis*	*Haplinis abbreviata*	*Haplinis diloris*	*Haplinis horningi*	*Haplinis subdola*	*Haplinis tegulata*	*Haplinis titan*	steps	ci	ri
94	–	–	–	–	–	–	–	0	0	0	0	0	1	0	0	0	0	0	0	0	0	0	0	0	0	0	0	0	0	0	0	0	0	0	0	0	0	0	0	0	0	0	0	0	1	1.00	0.00
95	–	–	–	–	–	–	–	2	1	1	0	1	0	0	0	0	0	0	0	0	0	0	0	0	0	0	0	0	0	0	0	0	0	0	0	0	0	0	0	0	0	0	0	0	3	0.67	0.50
96	0	0	1	1	1	1	1	1	1	1	1	1	1	1	1	1	1	1	1	1	1	1	1	1	1	1	1	1	1	1	1	1	1	1	1	1	1	1	1	1	1	1	1	1	1	1.00	1.00
97	0	0	0	1	0	0	0	0	0	0	0	0	0	0	0	0	0	0	0	0	0	0	0	0	0	1	1	1	1	1	0	0	0	0	0	0	0	0	0	0	0	0	0	0	2	0.50	0.80
98	0	0	0	0	2	0	0	2	0	0	0	0	0	0	2	0	0	0	0	0	0	2	0	2	2	1	2	1	2	2	2	2	0	0	2	2	2	0	0	0	0	0	0	0	9	0.22	0.50
99	1	1	1	1	1	0	0	1	0	0	0	0	0	0	0	0	0	0	0	0	0	0	0	0	0	0	0	0	0	0	0	0	0	0	0	0	0	0	0	0	0	0	0	0	2	0.50	0.80
100	0	0	0	0	1	0	–	0	0	1	0	0	0	1	0	0	0	0	0	0	0	0	0	1	1	0	0	0	0	0	0	0	0	0	0	0	0	0	0	0	0	0	0	0	4	0.25	0.25
101	0	0	0	0	0	0	1	1	0	0	0	0	0	0	0	0	0	0	0	0	0	0	1	0	0	0	0	0	0	0	0	0	0	0	0	0	0	0	0	0	0	0	0	0	3	0.33	0.00
102	1	1	1	1	1	1	1	0	1	1	1	1	1	1	1	1	1	1	1	1	1	1	1	1	1	1	0	1	1	1	1	1	1	1	1	1	1	0	0	1	1	1	1	1	4	0.25	0.00
103	1	0	1	0	1	1	1	–	1	1	1	1	1	1	1	1	1	1	1	1	1	1	1	1	1	1	–	1	1	1	1	1	1	1	1	1	1	–	–	1	1	1	1	1	2	0.50	0.00
104	0	0	0	0	–	1	2	2	2	2	2	2	2	2	1	0	0	0	2	2	1	0	1	1	1	0	2	2	2	2	2	2	1	1	2	2	1	1	2	1	1	2	2	2	13	0.15	0.42
105	0	0	0	0	–	–	2	2	2	2	2	2	2	2	1	1	0	0	2	2	2	0	1	1	1	0	1	2	2	2	1	1	1	1	1	1	2	1	3	1	2	1	3	3	11	0.27	0.65
106	0	0	1	1	–	0	0	1	1	1	1	1	1	1	1	1	1	1	1	1	1	1	1	1	1	1	1	1	1	1	1	1	1	1	1	1	1	1	1	1	1	1	1	1	2	0.50	0.67
107	0	0	0	1	0	1	1	1	1	1	1	1	1	1	1	1	1	1	1	1	1	1	1	1	1	1	1	1	1	1	1	1	1	1	1	1	1	1	1	1	1	1	1	1	2	0.50	0.67
108	0	0	0	0	0	0	0	1	1	1	1	1	1	1	1	1	1	1	1	1	1	0	1	1	1	0	0	0	0	0	1	1	1	1	1	1	1	1	1	1	1	1	1	1	3	0.33	0.83
109	0	0	0	0	0	0	0	0	0	0	0	0	0	0	0	0	0	0	0	0	0	1	0	0	0	0	0	0	0	0	0	0	0	0	0	0	0	0	0	0	0	0	0	0	1	1.00	0.00
110	0	0	0	0	1	0	0	0	1	1	1	1	1	1	1	1	1	1	1	1	1	1	1	0	0	?	0	0	0	0	1	1	1	1	1	1	1	1	1	1	1	1	1	1	3	0.33	0.83
111	0	0	0	0	0	0	0	0	1	1	1	1	1	1	1	1	1	1	1	0	1	1	0	0	0	0	0	0	0	0	1	1	1	1	1	1	1	1	1	1	1	1	1	1	3	0.33	0.88
112	–	–	–	–	–	–	–	–	0	0	0	0	1	1	1	1	1	1	1	–	1	1	–	–	–	–	–	–	–	–	1	0	1	1	0	1	1	0	0	1	1	1	1	1	5	0.20	0.43
113	0	0	0	0	0	0	0	1	1	1	1	1	1	1	1	1	1	1	1	0	1	0	0	1	1	0	0	0	0	0	1	1	1	1	1	1	1	0	1	1	1	1	1	1	5	0.20	0.73
114	1	1	1	0	0	0	0	0	1	1	1	1	1	1	1	0	1	1	1	1	1	0	0	1	1	0	0	0	0	0	2	0	0	1	0	0	0	1	1	2	2	1	2	2	12	0.17	0.52
115	0	0	1	0	0	0	1	0	1	1	1	1	1	1	1	1	1	1	1	1	1	1	1	0	0	0	0	0	0	0	0	1	1	1	1	1	1	0	1	1	1	1	1	1	6	0.17	0.64
116	1	1	1	1	1	0	0	1	0	0	1	1	1	1	1	1	1	1	0	1	1	1	0	0	0	1	0	0	1	1	0	1	0	0	0	0	1	0	0	1	0	0	1	1	12	0.08	0.39
117	0	1	1	1	0	0	0	1	0	0	1	1	1	1	1	1	1	0	0	1	1	0	0	0	0	0	0	0	1	0	0	0	0	0	0	0	1	0	0	1	0	0	1	0	12	0.08	0.31
118	0	0	0	0	0	0	0	0	0	0	0	0	1	1	1	0	1	0	0	0	0	0	0	0	0	0	0	0	0	0	0	0	0	0	0	0	0	0	0	0	0	0	0	0	3	0.33	0.33
119	0	1	1	0	0	0	0	0	0	0	0	0	0	0	0	0	0	0	0	0	0	0	0	0	0	0	0	0	0	0	0	0	0	0	0	0	0	0	0	0	0	0	0	0	2	0.50	0.00
120	0	0	1	1	1	1	0	0	0	0	1	1	1	1	1	1	1	1	1	1	1	1	1	0	0	1	1	1	1	1	0	1	1	1	1	1	1	2	2	2	2	2	2	2	6	0.33	0.71
121	0	0	1	0	1	1	0	0	1	0	0	0	1	0	0	0	0	0	0	1	1	1	0	0	0	1	0	1	0	0	0	0	0	0	0	0	0	0	0	0	0	1	1	1	10	0.10	0.25
122	0	0	1	0	0	0	0	0	0	0	0	0	0	0	0	0	0	0	0	0	0	0	0	0	0	0	0	0	0	0	0	0	0	0	0	0	0	0	0	0	0	0	1	1	2	0.50	0.50
123	0	0	0	0	0	0	0	0	0	0	0	0	0	0	0	0	0	0	0	0	0	0	0	0	0	0	0	0	0	0	0	1	1	1	0	1	0	0	1	1	0	1	1	1	4	0.25	0.63
124	0	0	0	0	0	0	0	0	0	0	0	0	0	0	0	0	0	0	0	0	0	0	0	0	0	0	0	0	0	0	0	0	1	0	1	1	0	1	0	1	0	0	0	1	6	0.17	0.00
125	1	0	0	1	1	1	0	1	1	1	1	1	1	1	1	1	1	1	1	1	1	1	1	1	1	1	1	1	1	1	1	1	1	1	1	1	1	1	1	1	1	1	1	1	3	0.33	0.00
126	0	0	0	1	0	0	0	1	0	0	0	0	0	0	0	0	0	0	0	0	0	0	0	0	0	0	0	0	0	0	0	0	0	0	0	0	0	0	0	0	0	0	0	0	2	0.50	0.00
127	0	0	0	1	0	0	0	1	0	0	1	1	0	0	0	0	0	0	0	0	0	0	0	0	0	0	0	0	0	0	0	1	1	1	1	1	1	1	1	1	1	1	1	1	4	0.25	0.81
128	0	–	–	0	–	–	–	1	–	–	–	–	–	–	–	–	–	–	–	–	–	–	–	–	–	–	–	–	–	–	–	0	0	0	1	0	0	1	0	1	0	0	0	0	4	0.25	0.00
129	1	–	–	1	–	–	–	1	–	–	–	–	–	–	–	–	–	–	–	–	–	–	–	–	–	–	–	–	–	–	–	0	0	0	1	0	0	1	1	1	1	0	0	0	3	0.33	0.71
130	1	–	–	1	–	–	–	0	–	–	–	–	–	–	–	–	–	–	–	–	–	–	–	–	–	–	–	–	–	–	–	1	1	1	1	1	1	1	0	0	0	0	1	1	3	0.33	0.50
131	0	0	0	0	0	0	0	0	0	0	1	1	0	0	0	0	0	0	0	0	0	0	0	0	0	0	0	0	0	0	0	0	0	0	0	0	0	0	0	0	0	0	0	0	1	1.00	1.00
132	0	0	0	0	0	0	0	0	0	0	0	0	0	0	0	0	0	0	0	0	0	0	0	0	0	0	0	0	0	0	0	0	1	0	1	1	1	1	0	0	0	0	0	0	3	0.33	0.50
133	0	1	0	0	1	0	0	0	0	0	0	0	1	0	1	1	1	0	0	0	0	1	1	0	0	1	1	1	1	1	0	0	0	0	0	0	0	0	0	0	0	0	0	0	6	0.17	0.58
134	0	0	0	0	1	0	0	0	0	0	0	0	1	1	1	1	0	0	0	1	0	1	1	0	0	1	1	0	0	0	1	0	0	0	0	0	0	0	0	0	0	0	0	0	7	0.14	0.40
135	0	0	0	0	0	0	0	0	0	0	0	0	0	0	0	0	0	0	0	0	0	0	0	1	1	0	0	0	0	0	1	0	0	0	0	0	0	0	0	0	0	0	0	0	2	0.50	0.50
136	0	0	0	0	0	0	0	0	0	0	0	0	0	0	0	0	0	1	1	0	1	0	0	0	0	0	0	0	1	1	0	0	0	0	1	1	1	0	1	0	0	1	1	0	7	0.14	0.40
137	1	1	0	1	1	1	0	0	1	1	1	1	1	1	1	1	1	1	1	1	1	1	1	1	1	1	1	1	1	1	1	1	1	1	0	0	0	0	0	0	0	0	0	0	4	0.25	0.75
138	0	2	0	1	0	1	–	1	2	2	2	2	0	0	0	0	0	0	0	0	0	0	0	2	2	0	0	0	0	0	0	0	0	0	1	1	1	1	1	1	1	1	1	1	7	0.29	0.72
139	1	1	0	1	1	1	1	1	1	1	1	1	1	1	1	1	1	1	1	1	1	1	1	1	1	1	1	1	1	1	1	0	0	0	0	0	0	0	0	0	0	0	0	0	2	0.50	0.92
140	0	0	1	1	1	1	0	1	1	0	1	1	1	1	1	1	1	1	1	1	1	1	1	1	1	1	1	1	1	1	1	1	1	1	1	1	1	1	1	1	1	1	1	1	3	0.33	0.33
141	0	0	0	1	0	1	0	1	0	0	0	0	0	0	0	0	0	0	0	0	0	0	0	0	0	0	0	0	0	0	0	0	0	0	0	0	0	0	0	0	0	0	0	0	3	0.33	0.00
142	1	0	1	1	1	1	0	0	1	0	1	1	1	1	1	1	1	1	1	1	1	1	1	1	1	1	1	1	1	1	1	1	1	1	1	1	1	1	1	1	1	1	1	1	4	0.25	0.00

(*Continued*)

Character	*Pimoa altioculata*	*Stemonyphantes lineata*	*Linyphia triangularis*	*Bolyphantes luteolus*	*Australolinyphia remota*	*Diplostyla concolor*	*Hilaira excisa*	*Cassafroneta forsteri*	*Novafroneta gladiatrix*	*Novafroneta vulgaris*	*Hyperafroneta obscura*	*Metafroneta sinuosa*	*Protoerigone otagoa*	*Pseudafroneta perplexa*	*Pseudafroneta pallida*	*Parafroneta minuta*	*Parafroneta haurokoae*	*Parafroneta demota*	*Parafroneta confusa*	*Parafroneta marrineri*	*Parafroneta westlandica*	*Trachyneta jocquei*	*Gibbafroneta gibbosa*	*Laminafroneta bidentata*	*Laminafroneta brevistyla*	*Afroneta bamilekei*	*Afroneta subfusca*	*Afroneta guttata*	*Afroneta lobeliae*	*Afroneta tenuivulva*	*Afromynoglenes parkeri*	*Promynoglenes silvestris*	*Promynoglenes nobilis*	*Promynoglenes grandis*	*Metamynoglenes helicoides*	*Metamynoglenes gracilis*	*Metamynoglenes incurvata*	*Haplinis insignis*	*Haplinis abbreviata*	*Haplinis diloris*	*Haplinis horningi*	*Haplinis subdola*	*Haplinis tegulata*	*Haplinis titan*	steps	ci	ri
143	0	–	1	1	1	0	–	–	1	–	0	0	0	1	1	0	0	0	0	0	0	0	1	0	0	0	0	0	1	1	0	0	1	0	1	1	1	1	1	1	1	1	1	1	9	0.11	0.58
144	0	–	2	0	0	2	–	–	1	–	2	2	2	2	2	2	2	2	2	2	2	2	2	0	0	2	2	2	2	2	0	2	2	2	0	0	0	0	0	0	0	0	0	0	6	0.33	0.73
145	2	–	0	2	2	0	–	–	0	–	1	1	0	0	0	0	0	0	0	0	0	0	1	0	0	0	0	0	0	0	0	1	1	1	0	0	2	2	2	2	2	2	2	2	7	0.29	0.67
146	1	–	1	1	0	1	–	–	1	–	0	0	1	1	1	1	1	1	1	1	1	1	1	0	0	1	1	1	1	1	0	1	1	1	1	1	1	0	0	0	0	0	0	0	5	0.20	0.67
147	0	0	1	0	0	0	0	0	0	0	0	0	1	1	1	1	1	1	1	1	1	0	0	0	0	0	0	1	1	1	1	1	1	1	1	1	1	1	1	1	1	1	0	0	5	0.20	0.78
148	0	0	0	0	1	0	0	0	0	0	0	0	1	1	1	1	1	1	1	1	1	1	1	1	1	1	1	1	1	1	1	1	1	1	1	1	1	1	1	1	1	1	1	1	2	0.50	0.90
149	0	1	0	0	1	0	0	1	1	0	0	0	1	1	1	1	1	1	1	1	1	1	0	1	1	0	1	1	1	1	1	1	1	1	1	1	1	1	1	1	1	1	1	1	7	0.14	0.33
150	–	1	–	–	1	–	–	0	0	–	–	–	0	0	0	0	0	0	0	0	0	0	–	0	0	–	0	0	0	0	0	1	1	1	1	1	1	1	1	1	1	1	1	1	2	0.50	0.93
151	–	2	–	–	2	–	–	0	2	–	–	?	1	2	1	1	1	2	2	1	2	1	–	0	0	–	1	1	1	1	2	2	2	2	2	2	2	2	2	2	2	2	2	2	6	0.33	0.64
152	–	3	–	–	3	–	–	0	0	–	–	–	0	0	0	0	0	0	0	0	0	0	–	0	0	–	0	0	0	0	0	2	3	3	2	1	1	0	1	2	2	2	1	2	7	0.43	0.64
153	1	0	0	0	0	0	0	0	0	0	0	0	0	1	1	1	1	0	0	1	0	0	0	0	0	0	0	0	0	0	0	0	0	0	0	0	0	0	0	0	0	0	0	0	5	0.20	0.20
154	1	1	1	1	1	1	1	0	1	1	0	1	1	1	1	1	0	0	0	1	1	1	0	1	1	1	1	1	0	1	1	1	1	1	1	1	1	1	1	1	1	1	0	1	7	0.14	0.14
155	1	1	1	1	1	1	0	1	1	1	0	1	1	1	1	1	0	1	1	1	1	1	0	1	1	0	0	1	0	0	1	1	1	1	1	1	1	0	1	1	1	1	1	1	7	0.14	0.25
156	1	1	1	1	1	1	0	0	0	0	0	0	0	0	0	0	0	0	0	0	0	0	0	1	0	0	0	0	0	0	0	0	0	0	0	0	0	0	0	1	0	0	0	1	4	0.25	0.63
157	0	1	1	1	1	1	0	0	0	0	0	0	0	1	0	0	0	0	0	0	0	0	0	0	0	0	0	0	0	0	0	0	0	0	0	0	0	0	0	0	0	0	0	0	3	0.33	0.60
158	4	3	3	1	3	2	1	2	3	3	1	3	2	3	2	2	0	1	2	2	1	2	1	3	3	2	2	2	3	3	3	3	2	2	3	2	2	2	3	3	2	3	3	3	18	0.22	0.33
159	2	2	2	1	2	1	1	1	2	2	1	2	2	2	1	1	0	0	1	1	1	0	1	2	2	2	2	2	2	2	2	2	2	2	1	1	2	1	2	2	2	2	0	2	13	0.15	0.31
160	0	0	0	0	0	0	0	0	0	0	0	0	0	0	0	0	0	0	0	0	0	0	0	0	0	0	1	0	1	0	0	0	0	0	0	0	0	0	0	0	0	0	0	0	2	0.50	0.00
161	0	0	1	0	0	0	0	0	0	0	0	0	0	0	0	0	0	0	0	0	0	0	0	0	1	0	1	1	1	1	?	0	0	0	0	0	0	0	0	0	0	0	0	0	3	0.33	0.60
162	2	0	0	0	0	0	0	0	1	1	1	1	2	1	0	1	0	1	1	2	1	0	1	1	1	1	1	1	2	2	1	1	0	0	1	1	1	1	1	1	1	1	2	2	10	0.20	0.53
163	2	0	0	0	0	0	0	0	1	1	0	1	1	1	0	0	0	1	1	2	1	0	0	0	1	0	0	1	1	2	1	0	0	0	1	1	1	1	1	1	1	1	2	2	11	0.18	0.59
164	2	1	2	1	1	2	0	1	1	2	1	1	1	1	1	1	0	1	1	2	1	1	1	1	2	1	0	1	2	2	1	1	1	1	1	1	1	1	1	1	1	1	1	1	10	0.20	0.11
165	1	1	1	0	1	1	0	0	1	1	0	0	0	1	0	0	0	0	0	1	0	0	1	1	1	1	1	1	1	1	1	0	0	0	0	0	0	0	0	0	0	0	0	1	8	0.13	0.61
166	0	0	0	0	0	0	0	0	0	0	0	0	0	0	0	0	0	0	0	0	0	1	0	0	0	0	0	0	0	0	0	0	0	0	0	0	0	0	0	0	0	0	0	0	1	1.00	0.00
167	2	1	2	1	1	1	1	0	1	1	1	1	1	1	1	1	0	1	1	2	1	1	1	1	1	1	1	1	1	1	1	1	1	1	1	1	1	1	1	1	1	1	1	1	5	0.40	0.00
168	2	1	2	1	1	1	0	0	1	0	0	0	0	0	0	1	0	0	0	2	0	0	1	1	1	1	1	1	2	2	0	0	0	0	0	0	0	0	0	0	0	0	0	0	8	0.25	0.60
169	2	2	2	1	2	0	0	0	1	1	1	1	1	1	1	0	0	0	1	2	0	0	0	1	1	1	1	2	1	1	1	1	1	0	1	1	1	1	1	1	1	1	1	1	10	0.20	0.43
170	2	2	2	1	2	0	0	0	0	0	0	0	0	0	0	0	0	0	0	1	0	0	0	1	1	1	1	2	1	1	0	0	0	0	0	0	0	0	0	0	0	0	0	0	5	0.40	0.73
171	1	1	0	0	1	0	0	0	0	0	0	0	0	0	0	0	0	0	0	0	0	0	0	0	0	0	1	1	1	1	0	0	0	0	0	0	0	0	0	0	0	0	0	0	3	0.33	0.67
172	1	1	1	0	1	0	0	0	0	0	0	0	0	0	0	0	0	0	0	1	0	0	0	1	1	1	1	1	1	1	1	0	0	0	0	0	0	0	0	0	0	0	0	0	5	0.20	0.67
173	0	2	2	0	0	0	0	0	0	0	0	0	0	0	0	0	0	0	0	1	0	0	0	2	2	2	2	2	2	2	2	0	0	0	0	0	0	0	0	0	1	0	0	1	7	0.29	0.55
174	2	1	1	1	1	0	0	0	2	1	1	1	1	1	0	1	0	1	1	2	1	0	1	1	1	1	1	1	2	2	1	1	1	1	1	1	1	1	2	1	2	1	2	2	12	0.17	0.23
175	0	1	1	1	1	0	0	0	0	0	0	0	0	0	0	0	0	0	0	1	1	0	0	1	1	1	1	1	1	1	1	0	0	0	0	0	0	0	0	0	0	0	0	1	6	0.17	0.64
176	2	1	1	1	0	0	0	0	1	0	0	0	0	0	0	0	0	0	0	2	0	0	1	1	1	1	1	1	2	2	0	0	0	0	0	0	0	0	0	0	2	0	0	0	7	0.29	0.62
177	0	1	1	1	1	0	0	0	1	1	1	1	1	1	1	1	0	1	1	1	1	0	0	1	1	1	1	1	1	1	1	1	1	1	1	1	1	1	1	1	1	1	1	1	6	0.17	0.17
178	2	2	2	1	0	0	0	0	1	1	2	1	1	1	0	1	0	1	1	2	1	0	1	1	1	1	1	2	2	2	1	1	1	1	1	1	1	1	1	2	2	1	2	1	11	0.18	0.44
179	2	0	0	0	1	0	0	0	0	0	0	0	0	0	0	0	0	0	0	2	0	0	0	1	0	0	0	0	2	1	1	0	0	0	0	0	0	0	0	0	1	0	0	0	8	0.25	0.00
180	1	1	0	0	0	0	0	0	0	0	0	0	0	0	0	0	?	0	0	0	0	0	0	0	0	0	0	0	1	1	0	0	0	0	0	0	0	0	0	0	0	0	0	0	2	0.50	0.67
181	1	0	0	0	0	0	0	0	0	0	0	0	0	0	0	0	?	0	0	1	0	0	0	1	1	1	1	1	1	1	0	0	0	0	0	0	0	0	0	0	0	0	0	0	3	0.33	0.75
182	0	2	2	0	0	0	0	1	2	2	2	2	2	2	2	2	2	2	2	2	2	0	2	2	2	2	2	2	2	2	2	2	2	2	2	2	2	2	2	2	2	2	2	2	5	0.40	0.40
183	2	0	2	1	1	0	0	0	0	0	0	0	0	1	0	0	0	0	0	1	0	0	0	1	1	0	1	1	1	1	1	0	0	0	0	0	0	0	0	0	1	0	0	1	11	0.18	0.31
184	2	1	2	1	0	0	0	0	0	0	0	1	1	1	0	0	0	1	1	1	1	0	0	0	1	0	0	0	1	1	0	0	0	0	0	0	0	0	1	1	2	1	2	1	11	0.18	0.50
185	2	2	1	1	0	0	0	0	0	0	0	0	0	2	0	0	0	0	0	2	0	0	0	0	1	0	0	0	0	0	0	0	0	0	0	0	0	0	0	1	2	0	1	0	8	0.25	0.25
186	1	1	1	0	0	0	0	0	0	0	0	0	0	0	0	0	0	0	0	1	0	0	0	0	0	0	0	0	1	1	0	0	0	0	0	0	0	0	0	0	1	0	1	0	6	0.17	0.29
187	0	1	1	0	0	0	0	0	0	0	1	1	1	0	0	0	0	0	1	1	1	0	0	0	0	0	0	0	0	0	0	0	0	0	0	0	0	1	1	1	1	1	1	1	6	0.17	0.64
188	1	1	0	0	0	0	1	1	1	1	1	1	1	1	1	0	0	1	1	1	1	0	1	1	1	1	1	1	1	1	1	1	1	1	1	1	1	1	1	1	1	1	1	1	5	0.20	0.33
189	1	1	0	0	0	0	0	0	0	0	0	0	1	1	0	0	1	1	1	1	0	0	0	0	0	0	0	0	0	0	0	1	1	1	1	1	1	1	1	0	0	0	1	1	7	0.14	0.65
190	1	1	1	1	1	1	0	1	0	0	0	0	0	1	0	0	0	0	0	1	0	1	1	1	1	1	1	1	1	1	1	0	0	0	0	0	0	0	0	0	0	0	0	0	6	0.17	0.72

Appendix 5

Character mappings and apomorphy lists

In this section we discuss clades of interest and their character support. We focus on synapomorphic character-state changes derived from an ACCTRAN optimization (black squares in Figs 2–4) and the respective Bremer support (BS) and jackknife (JK) values of the equally weighted analysis. Only synapomorphies that are unaltered or reversed only in very few taxa are listed. We also provide new diagnoses for the genera included in the phylogeny and refer to the original descriptions.

Clades 1–6: Subfamily relationships. Previous phylogenetic studies have not agreed on the placement of mynoglenines within Linyphiidae and the present study does not attempt to investigate this further. In order to do that, we would have to include many more taxa and characters. This should be kept in mind when referring to the subfamily relationships discovered in the current analysis. See comments about outgroup selection under "Methods, taxon sampling".

Mynoglenines have been suggested as sister-group to erigonines (Wunderlich, 1986; Miller and Hormiga, 2004; current study using *k* values of 5 or more) or as an early lineage within linyphiids sister to all other subfamilies except Stemonyphantinae (Hormiga, 1994b; Arnedo et al., 2009: fig. 3). The latest and most comprehensive phylogenetic study of Linyphiidae and all its subfamilies (Arnedo et al., 2009) suggests either a sister-group relationship between mynoglenines and the Australian genus *Australolinyphia* (direct optimization; also current analysis using *k* values of 1–4); or a sister-group relationship between Mynogleninae and a clade including *Australolinyphia*, *Laetesia* (Australia and New Zealand), *Bathyphantes* (worldwide), and *Diplostyla* (holarctic) (Bayesian and parsimony).

We used 39 of the morphological characters of Arnedo et al. (2009), four from Miller and Hormiga (2004), and added another 147 new characters (Appendix 3) to the current morphological matrix, and found statistical support (BS: 5; JK: 79%; Fig. 1) for a sister-group relationship between mynoglenines and erigonines using equal weights and implied weights with *k* values of 5 and above. With *k* values 1–4 we find support for a sister-group relationship between mynoglenines and *Australolinyphia remota*.

Clade 1: Linyphiidae are supported by two unaltered characters, the presence of a suprategulum (ch54, Fig. 9c), and a radix (ch76, Fig. 11d). BS: >20, JK: 100%.

Clade 2 is supported by two unaltered character states, the presence of an embolic membrane (ch64, Fig. 13a), and the AMEs being smaller than the PMEs (ch96, Fig. 14b). BS: 7, JK: 93%.

Clade 3: The bifurcated distal section of the suprategulum (ch60) is a synapomorphy of the sister-group relationship between *Linyphia triangularis* and *Bolyphantes luteolus* but is also present in *Hyperafroneta*. BS: 1, JK: <50%.

Clade 4 is not supported by any unreversed synapomorphies. However, the alveolus is much shorter than the cymbium (ch10, Fig. 10b) in all taxa within this clade except in *Hilaira excisa*. BS: 3, JK: 70%.

Clade 5 is not supported by any unaltered synapomorphies. However, all taxa in this clade except *Cassafroneta forsteri* have only one macroseta below the AME (ch99, Fig. 14b). BS: 5, JK: 87%.

Clade 6: The sister-group relationship between Erigoninae and Mynogleninae is not supported by any unaltered synapomorphies. BS: 5, JK: 79%. However, Miller and Hormiga (2004) also found unambiguous support for this sister-group relationship based on the reduction of the clypeal setae from several to one (our character 99, synapomorphy of clade 5, with one reversal in *Cassafroneta*), the loss of retrolateral (our character 168, synapomorphy of this clade with several reversals), and ventral macrosetae on tibia I and the loss of ventral macrosetae on metatarsus I (characters that we did not score).

Clade 7: Mynogleninae. Lehtinen (1967) established the subfamily Mynogleninae for the genera *Mynoglenes* (a junior synonym of *Haplinis* by Millidge, 1984) and *Paro* (transferred to Linyphiinae by Ledoux and Hallé, 1995), based on "the presence of numerous metatarsal trichobothria and the exceptional type of modifications of the carapace". Blest (1979, p. 96) and Wunderlich (1986, p. 121) described the morphology of Mynogleninae in more detail: males and females with subocular sulci, tibia IV usually with two dorsal macrosetae, chaetotaxy variable but tibia III–IV and metatarsus III–IV often with distal macrosetae, haplotracheate trachea, male and female palpal femur with stridulatory bristle, simple paracymbium, radix small and continuous with embolus, lack of a lamella characteristica, and lack of a terminal apophysis; epigyne with or without scape. Both also mention that the female palp lacks a claw (which has been demonstrated to be an observational error by Hormiga, 1994b) and the lack of an embolic membrane. The absence of an embolic membrane is ambiguous: Blest (1979) described a membraneous, more or less sclerotized structure in mynoglenines, which he called a "conductor". This may be the embolic membrane, which is our hypothesis.

All phylogenetic analyses carried out to date support the monophyly of the subfamily Mynogleninae (Hormiga, 1993, 1994b, 2000; Miller and Hormiga, 2004; Arnedo et al., 2009), although only few mynoglenine exemplars have been included in these studies (a maximum of three). Mynoglenines can be easily diagnosed morphologically by the presence of clypeal sulci (or pits) in both sexes with cuticular pores served by glands (Arnedo et al., 2009). The monophyly of mynoglenines is also well supported (BS: 5, JK: 84%) in our study, which includes 37 mynoglenine exemplars representing 15 genera. The subfamily is supported by three unreversed synapomorphies: the attachment of the embolic membrane to the tegulum (ch69, Fig. 12a), the indistinct, small radix (ch77, Fig. 11d), and the subocular sulci (ch92, Fig. 14b). By far the most distinct character defining the mynoglenines is the subocular sulci that are present in both sexes as well as juveniles.

Another 17 character-state changes support the monophyly of Mynogleninae, among which two are worth mentioning as they also occur only in *Australolinyphia remota* (a suggested close relative of mynoglenines in former studies, e.g. Blest, 1979; Arnedo et al., 2009). These are the fusion of the basal part of the suprategulum to the tegulum (ch55, Fig. 9e) and the presence of a foramen in the tegulum (ch63, Fig. 13a).

Clades 7–11: *Cassafroneta*, *Novafroneta*, *Hyperafroneta*, and *Metafroneta* are the earliest lineages within the mynoglenines (Fig. 1). Generally, they have simpler copulatory organs than the more distal mynoglenines (clade 30) and even lack some classic mynoglenine synapomorphies.

***Cassafroneta* Blest, 1979:** This monotypic genus from New Zealand is sister to all other mynoglenine taxa (Fig. 2b). Males have a distinct cephalic lobe (ch101; Blest, 1979: figs 582, 583) similar to that present in the African genus *Gibbafroneta* and in some erigonines. The frontal third of the lobe of *Cassafroneta* is densely covered with forward-pointing setae (Blest, 1979: figs 582, 583). The cephalothorax and the large subocular sulci are very distinctive (Blest, 1979). The circular shape of the sulci in the males (ch95; Blest, 1979: figs 582) is autapomorphic for the genus. It is the only scored species with a glabrous paracymbial base (ch28) and a single ventral distal macroseta on tibia IV (ch182). The broad and short embolic membrane situated retrolateral to the embolus (Blest, 1979: fig. 584) is unique among the scored mynoglenines. Unlike in other mynoglenines, the embolic membrane ("conductor") is broadly attached to the tegulum (Blest, 1979: fig. 584). Based on our observations on unexpanded palps, the distal broad part is free-standing while only the basal part is attached to the tegulum as in other

mynoglenines. The short and strongly sclerotized embolus is also typical (Blest, 1979). It is lamellar and distally broadened (Blest, 1979: fig. 584). *Cassafroneta* lacks the mynoglenine tegular process (ch48) just like *Novafroneta* (Fig. 13a). The females of *Cassafroneta* can be recognized by the ventrally protruding lateral sides of the epigyne (Fig. 17a, ELS).

Clade 8 is not supported by any unaltered synapomorphies. However, the development of a bifid prolongation of the pedicel sternite (ch111, Fig. 14e: PBP) is noteworthy, despite its loss in *Parafroneta marrineri* and clade 23. BS: 5, JS: 72%.

Clade 9: *Novafroneta* Blest, 1979. The monophyly of this genus is highly supported in the current analysis (BS: 11, JK: 100%, Fig. 1). According to Blest (1979), species of *Novafroneta* have a long, slender suprategulum and embolic membrane. They lack the mynoglenine tegular process (ch48, Fig. 13a). However, *Novafroneta vulgaris* and *N. gladiatrix* have a pronounced "ridge" that connects the tegulum with the embolic membrane. This might be the homologue of the mynoglenine tegular process and may represent an intermediate state of the more distinct mynoglenine tegular process found in all other genera (clade 10). The embolic membrane of *Novafroneta* has a uniquely modified tip, looking like a membraneous broadened bundle (ch68, Fig. 13a: EM). Unique synapomorphies are also the dorsally bent tibia (ch3, Fig. 10b), the retrolateral thin marginal expansion of the tibia (ch7, Fig. 10b), the presence of only one seta at the paracymbial base (ch28), the very thin tegular sperm duct (ch44, Fig. 10b), and the convoluted sperm duct in the radix (ch82, Fig. 13a; Blest, 1979). The epigyne lacks a scape and the ventral and dorsal plates are fused (Blest, 1979: fig. 512).

Clade 10 is supported by a Bremer value of 1 (JK: < 50%), and the mynoglenine tegular process (ch48, e.g. Fig. 9c), which was considered as a potential homologue of the protegulum in other linyphiids (Hormiga, 2000, p. 6; in character 10; Miller and Hormiga, 2004, p. 419, in character 16). It is present in all scored mynoglenine species except the genera *Cassafroneta* and *Novafroneta*.

Clade 11: *Hyperafroneta* Blest, 1979 and *Metafroneta* Blest, 1979. The sister-group relationship between these two genera (clade 11, Fig. 2b) is well supported (BS: 6, JK: 86%). Their copulatory organs (males and females) differ distinctly from all other mynoglenines (Blest, 1979). The male palps, in particular, are distinctly different: they share the robust, curved lamellar embolus (ch86; Fig. 12c,e) and a unique type of epigyne, where the median extension, the dorsal plate scape, and the surrounding tissue are on the same level (ch131, Fig. 17c; Blest, 1979: figs 573, 577). In addition to the typical embolus, Blest (1979) also mentions that the sperm duct of *Metafroneta* directs distally. As for the females, we agree there is no scape present in both these genera, but an anterior socket (Blest, 1979). The central structure, resembling a scape, is a ventrally protruding part of the dorsal plate and not a free-standing structure such as a scape would be. In *Metafroneta*, this median structure is also bordered by medially extended lateral sides (ch127, Fig. 17c). These structures are also present in *Hyperafroneta*, but are less pronounced and restricted to the posterior half of the epigyne. The vulva of both genera lack distinct bursae and the receptacula are pear-shaped.

The surface of the carapace is smooth in *Hyperafroneta* and rugose in *Metafroneta* (Blest, 1979). The monotypic genus *Hyperafroneta* has some additional autapomorphies, including a bifid suprategulum (ch60; Fig. 12c: SPT) and a distinct dichotomous side arm (Blest, 1979) arising posteriorly from the embolus (ch90; Fig. 12c: ESA), which are also found in some outgroup taxa. However, the few autapomorphies of *Hyperafroneta* might not justify the establishment of a monotypic genus. A synonymy of *Hyperafroneta* with *Metafroneta* is suggested based on our phylogenetic results but is not formally proposed here.

Clade 12: Despite the low support values (BS: 1, JK: > 50%), some synapomorphies support this clade, such as the two turns of the sperm duct in the tegulum (ch43, Fig. 13b, reduced to one in *Haplinis*) and the turning point of the copulatory duct (ch148; Blest, 1979: fig. 478), which is also present in *Australolinyphia*. The connection between the bifid prolongations of the pedicel sternite (ch112) is also synapomorphic for this clade, but subsequently reduced four times.

Clade 13: The sister relationship between *Protoerigone* and *Pseudafroneta perplexa* is weakly supported (BS: 1, JK: < 50%) and disappears under implied weights of $k = 2$–41 (Fig. 5). *Pseudafroneta perplexa* resembles taxa from clade 30, which is reflected in a suggested sister-group relationship (Figs 1 and 2b) when using k values of 2–41.

No unique synapomorphies support this clade, but one unusual character is worth mentioning: femur I of *Protoerigone otagoa* and *Pseudafroneta perplexa* is scaly at the retrolateral side adjacent to the trochanter joint (ch118, Fig. 13f). This state is also found in *Pseudafroneta pallida* and *Parafroneta haurokoae*.

***Protoerigone* Blest, 1979** was established to account for the deeply invaginated subocular sulci (ch94, autapomorphy; Blest, 1979: fig. 609) found in males of this genus (two described species). Otherwise, these species closely resemble *Parafroneta* (Blest, 1979). The suprategulum is a strongly sclerotized hook (ch67, e.g. Fig. 9e) and the epigynal scape is reduced to a knob or bar (ch143, e.g. Fig. 17f; Blest, 1979). Using implied weights, *Protoerigone* emerges in clade 14 either as sister to clade 30 ($k = 2$–4) or sister to clade 15 ($k = 5$–41).

***Pseudafroneta* Blest, 1979** is paraphyletic in the current analysis. A diagnosis would therefore cause more problems than stability. Blest (1979) suggested as synapomorphy for *Pseudafroneta* that the embolic membrane and the embolic division form a complex together, which is separated from the tegulum.

The filiform embolus of *Pseudafroneta perplexa* resembles that of *Haplinis* and other members of clade 30, while the robust embolus of *Pseudafroneta pallida* is more like what is seen in *Afroneta* and other members of clade 15. We agree with Blest (1979) that *Pseudafroneta* shares many characters with *Parafroneta* and in particular the shape of the epigyne. A comparison of all described *Pseudafroneta* species (figures in Blest, 1979) reveals that the palpal morphology of *P. perplexa* is representative for all *Pseudafroneta* species except *P. pallida*.

Clade 14 has low support values (BS: 1, JK: > 50%) and is supported by only one synapomorphy: the four retromarginal denticles on the chelicerae (ch105, Fig. 14c), a state that is reversed several times within the clade.

Clade 15 contains taxa with simpler palpal morphologies, i.e. fewer appendices than in most other taxa distal to node 14. It includes all African genera (*Trachyneta*, *Gibbafroneta*, *Laminafroneta*, and *Afroneta*) except *Afromynoglenes*, and also *Pseudafroneta pallida* and *Parafroneta* from New Zealand. Although this clade is recovered in all topologies using k values of 5 and above (including equal weights), it is weakly supported (BS: 1, JK: < 50%), including no synapomorphies (Fig. 2b). However, it shares characters with the more basal taxa, such as the teardrop-shaped conformation of the radix and the embolus (ch79, Fig. 11e), which are present in all mynoglenines except *Pseudafroneta perplexa* and clade 30.

Clade 16: The sister relationship between *Pseudafroneta pallida* and *Parafroneta* is weakly supported (BS: 1, JK: < 50%) and is likely to change in future analyses. The special position of *Pseudafroneta pallida* is discussed in more detail in the section on *Pseudafroneta*.

Clades 17–21: *Parafroneta* Blest, 1979 emerged as paraphyletic when using k values of 1, but monophyletic in all other analyses. The genus *Parafroneta* and the individual nodes within the genus have low support (Bremer value of 1 and jackknife values below 50%), and are not supported by any synapomorphy (Figs 1 and 3). The morphology of their copulatory organs resembles those of the African taxa (clade 22). They share with *Trachyneta* a teardrop-shaped radix with a pointed proximal end (ch80, Fig. 11f).

Blest (1979) mentions the following descriptive characters, which are all also found in e.g. *Afroneta* and most other African mynoglenines within clade 22: long and narrow, extremely simple male palps, with an indistinct suprategulum, a transparent narrow embolic membrane and a more or less straight distally directed embolus on a teardrop-shaped radix (e.g. Fig. 13b; Blest, 1979: fig. 550). The female epigyne also share most characters within clade 22, i.e. the highly homoplasious knob-like scape (ch143, Fig. 17f) situated posteriorly ("rudimentary posterior socket" in Blest, 1979).

Clade 22–24: These clades define the relationships between the three species-poor genera *Trachyneta* (two species), *Gibbafroneta* (one species) and *Laminafroneta* (three species). They are weakly supported (BS: 1, JK: < 50%, Figs 1 and 3) and likely to change position in future analyses due to the lack of informative morphological characters. The overall similarity and simplicity of their copulatory organs makes it difficult to find characters for a morphological analysis, and molecular data should be collected to address this problem.

***Trachyneta* Holm, 1968** is represented by one of the two described species (Fig. 3). It is difficult to separate from *Afroneta*, but both sexes lack a trichobothrium on metatarsus IV and have only one instead of two macrosetae on tibia IV (Holm, 1968; Merrett, 2004). In the current analysis, the tibial spine (macrosetae) formula 2221 is an autapomorphy for *Trachyneta* (ch166). However, the most distinct diagnostic character for males (lacking in females) is a distal bump on the lateral side of the chelicerae, mentioned by Holm (1968) when he described *T. extensa*. It is also present in *T. jocquei* and acts as autapomorphy in the current analysis (ch109; Holm, 1968: fig. 65). Moreover, the embolic membrane is highly sclerotized (ch80) and similar to *Laminafroneta* (Fig. 12d), but is unlike that of *Afroneta* and *Gibbafroneta* (Holm, 1968; Merrett, 2004).

***Gibbafroneta* Merrett, 2004:** We found no synapomorphy to support this monotypic genus (Fig. 3). However, males can be recognized by the hirsute post-PME cephalic lobe (ch101; Merrett, 2004: fig. 75), which is present in a similar form in *Cassafroneta forsteri* from New Zealand and the erigonine *Hilaira excisa*. In addition, both sexes have relatively short legs, with tibia, metatarsi, and tarsi of nearly equal length (Holm, 1968; Merrett, 2004). The female vulva is short and lacks bursae (ch149; Merrett, 2004: fig. 79), which is otherwise only found in four other mynoglenines *Novafroneta vulgaris*, *Hyperafroneta*, *Metafroneta*, and *Afroneta bamilekei*.

Clade 25: *Laminafroneta* Merrett, 2004. The genus *Laminafroneta* is well supported (BS: 8, JK: 99%, Fig. 1) but lacks unique synapomorphies (Fig. 3). However, the genus can be diagnosed by a number of characters that are absent or rare within mynoglenines. These include the long proximal setae on the paracymbium (ch29, Fig. 9e, which are unique among the scored mynoglenines); and the inner connection of the paracymbium (ch38, Fig. 9e), which is also found in *Novafroneta gladiatrix* and *Pseudafroneta perplexa*. Merrett (2004: figs 81 and 86) describes the "separate leaf-like sclerite which partially encloses the distal end of the embolus" as diagnostic for *Laminafroneta*. We consider this structure as a highly sclerotized embolic membrane (ch67, Fig. 12d), which is also found in *Hyperafroneta*, *Pseudafroneta pallida*, and *Trachyneta*. Females of *Laminafroneta* (and *Cassafroneta*, *Novafroneta*, and *Afromynoglenes*) lack a central depression on the ventral plate (ch120). Merrett (2004) also mentions the broad triangular sclerotized dorsal plate in females as diagnostic. We interpret it as the sclerotized anterior margin of the copulatory duct (ch135, Fig. 16e), a synapomorphy of *Laminafroneta* (also occurring in *Afromynoglenes parkeri*)

Clade 26–29: *Afroneta* Holm, 1968. The monophyly of *Afroneta* is not well supported (BS: 1, JK: < 50%) and lacks unreversed synapomorphies (Fig. 3). The problem might be the morphological similarity and genital simplicity of *Trachyneta*, *Gibbafroneta*, *Laminafroneta*, and *Afroneta*. However, among many other characters, Holm (1968) mentions the steadily tapering distal directed embolus on the simple radix, the membraneous embolic membrane, and the posterior knob-like scape on the epigyne. The membraneous embolic membrane (ch67, e.g. Fig. 12a) is found in all species of clade 15 except *Pseudafroneta pallida*, *Laminafroneta*, and *Trachyneta*. A steadily tapering embolus is also found in e.g. *Parafroneta* (Fig. 6) and *Trachyneta*. The knob-like scape (ch143) is also found in many other genera such as *Parafroneta* (Fig. 17f).

Males can be recognized by having a more or less unsclerotized tegular mynoglenine process (ch51, Fig. 9b), also present in *Trachyneta* and *Gibbafroneta*. Moreover, all scored species of *Afroneta* have PMEs larger than the PLEs (ch97, Fig. 14a). Such size differences are not seen in any other scored mynoglenines (e.g. Fig. 14b), but in one outgroup taxon, *Bolyphantes luteolus*. Besides *Trachyneta*, *Afroneta* is the only mynoglenine genus with a free-standing setal base that is nearly flush with the chelicerae (ch108, Fig. 14d). Furthermore, with the exception of *Afroneta bamilekei*, *Afroneta* is the only mynoglenine taxon that has one ventral proximal prolateral macroseta on tibia I (ch171, Fig. 15f).

Clade 30 includes all mynoglenines with relatively complex embolic division and long emboli, but the clade has weak support (BS: 2, JK: < 50%). No unreversed synapomorphy defines this clade. However, the clade is supported by homoplastic characters that are shared with some of the outgroup taxa: the tegular retrolateral lobe (ch45, Fig. 9d, TRL), the enlarged embolic membrane wrapping the embolus (ch70, Fig. 12b, EM), the ventrally twisted column connecting the radix and the tegulum (ch78, Fig. 12b), and the initially proximal oriented embolus (ch83, Fig. 11a).

***Afromynoglenes* Merrett and Russell-Smith, 1996:** This monotypic genus was established to account for the extraordinary male palpal morphology. The authors appropriately named this African genus to account for its close similarity to *Promynoglenes*, *Metamynoglenes*, and *Haplinis* (formerly *Mynoglenes*). The close resemblance is also reflected in the cladistic analysis, as *Afromynoglenes* emerges as sister taxon to all derived New Zealand taxa of clade 31 (Fig. 4). Merrett and Russell-Smith (1996) give the following diagnostic characters: males have a very long embolus, forming a loop; they are equipped with a unique embolic membrane, paracymbium, and tegular mynoglenine process; the females are recognized mainly by the exceptionally long, curved bursae (Merrett and Russell-Smith, 1996: fig. 16). Autapomorphic characters for *Afromynoglenes*, such as the unique broadened embolic membrane covering the whole prolateral side of the palp (Merrett and Russell-Smith, 1996: fig. 16) and the correspondingly elongated embolus and bursa, was left out of the analysis as autapomorphies do not contain any phylogenetic grouping information.

Clade 31 including *Promynoglenes* as sister to *Metamynoglenes* plus *Haplinis* is well supported (BS: 6, JK: 95%, Fig. 4) but lacks unaltered synapomorphies.

Clades 32 and 33: *Promynoglenes* Blest, 1979. The monophyly of *Promynoglenes* is highly supported (BS: 9, JK: 99%, Figs 1 and 4). This genus was defined by Blest (1979) based on the broad paracymbium with a small distal process (ch36, Fig. 10c), the ventral ledge emerging from the prolateral side of the cymbium (ch17, Fig. 12f, CPL), the small tegular mynoglenine process, the long coiled embolus (ch86, Fig. 13c), and a long and delicate epigynal scape (Blest, 1979).

The ledge is also found in *Metamynoglenes* (Fig. 12f) and in a vestigial form as a ridge in *Afromynoglenes* (ch17). However, it is only well developed (as an apophysis) in *Promynoglenes* (ch18, Fig. 13c, CPA) and *Metamynoglenes helicoides* (ch18, Fig. 11d). The broad paracymbium with the small distal process (ch36) is also found in *Metamynoglenes*, but *Promynoglenes* lacks the mesal broadening (ch37, cf. Figs 12f and 10c). Our analysis revealed additional unique synapomorphies for the genus: a ventrally flattened stubbly area at the prolateral side of the cymbium (ch15, Fig. 11d: CPF), a small additional knob retrolateral to the tegular mynoglenine process (ch52, Fig. 10c: TMK), a dagger-like suprategulum (ch59, Fig. 10c),

and a circular (coiled) embolus restricted to two dimensions (ch86, Fig. 13c).

Clade 34 is weakly supported (BS: 2, JK: < 50%), lacking any synapomorphic characters.

Clades 35 and 36: *Metamynoglenes* Blest, 1979. The monophyly of this genus is highly supported (BS: 5, JK: 97%, Fig. 1). Blest (1979) defined it on the basis of the broad paracymbium with a small distal protuberance (ch36, Fig. 10c), a distinct mynoglenine tegular process, a thin curved hook-like suprategulum (ch59, Fig. 10a), a spiniform embolus with a distinct radical component, and an anteriorly displaced epigynal scape. We found additional unique synapomorphies for *Metamynoglenes*: a mesally broadened paracymbium (ch37; Fig. 12f: PMB), a pointed tegular retrolateral lobe (ch45, ch46, Fig. 10a), and a thin long hook-like suprategulum (ch59, Fig. 10a). The retrolateral appendix (ch81; Fig. 12f: RRA) mentioned by Blest (1979: 129) as "distinct radical component" is very typical for *Metamynoglenes* but is also present in *Pseudafroneta perplexa*, thus arguing for a close relationship between the two taxa.

Clades 37–42: *Haplinis* Simon, 1894. *Mynoglenes* was redescribed in detail by Blest (1979) and synonymized with *Haplinis* by Millidge (1984). Blest (1979) points out that this genus includes species from a broad variety of forms and that it is therefore relatively difficult to circumscribe. Accounting for this variety, Blest (1979) defined species groups to simplify determination, rather than as indicator of relationships. We included one species of each of his species groups and found a relatively high support for the genus (BS: 7, JK: 83%), and recognize five synapomorphies: the paracymbial hairs extending from the sclerotized area to the membraneous part (ch30, Fig. 9d, altered in clade 39), a ventral mesal inwards fold on the embolic membrane (ch71, Fig. 9d, reduced in *H. horningi* and *H. titan*), and a filiform, three-dimensional embolus (ch86, Fig. 11a), which also occurs in *Afromynoglenes*. Unaltered synapomorphies are the distinct ventral ectal outwards fold (ch73, Fig. 12b: EME), which is an extension of the embolic membrane and mentioned as a diagnostic feature by Blest (1979), and the epigyne that is defined as two nearly circular depressions (ch120, Fig. 16d). Blest (1979) also notes the typical looped embolus sometimes curving along the prolateral side of the cymbium and also the sickle-shaped paracymbium. We scored this type of paracymbium as the oval hook (ch36, Fig. 9c), which is typical for *Haplinis* but also found in *Metafroneta sinuosa*.